The Role of Diacylglycerol Kinase Zeta in Mechanotransduction:

A Positive Regulator of Skeletal Muscle Mass

By

Jae-Sung You

A dissertation submitted in partial fulfillment of

the requirements for the degree of

Doctor of Philosophy

(Cellular and Molecular Biology)

at the

UNIVERSITY OF WISCONSIN-MADISON

2016

Date of final oral examination: 7/8/2016

The dissertation is approved by the following members of the Final Oral Committee:

William M. Bement, Professor, Zoology
Shigeki Miyamoto, Professor, Oncology
Marisa S. Otegui, Associate Professor, Botany
James M. Ntambi, Professor, Biochemistry
Troy A. Hornberger, Associate Professor, Comparative Biosciences

Abstract

Mechanical loading plays a major role in the regulation of skeletal muscle mass, and the maintenance of muscle mass profoundly influences our health and quality of life. Although the molecular pathways that link mechanical loading to the control of muscle mass (i.e., mechanotransduction) remain ill-defined, recent advancements in our knowledge indicate that signaling by the mammalian/mechanistic target of rapamycin (mTOR) is a key component of the mechanotransduction pathway. Defining components of the mechanotransduction pathway, such as mTOR signaling, is important because it helps advance the development of therapies that can mimic the effects of mechanical loading and, in turn, preserve muscle mass during atrophic conditions. Indeed, in this study, by using pharmacological, mechanical, and genetic means to directly modulate mTOR signaling, I demonstrated that the activation of mTOR signaling is both necessary and sufficient to alleviate the immobilization-induced decreases in protein synthesis and muscle mass in mice. Given the importance of mTOR signaling in the maintenance of muscle mass, I began to interrogate how mechanical stimuli activate mTOR signaling, by employing an *ex vivo* passive stretch model of mechanical stimulation in mice. Based on previous studies, it has been suggested that mechanical stimuli activate mTOR signaling through a phospholipase D (PLD)-dependent increase in the concentration of phosphatidic acid (PA). Consistent with the role of PA, the results in this study indicated that mechanical stimuli activate mTOR signaling, and protein synthesis, through a mechanism that involves a direct interaction of PA with mTOR. Surprisingly, however, the results also indicated that the zeta isoform of diacylglycerol kinase (DGKζ), but not PLD, plays an important role in the mechanically-induced increases in PA and mTOR signaling. Furthermore, it was shown that the overexpression of DGKζ is sufficient to induce muscle fiber hypertrophy through an mTOR-dependent mechanism that requires DGKζ kinase activity (i.e., the synthesis of PA). Therefore, these results suggest that DGKζ could be a fundamental component of the mechanism(s) through which mechanical loading increases mTOR signaling, protein synthesis, and skeletal muscle mass. To test this possibility, I next employed a mechanical overload (OV) model, which induces rapid muscle hypertrophy *in vivo*. As hypothesized, the results demonstrated that DGKζ plays an essential role in the OV-induced rapid muscle

hypertrophy. Unexpectedly though, the results also demonstrated that DGKζ not only promotes the activation of mTOR signaling and protein synthesis, but it also attenuates the induction of proteasome-dependent protein degradation and the ubiquitin-proteasome-system (UPS). Subsequent experiments revealed that nuclear DGKζ is a potent inhibitor of the Forkhead box O transcription factor, which promotes the induction of the UPS. I also found that increased expression of DGKζ can mitigate various types of muscle fiber atrophy, demonstrating that DGKζ is a potential therapeutic target for preventing muscle atrophy. Taken together, this study identifies DGKζ as a critical component of the mechanotransduction pathway through which mechanical loading promotes the activation of PA-mTOR signaling and protein synthesis, while attenuating the induction of the UPS and protein degradation, to facilitate skeletal muscle hypertrophy.

This dissertation is dedicated to the late Bok-soon Chang, my grandmother.

Acknowledgements

First of all, I would like to thank my advisor, Dr. Troy Hornberger, for guiding me through this journey. He has shown and taught me all the qualities that a principal investigator should have as a scientist, lab manager, and mentor. Thanks to his guidance, I was able to keep my passion for research and grow up both intellectually and personally. He often told me, “Your success is my success. I am working for it”. This is just one of many unforgettable words that he has given to me, but it really reflects how much he wholeheartedly supported me for my success. Undoubtedly, He is my bona fide academic father. I would also like thank the members of my dissertation committee, Drs. William Bement, Shigeki Miyamoto, Marisa Otegui, and James Ntambi. They gave me helpful advice and feedback for successful progress of my research. I was lucky to have such nice committee members.

I would like to sincerely acknowledge all my colleagues in Dr. Hornberger’s laboratory: Craig Goodman, Brittany Jacobs, John Fry, Rachel McNally, Rocky Blanco and many undergraduate research assistants including my three mentees, Chan-Ran Kim, Garret Anderson, and Matthew Dooley. They helped my research a lot and made my life in the lab much warmer and happier. Especially, I cannot emphasize enough how much I appreciate Brittany Jacobs being my soulmate in the lab during the entire period of my PhD. I would also like to acknowledge Kwanjeong Educational Foundation for supporting my PhD life financially. I am very grateful to many friends in Korean Presbyterian Church of Madison and in Wisconsin Knights baseball team. They have always cheered me up and made my life in Madison more balanced and enjoyable.

I would like to express profound gratitude to my loving parents and parents-in-law for giving me their endless love, care, and encouragement. I also thank my sister and brother-in-law for their concern about my life abroad. Lastly, I cannot find any word to express my deepest gratitude and love to my wonderful wife, Iseul Choi. Simply put, I could have not won through this journey without her love and supports. I am truly blessed to have her in my life.

God, my savior, I want to extend my special thanks to you for giving me all of these great people and guiding me until now.

Table of Contents

List of Figures

Chapter 1

Introduction

Skeletal muscle structure, function, plasticity, and significance

The structure of skeletal muscle is illustrated in Figure 1-1. Skeletal muscle is composed of many fascicles of multinucleated muscle cells called muscle fibers. Each muscle fiber contains numerous chains of myofibrils that are made of many myofibrillar proteins such as actin, myosin, and titin. These proteins are organized into two types of filaments of myofibrils: thick and thin filaments. Specifically, thick filaments consist primarily of myosin proteins, and thin filaments consist primarily of actin proteins. Muscle contractions occur by the cyclic interaction between actin and myosin, and subsequent myofilament sliding. Thus, the amount of myofibrillar proteins and myofibrils in a muscle fiber is directly associated with the fiber's force-generating capacity, and is a key determinant of the muscle fiber size. Typically, muscle (fiber) hypertrophy or atrophy refers to the cross-sectional increase or decrease in myofibril size, respectively.

Muscle fibers are formed by myoblast fusion in a process known as myogenesis (1). During postnatal development, these muscle fibers become physically and biochemically distinct fiber types (type 1, 2a, 2x, type 2b, or hybrid) depending on the genetic nature of each muscle fiber as well as the types of innervating motor nerve (2-5). These different types of muscle fibers express different isoforms of myosin heavy chain (MHC) which are commonly used for fiber-typing (see Figure 2-8). Skeletal muscle contains a heterogeneous mixture of the distinct muscle fiber types. Thus, depending on the composition of the fiber types, each skeletal muscle exhibits its unique functional property that is suited for performing a specific task, such as standing for a long period of time or sprinting for a short period of time.

In the human body, there are approximately 650 different skeletal muscles (6). These muscles work alone or in combination in their specific location (i.e., origin and insertion), creating a wide variety of human movements/positions and other essential functions for our life (e.g. diaphragm in breathing). Furthermore, as mentioned above, these performances are optimized by the appropriate selection of fiber type composition within the working muscles. Therefore, skeletal muscles possess intricate and extensive structural features that allow them to function as a motor in the human body.

Skeletal muscles consume a lot of energy (i.e., ATP) during every cyclic interaction between actin and myosin, and importantly, these active muscles comprise approximately 45% of total body mass. Therefore, in addition to generating force, skeletal muscles can also play a critical role in the regulation of whole-body energy metabolism. For example, epidemiologic studies have shown that skeletal muscle mass is inversely associated with several metabolic disorders such as obesity, diabetes, and metabolic syndromes (7-9). These studies indicate that the maintenance of skeletal muscle mass is not only keeping our body physically functional, but also metabolically healthy.

As discussed above, skeletal muscle functions are directly associated with its mass, and thus, the maintenance of skeletal muscle mass will contribute significantly to health and quality of life. However, skeletal muscle mass can be reduced by a variety of factors such as physical inactivity (e.g., immobilization, bed rest, and unloading), injuries (e.g., muscle, nerve, and tendon injuries), diseases (i.e., cachexia), malnutrition, and aging (10). Specifically, with aging, both sedentary and active adults will lose up to 30-40% of their muscle mass, and this reduction in muscle mass is associated with disability, loss of independence, an increased risk of morbidity and mortality, along with an estimated $18.5 billion in annual healthcare costs in the United States alone (11-14).

In contrast, skeletal muscle mass can be increased by various stimuli, and one of the most powerful stimuli is mechanical loading/stimuli (e.g., mechanical overload, eccentric contractions, and chronic stretch) (15-19). Mechanical loading can also contribute to the maintenance of skeletal muscle mass during atrophic conditions including physical inactivity and aging (20-24). Thus, it is widely believed that understanding the molecular process that links mechanical loading to the control of muscle mass (i.e., mechanotransduction) will provide insights into the development of therapies that are aimed at mimicking the effect of mechanical loading, and in turn, prevent muscle atrophy. In the next sections, some of the molecular mechanisms that have been tested for their potential role in the mechanical load-induced hypertrophy will be discussed.

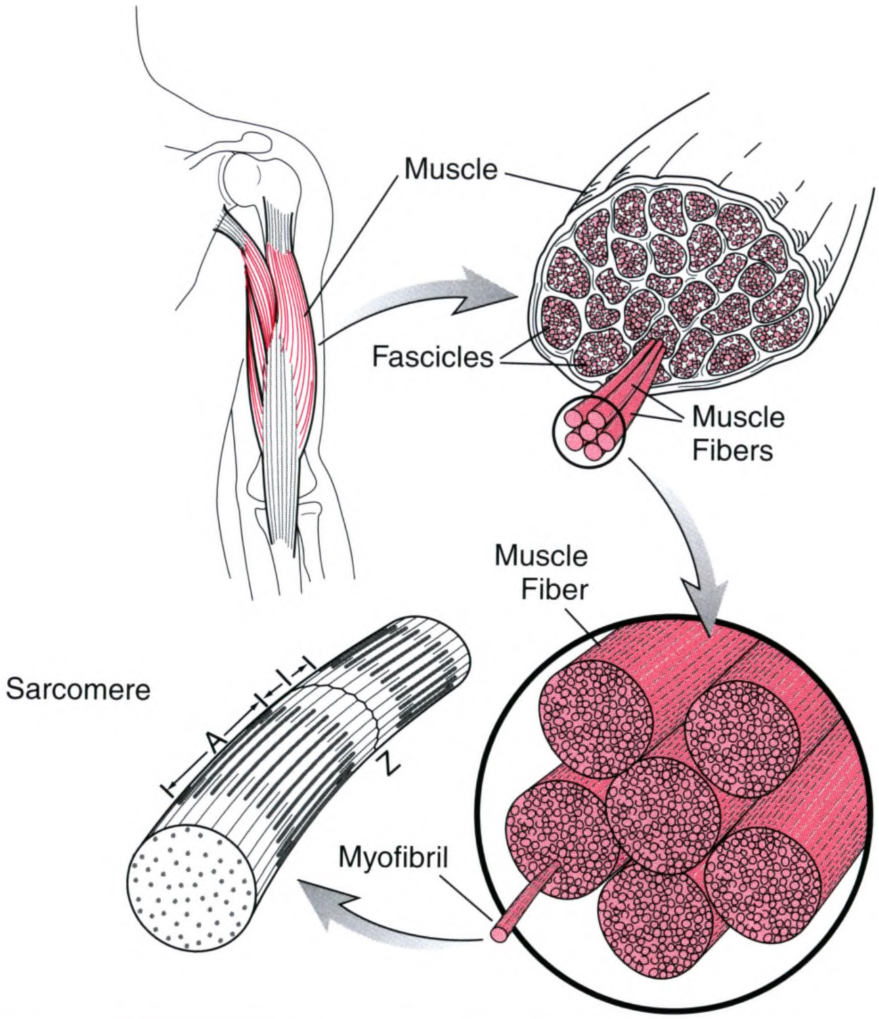

Figure 1-1. Structural hierarchy of skeletal muscle. Whole skeletal muscles (here a biceps muscle is shown) are composed of numerous fascicles of muscle fibers. Muscle fibers are composed of myofibrils arranged in parallel. Myofibrils are composed of sarcomeres arranged in series. Sarcomeres are composed of interdigitating myosin and actin filaments. Adapted from (25)

The role of mTOR in the mechanically-induced skeletal muscle hypertrophy

Mechanical loading induces skeletal muscle hypertrophy by increasing the rate of protein synthesis greater than the rate of protein degradation. Although mechanical loading has been shown to affect both translational efficiency (i.e., initiation, elongation, and termination) and translational capacity (i.e., the number of ribosomes), the primary effect of mechanical loading on protein synthesis appears to occur at the level of translational efficiency, and more specifically, translation initiation (i.e., the binding of a ribosome to the mRNA) (18, 26). For example, mechanical loading has been shown to promote a selective increase in the binding of the polysomal pool to the proportion of 5' terminal oligopyrimidine tract (5'TOP)-containing mRNAs that encode proteins central to the growth process (e.g. ribosomal proteins and translation factors) (27, 28).

The translation of mRNAs that contain a 5'TOP structure is inhibited by the drug called rapamycin (29). Consistent with the role of 5'TOP mRNAs in the expression of growth-related proteins, many studies have shown that rapamycin prevents mechanically-induced increases in protein synthesis and skeletal muscle mass (30-35). These observations suggest that components of the rapamycin-sensitive pathway play a critical role in the mechanical regulation of protein synthesis and skeletal muscle mass.

In cells, rapamycin forms a complex with the FKBP12 protein, and this complex has been shown to bind to the FKBP12-rapamycin binding (FRB) domain of a protein kinase called mammalian/mechanistic target of rapamycin (mTOR) (36, 37). A point mutation of the FRB domain inhibits the interaction of mTOR with the FKBP12-rapamycin complex and renders this mutant of mTOR rapamycin-resistant (RR-mTOR) (38, 39). Furthermore, numerous studies have shown that various forms of mechanical stimuli are sufficient to induce phosphorylation of direct mTOR substrates such as $p70^{S6k}$ (30-35). Inspired by these findings, Goodman et al. tested if mTOR is the rapamycin-sensitive element that confers mechanically-induced muscle growth (35). By using transgenic mice with muscle-specific expression of RR-mTOR, they found that the growth inhibitory effect of rapamycin is completely rescued in RR-mTOR mice. However, the rescue effect is not observed in mice that express a rapamycin-resistant, but kinase-dead, mutant of mTOR. Based on these findings, it was concluded that mTOR, within skeletal muscle cells, is

the primary rapamycin-sensitive element that confers the mechanically-induced hypertrophic response, and that mTOR kinase activity is necessary for this event. This conclusion is important because, as mentioned earlier, identifying the molecular mechanism through which mechanical loading increases muscle mass will help to develop therapies that are aimed preventing muscle atrophy. Indeed, in Chapter 2, by using immobilization model, I confirm the therapeutic potential of targeting mTOR signaling for the prevention of muscle atrophy.

The potential mechanisms underlying the mechanical activation of mTOR signaling (Figure 1-2)

Since mTOR was identified as a crucial component in the mechanotransduction pathway that promotes muscle growth, numerous investigations have been aimed at defining how mechanical stimuli activate mTOR signaling. These studies tested a potential role of several candidates that are well-established as upstream mTOR activators, such as class I phosphoinositide-3 kinase (PI3K)/protein kinase B (PKB) and amino acids.

The potential involvement of PI3K/PKB pathway in the mechanical activation of mTOR signaling was first supported by several studies which have shown that *i)* mechanical stimuli increase the content of IGF-1 which is known to activate the PI3K→PKB→mTOR pathway and induce skeletal muscle growth (40-42), *ii)* mechanical stimuli activate signaling through the PI3K→ PKB (34, 43-52), and *iii)* forced activation of the PI3K→PKB pathway activates mTOR signaling and induces skeletal muscle growth via a rapamycin-sensitive mechanism (34, 53, 54). Taken together, these observations provided a hypothesis that mechanical loading activates mTOR signaling and muscle growth through a mechanism involving the IGF-1→PI3K→PKB→mTOR pathway. However, this hypothesis was challenged by subsequent studies which have shown that *i*) transgenic mice with muscle-specific expression of dominant negative IGF-1 receptor fail to show an increase in PKB phosphorylation following IGF-1 stimulation, but still exhibit a normal hypertrophic response following mechanical overload (55), *ii*) eccentric contractions induces signaling through the PI3K→PKB, but this was a very transient event and markedly different from the prolonged activation of mTOR signaling (56), and *iii*) pharmacological inhibition of PI3K with

wortmannin, or genetic deletion of PKB1, does not block the mechanical activation of mTOR signaling (31, 56, 57). Overall, these results indicate that mechanical loading activates mTOR signaling through a PI3K/PKB-independent mechanism.

The potential involvement of amino acids in the mechanical activation of mTOR signaling was also proposed by several findings. For example, amino acids, unlike growth factors (e.g., IGF1), have shown to activate mTOR signaling through a PI3K/PKB-independent mechanism (58, 59). Furthermore, mechanical loading was able to increase amino acid uptake (60, 61). Despite these findings, the proposed role of amino acids was challenged by other reports that *i*) the activation of mTOR following eccentric contractions precedes the increase in intracellular amino acids (61), *ii*) in isolated skeletal muscles, mechanical stimuli can activate mTOR in the absence of exogenous amino acids (62), and *iii*) wortmannin prevents the activation of mTOR signaling by amino acids but not by mechanical stimuli (62). Combined, it appears that mechanical loading activates mTOR signaling via a mechanism that is distinct from the amino acids-triggered mechanism.

The results from the above studies, along with others, indicate that mechanical loading activates mTOR signaling through a unique mechanism that does not require typical candidates such as PI3K, PKB, exogenous nutrients, phospholipase C, or intracellular calcium (31, 56, 62, 63). However, the identity of this unique mechanism remains unclear. Nonetheless, an emerging body of evidence suggests that phosphatidic acid, (PA), a potent activator of mTOR, may play a key role in the mechanical activation of mTOR signaling (56, 63-66). Furthermore, among many enzymes that are involved in the regulation of PA [e.g. phospholipase D (PLD), diacylglycerol kinase ζ (DGKζ or DAGKζ), etc], PLD appears to be essential for the potential role of PA in the mechanical activation of mTOR signaling (56, 63). The studies in Chapter 3 and 4 were inspired by this evidence, and thus explore the potential role of PA and PLD in the mechanical activation of mTOR signaling. The results from these studies indicate that DGKζ, but not PLD, plays an important role in the mechanical activation of PA-mTOR signaling. These findings led me to further investigate DGKζ, and as a result, in Chapter 5, I report various novel functions of DGKζ that collectively contribute to the mechanical load-induced skeletal muscle hypertrophy.

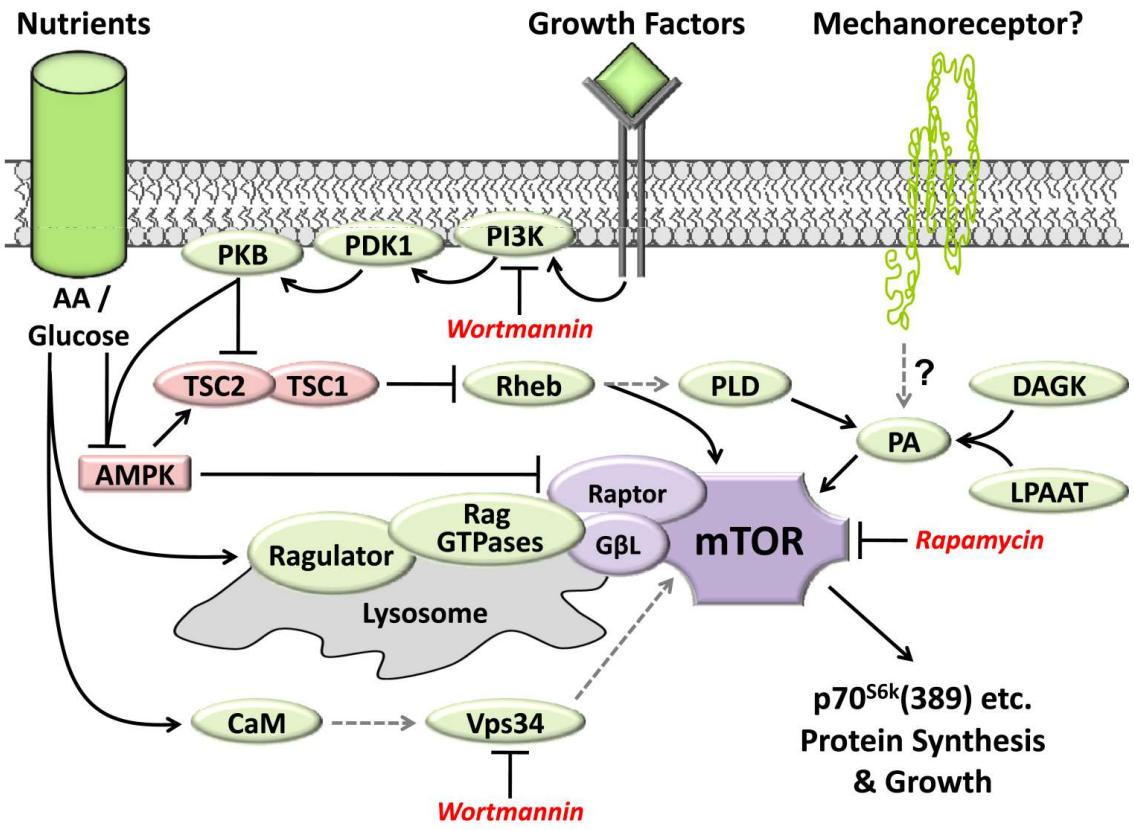

Figure 1-2. Schematic of the general mechanisms that regulate mTOR Signaling. Signaling by mTOR can be activated by numerous stimuli including growth factors, nutrients and mechanical loading. mTOR exists in complexes with other proteins, and some of the components of the mTOR complex are shaded in purple. The signaling molecules that stimulate mTOR signaling are shaded in green, while molecules that inhibit mTOR signaling are shaded in red. Dashed lines represent links in the regulatory pathways that have not been clearly established. Adapted from (67)

Chapter 2

The Role of mTOR Signaling in the Regulation of Protein Synthesis and Muscle Mass during Immobilization

Jae-Sung You[1,2], Garrett B. Anderson[2], Troy A. Hornberger[1,2,*]

[1]Program in Cellular and Molecular Biology and [2]Department of Comparative Biosciences in the School of Veterinary Medicine, University of Wisconsin - Madison, WI 53706 USA

Corresponding authors: Troy Alan Hornberger (Address: 2015 Linden Drive, Madison, WI 53706, USA; Phone: 608.695.2847; E-mail: troy.hornberger@wisc.edu),

Author contributions: J.-S.Y. and T.A.H. conceived and designed the experiments. J.-S.Y. and G.B.A. performed the experiments and analyzed the data. J.-S.Y. and T.A.H. wrote the paper.

This chapter was published in: *Disease Models and Mechanisms*. 2015 Sep 1;8(9):1059-69 and modified slightly to comply with the format of this dissertation

Abstract

The maintenance of skeletal muscle mass contributes significantly to health and issues associated with the quality of life. It has been well recognized that skeletal muscle mass is regulated by mechanically-induced changes in protein synthesis and that signaling by mTOR is necessary for an increase in protein synthesis and the hypertrophy that occurs in response to increased mechanical loading. However, the role of mTOR signaling in the regulation of protein synthesis and muscle mass during decreased mechanical loading remains largely undefined. In order to define the role of mTOR signaling, we employed a mouse model of hindlimb immobilization along with pharmacological, mechanical, and genetic means to modulate mTOR signaling. The results first showed that immobilization induced a decrease in the global rates of protein synthesis and muscle mass. Interestingly, immobilization also induced an increase in mTOR signaling, eIF4F complex formation, and cap-dependent translation. Blocking mTOR signaling during immobilization with rapamycin not only impaired the increase in eIF4F complex formation, but also augmented the decreases in global protein synthesis and muscle mass. On the other hand, stimulating immobilized muscles with isometric contractions enhanced mTOR signaling and rescued the immobilization-induced decrease in global protein synthesis through a rapamycin-sensitive mechanism that was independent of ribosome biogenesis. Unexpectedly, the effects of isometric contractions were also independent of eIF4F complex formation. Similar to isometric contractions, overexpression of Rheb in immobilized muscles enhanced mTOR signaling, cap-dependent translation, and global protein synthesis, and prevented the loss of fiber size. Therefore, we conclude that the activation of mTOR signaling is both necessary, and sufficient, to alleviate the decreases in protein synthesis and muscle mass that occur during immobilization. Furthermore, these results indicate that the activation of mTOR signaling is a viable target for therapies that are aimed at preventing muscle atrophy during periods of mechanical unloading.

Introduction

Skeletal muscle is the largest organ in human body and the loss of its mass is highly associated with a low quality of life, an increased risk of morbidity and mortality, as well as elevated healthcare costs (9, 11, 12, 68). Importantly, a profound loss of skeletal muscle mass can occur during various conditions that result in mechanical unloading (i.e. disuse atrophy). For example, most orthopedic injuries and non-orthopedic diseases require immobilization of body parts and bed rest, respectively, and, during the initial 2-3 weeks of this period, a rapid disuse atrophy occurs at a rate of approximately 0.5% of total muscle mass per day (69, 70). Thus, the development of therapies that are aimed at preserving muscle mass during mechanical unloading is of great clinical and fiscal significance.

Skeletal muscle mass is ultimately determined by the balance between the rate of protein synthesis and protein degradation (71). For instance, a net decrease in protein synthesis and/or a net increase in protein degradation can lead to disuse atrophy. Indeed, both decreased rates of protein synthesis and increased rates of protein degradation have been observed in several animal models of disuse atrophy (72). Similarly, decreased rates of protein synthesis have also been observed in numerous human models of disuse atrophy, but whether changes in the rate of protein degradation contribute to the atrophic response in humans is less clear (69, 73). As such, it has generally been concluded that disuse atrophy is primarily driven by a decrease in the rate of protein synthesis, and thus, preventing the decline in protein synthesis could be a viable target for therapies that are aimed at preventing disuse atrophy (69, 73).

Previous studies have shown that a variety of stimuli such as nutrients, growth factors, and mechanical loading, can regulate protein synthesis in skeletal muscle and this regulation occurs primarily at the level of translation initiation (74). Furthermore, the regulation of translation initiation by these stimuli is largely mediated by a protein kinase called the mammalian (or the mechanistic) target of rapamycin (mTOR) which exists in at least two characteristically distinct complexes; a) the rapamycin-sensitive mTOR complex 1 (mTORC1), and b) the rapamycin-insensitive mTOR complex 2 (mTORC2) (75). Numerous studies have shown that signaling by mTORC1, and / or an unidentified rapamycin-sensitive form of mTOR (referred to as mTOR hereafter unless otherwise noted) regulates cap-dependent

initiation of translation through the phosphorylation of substrates such as eukaryotic initiation factor (eIF) 4E binding protein 1 (4E-BP1) and p70 ribosomal protein S6 kinase ($p70^{S6k}$). For example, the phosphorylation of 4E-BP1 can promote translation initiation by enhancing the formation of the elF4F complex which, in turn, recruits the 43S preinitiation complex to the 5' cap of most mRNAs (76, 77). Moreover, phosphorylated and activated $p70^{S6k}$ can promote an increase in the helicase activity of eIF4A, a component of eIF4F, and thus provide an additional stimulus for translation initiation (78). Finally, it has been demonstrated that the activation of mTOR via the overexpression of Rheb, a direct activator of mTOR, is sufficient to induce an increase in $p70^{S6k}$ phosphorylation, cap-dependent translation, and protein synthesis in skeletal muscles with normal activity (79, 80). Therefore, the control of translation initiation by mTOR is considered to be one of the key steps for the regulation of protein synthesis in skeletal muscle.

A direct link between mTOR signaling and the regulation of protein synthesis and muscle mass has been well documented in models of elevated mechanical loading. For instance, it has been shown that rapamycin, a highly specific inhibitor of mTOR signaling, can prevent the increases in $p70^{S6k}$ phosphorylation and protein synthesis that are induced by various forms of mechanical loading such as resistance exercise, blood flow restriction exercise, and passive stretch (30-33). It has also been shown that rapamycin can prevent chronic mechanical overload-induced increases in fiber size (i.e., hypertrophy) (34, 35). Based on these points, it has become widely accepted that rapamycin-sensitive mTOR signaling plays a central role in the regulation of protein synthesis and muscle mass during periods of increased mechanical loading. However, the potential role of mTOR signaling in the regulation of protein synthesis and muscle mass during mechanical unloading has remained largely undefined. Therefore, the primary goal of this study was to define the role of mTOR signaling in the regulation of protein synthesis and muscle mass during mechanical unloading. More specifically, using a new mouse model of hindlimb immobilization, we attempted to: 1) characterize immobilization-induced changes in mTOR signaling, protein synthesis, and muscle mass, 2) define the role of mTOR in these changes, and 3) determine if forced activation of mTOR signaling can rescue the decline in protein synthesis and fiber size that is

observed in immobilized muscles. Combined, the results from our study have demonstrated that, during immobilization, the activation of mTOR signaling is both necessary, and sufficient, to alleviate decreases in protein synthesis and muscle mass. Hence, this study highlights that the activation of mTOR signaling could serve as a viable target for therapies that are aimed at preventing atrophy during periods of mechanical unloading.

Results

Immobilization decreases the global rates of protein synthesis and muscle mass, but activates mTOR signaling and cap-dependent translation. - In this study, we employed a new mouse model of unilateral hindlimb immobilization that externally immobilizes both the knee and ankle joints in a highly convenient, stable, and safe manner (Figure 2-1A). With this method, we found that the mass of the five major muscles involved in ankle joint movement were significantly reduced after 7 days of immobilization (Figure 2-1B) (note: the animal body weight decreases slightly during the first 2 days of immobilization, Figure 2-2). Furthermore, with the SUnSET technique, we found that all of the muscles displayed a significant decrease in the amount of puromycin-labeled peptides during the course of immobilization which demonstrates that immobilization induced a decrease in the global rates of protein synthesis (Figure 2-1C). Combined, these results validate the effectiveness of our immobilization model and indicate that the decreases in muscle mass were due, at least in part, to a decrease in the rate of protein synthesis.

Previous studies have shown that the activation of mTOR signaling is necessary for the increases in protein synthesis and muscle mass that occur in response to elevated mechanical loading (30-35). Based on these reports, we hypothesized that mechanical unloading with immobilization would lead to a reduction in mTOR signaling and that this, in turn, would contribute to the immobilization-induced decreases in protein synthesis and muscle mass. However, in contrast to this hypothesis, we observed that mTOR signaling, as revealed by the phosphorylated to total ratio of $p70^{S6k}$ (T389), was elevated by immobilization (Figure 2-1D). Surprisingly, yet consistent with the role of mTOR in the regulation of

cap-dependent translation, we also found that immobilization induced an increase in cap-dependent translation in muscles that had been transfected with a dual-luciferase bicistronic reporter of cap-dependent translation (Figure 2-1E) (79). Therefore, these results indicate that immobilization induces a decrease in the global rate of protein synthesis via a mechanism that is independent of mTOR signaling and cap-dependent translation.

Previous studies have demonstrated that an increase in phosphatidylinositol 3-kinase (PI3K)/protein kinase B (PKB) activity can activate mTOR signaling by inhibiting the tuberous sclerosis complex (TSC) which converts active GTP-Rheb into inactive GDP-Rheb (81). Thus, in an effort to gain insight into mechanism through which immobilization activates mTOR signaling, we examined the phosphorylation status of PKB on the T308 residue as a marker of PI3K/PKB activity. As shown in Figure 2-1D, the results demonstrated that neither changes in the phosphorylated to total ratio of PKB (an index of PI3K activity) nor the total amount of phosphorylated PKB (a marker of total PKB activity) were correlated with the immobilization-induced activation of mTOR signaling. When combined, these results suggest that the immobilization-induced activation of mTOR signaling is mediated by a PI3K/PKB-independent mechanism.

Rapamycin exacerbates immobilization-induced decreases in protein synthesis and muscle mass. - Our observation that immobilization induces the activation of mTOR signaling was unexpected, but it was not entirely surprising because recent studies have shown that denervation of the sciatic nerve, which induces neurogenic atrophy, also results in the activation of mTOR signaling (82, 83). However, the functional role of mTOR activation in neurogenic atrophy is not entirely clear because, during denervation, the activation of mTOR signaling can not only increase protein synthesis, but it can also increase protein degradation through a negative feedback inhibition of the anti-catabolic PI3K/PKB signaling pathway (82-85). Thus, we set out to define the role that mTOR activation plays in immobilization-induced atrophy. To accomplish this, we first performed an experiment in which mice were treated with rapamycin during the period of immobilization. As shown in Figure 2-3A, rapamycin effectively inhibited the increase in $p70^{S6k}$ (T389) phosphorylation that was observed in the Extensor

Digitorum Longus (EDL) muscles after 3 and 7 days of immobilization. In these analyses, we also examined the phosphorylation status of the (S240/244) residues on the ribosomal S6 protein which are downstream substrates of $p70^{S6k}$ (86). As expected, immobilization induced an increase in S6 (S240/244) phosphorylation and rapamycin significantly reduced the phosphorylation of these sites. Moreover, we found that immobilization induced an increase in the total amount of the S6 protein and this event was completely inhibited by rapamycin. Finally, and most importantly, our results demonstrated that rapamycin exacerbates the reductions in muscle mass and fiber size that occurs after 7 days of immobilization (Figure 2-3, B-D).

As mentioned above, the activation of mTOR can increase the rates of protein synthesis and degradation, and thus, rapamycin could potentially inhibit mTOR-mediated increases in both protein synthesis and degradation during immobilization. Consistent with this suggestion, we found that rapamycin exacerbated the immobilization-induced decrease in the rates of protein synthesis at day 3 (Figure 2-3C). Furthermore, our results in Figure 2-1C revealed that after 7 days of immobilization, the rate of protein synthesis in EDL muscles rebounds to a level that is higher than that observed in control muscles and, as shown in Figure 2-3C, this effect was attenuated in mice that had been treated with rapamycin. However, in contrast to its clear effects on protein synthesis, rapamycin only slightly inhibited the immobilization-induced increase in global ubiquitination (a marker for protein degradation), and this effect was only present in muscles that had been subjected to 7 days of immobilization (Figure 2-3D). As shown in Figure 2-4, we also obtained similar results when examining mTOR signaling events, muscle mass, rates of protein synthesis, and global ubiquitination in Gastrocnemius muscles. Therefore, it can be firmly concluded that the immobilization-induced activation of mTOR signaling helps to prevent the loss of muscle mass and this effect is primarily driven through the anabolism-favoring effect of mTOR signaling.

In immobilized muscles, isometric contractions enhance mTOR signaling and rescue the decrease in protein synthesis via a rapamycin-sensitive mechanism. - Previous human studies have shown that electrically-evoked contractions can prevent disuse-induced reductions in the rate of protein

synthesis and muscle size (23, 24). Although the molecular mechanisms behind this effect are not known, current evidence suggests that the activation of mTOR signaling may be involved. For instance, previous studies have shown that the activation of mTOR signaling positively correlates with contraction-induced increases in the rate of protein synthesis and training-induced increases in muscle mass (87-89). Therefore, we reasoned that a further activation of mTOR signaling during immobilization, via electrically-evoked contractions, might alleviate the immobilization-induced decrease in protein synthesis. To test this, we treated control and 3 day immobilized mice with or without an acute bolus of rapamycin and then subjected the mice to a bout of isometric contractions or a sham condition (Figure 2-5A). As shown in Figure 2-5B, isometric contractions enhanced the level of mTOR signaling in immobilized muscles, and rapamycin abolished this effect. Moreover, in immobilized muscles, isometric contractions enhanced the rate of protein synthesis, and again, this effect was completely abolished by rapamycin (Figure 2-5C). Combined, these results indicate that isometric contractions can prevent the immobilization-induced decrease in protein synthesis and this effect is mediated by a rapamycin-sensitive / mTOR-dependent mechanism.

Next, we set out to identify the possible mechanisms that were responsible for the mTOR-dependent effect of isometric contractions on protein synthesis. While cap-dependent regulation of translation initiation (i.e. translational efficiency) is the best characterized downstream function of mTOR, mTOR can also regulate protein synthesis via changes in translational capacity (90). Hence, we first measured total RNA levels as a marker of translational capacity. The results of these analyses indicated that total RNA was not affected by isometric contractions (Figure 2-5D). Similar results were also obtained when we examined the levels of 28S+18S rRNA and the S6 ribosomal protein (Figure 2-5, B and E). Taken together, these results suggest that the mTOR-dependent effect of isometric contractions on protein synthesis is mediated through changes in translational efficiency.

In immobilized muscles, Rheb overexpression enhances mTOR signaling, cap-dependent translation, protein synthesis, and rescues the decrease in fiber size. - The results from Figure 2-5 suggest that, in immobilized muscles, the activation of mTOR signaling can induce an increase in the rate

of protein synthesis which may help to prevent disuse atrophy. To more directly investigate this possibility, we used overexpression of Rheb as a means for inducing the activation of mTOR signaling in immobilized muscles. As shown in Figure 2-6A, we confirmed that the overexpression of Rheb in immobilized muscles was sufficient to induce the activation of mTOR signaling as revealed by an increase in the T389 phosphorylation of cotransfected GST-p70. Furthermore, we determined that the overexpression of Rheb was sufficient to induce an increase in both cap-dependent translation and the global rate of protein synthesis (Figure 2-6, B and C). Finally, and most significantly, we demonstrated that the overexpression of Rheb robustly increased the size of fibers and prevented the atrophy that occurred during immobilization (Figure 2-6D). Combined, these results indicate that the forced activation of mTOR signaling during immobilization can prevent disuse atrophy, at least in part, by promoting an increase in protein synthesis via enhanced cap-dependent translation.

eIF4F formation is enhanced by immobilization in a rapamycin-sensitive manner, but not further enhanced by isometric contractions. - To gain insight into molecular mechanisms through which the activation of mTOR signaling promotes cap-dependent translation / protein synthesis during immobilization, we first examined the effects of immobilization on the association of eIF4E with 4E-BP1 and eIF4G. As described in the introduction, mTOR-dependent increases in 4E-BP1 phosphorylation can lead to the dissociation of 4E-BP1 from eIF4E while simultaneously enhancing the association of eIF4E with eIF4G (i.e., the formation of eIF4F complex which is critical for the cap-dependent initiation of translation). Consistent with these mechanisms, we found that immobilization induced a decrease in the ratio of 4E-BP1:eIF4E and an increase in the ratio of eIF4G:eIF4E, and that these events were sensitive to the inhibitory effects of rapamycin (compare 1st, 3rd, and 5th bars from the left in Figure 2-7, A and B). Interestingly, the immobilization-induced increase in eIF4F formation did not appear to be entirely inhibited by rapamycin and this effect might be explained by our observation of a rapamycin-insensitive increase in the S209 phosphorylation of eIF4E which can stabilize the eIF4F complex (Figure 2-7C) (91). In either case, our results suggest that an mTOR-dependent increase in the formation of the eIF4F

complex contributes to the increase in cap-dependent translation, and thereby, an alleviation of the decrease in protein synthesis that occurs during immobilization.

Next, we examined the effects of isometric contractions on the association of eIF4E with 4E-BP1 and eIF4G. Unexpectedly, the results revealed that neither the ratio of 4E-BP1:eIF4E nor the ratio of eIF4G:eIF4E was altered by isometric contractions in immobilized muscles (compare 3rd and 4th bars from the left in Figure 2-7, A and B). Therefore, we examined another rapamycin-sensitive regulatory event in protein synthesis which involves the eukaryotic elongation factor 2 (eEF2). eEF2 is a GTP-binding translation elongation factor that loses its ability to bind to the ribosome (i.e., inactivation) when phosphorylated on the T56 residue by eEF2 kinase (eEF2K) (92). Importantly, the activity of eEF2K can be negatively regulated by mTOR (93). Hence, the activation of mTOR should lead to an increase in the amount of T56-non-phosphorylated eEF2 and, in-turn, an increase in the rate of protein synthesis. As shown in Figure 2-7C, we found that isometric contractions led to a decrease in the amount of T56-phosphorylated eEF2 along with an increase in the amount of total eEF2. Thus, these results indicate that isometric contractions promote an increase in the amount of T56-non-phosphorylated eEF2; however, this effect was not inhibited by rapamycin (Figure 2-7C). When taken together, our results suggest that, in immobilized muscles, the isometric contraction-induced increase in protein synthesis is mediated through a unique rapamycin-sensitive / mTOR-dependent mechanism that does not involve changes in eIF4F formation or eEF2 activity.

Immobilization induces fiber type-dependent decreases in protein synthesis and fiber size that are not associated with the level of mTOR activity. - We have previously shown that the regulation of fiber size in response to mechanical overload and food deprivation varies among different fiber types, and that this variation is associated with similar fiber type-dependent alterations in the rate of protein synthesis and mTOR activity as revealed by S6 (S240/244) phosphorylation (94). Furthermore, in Figure 2-3D, immobilization appeared to preferentially reduce the size of larger fibers. Hence, we wondered if changes in fiber size and protein synthesis during immobilization are also fiber type-dependent, and if these changes are associated with similar alterations in the level of mTOR signaling.

Specifically, we hypothesized that the magnitude of any fiber type-dependent decreases in protein synthesis would be inversely correlated with the magnitude of mTOR activation. As shown in Figure 2-8B, we first determined that immobilization decreases the size of fibers in EDL muscles with the following fiber type-dependent order: $1 \leq 2A < 2X = 2B$. Interestingly, it was also found that immobilization decreases the rates of protein synthesis in a similar fiber type-dependent fashion with type $1 < 2A < 2X < 2B$ (Figure 2-8C) (note: similar results were also observed in TA muscles, data not shown). On the other hand, we were not able to detect an inverse correlation between the fiber type-dependent regulation of protein synthesis and the level of mTOR signaling as revealed by S6 (S240/244) phosphorylation (Figure 2-8D). Therefore, these results suggest that; 1) the regulation of protein synthesis during immobilization largely influences the extent of disuse atrophy, and 2) the fiber type-dependent decreases in the rate of protein synthesis are not mediated through fiber-type-dependent differences in the regulation of mTOR signaling.

Discussion

The maintenance of skeletal muscle mass contributes significantly to health and issues associated with the quality of life. However, many primary conditions necessitate the immobilization of body parts which results in mechanical unloading. During mechanical unloading, skeletal muscles undergo rapid disuse atrophy and this occurs primarily through a decrease in the rate of protein synthesis (73, 95). Hence, defining how mechanical unloading impairs protein synthesis and induces atrophy has remained a long-standing question. Accordingly, several hypotheses have been proposed to explain this phenomenon, and one that has received a large amount of interest suggests that a decrease in anabolic mTOR signaling may be involved (72, 96). Indeed, previous animal studies have shown that various forms of mechanical unloading, such as hindlimb immobilization and hindlimb suspension, can induce decreases in mTOR signaling and protein synthesis (96-98). Yet, several human studies with immobilization have casted doubt on this hypothesis because they observed decreases in the rates of protein synthesis and muscle mass in the absence of changes in mTOR signaling (70, 99). Thus, it appears that, at least in humans, an

mTOR-independent pathway plays a predominant role in the regulation of protein synthesis and muscle mass during mechanical unloading. In this study, we provide several lines of evidence that support this possibility by identifying that: 1) immobilization decreases the rate of protein synthesis and muscle mass while simultaneously increasing mTOR activity, and 2) the activation of mTOR via Rheb overexpression can robustly increase the size of fibers in immobilized muscles, but Rheb-overexpressing fibers still undergo immobilization-induced atrophy to almost the same extent as GFP-overexpressing and non-transfected fibers. This latter observation is particularly noteworthy because it strongly suggests that the mechanism through which immobilization reduces muscle size is primarily mediated by a pathway that negatively affects the balance between protein synthesis and degradation in a manner that is parallel to the mTOR signaling pathway.

To date, the identity of the mTOR-independent pathway that drives mechanical unloading-induced declines in protein synthesis and / or muscle mass remains unknown; however, our observation that immobilization induces fiber type-dependent decreases in the rates of protein synthesis and fiber size may provide some clues. For example, it has been demonstrated that more oxidative fiber types have higher levels of peroxisome proliferator-activated receptor γ coactivator 1α (PGC1α) than glycolytic fiber types, and that overexpression of PGC1α inhibits the expression of atrophy-related genes as well as denervation- and fasting-induced muscle atrophy (100-102). Hence, in our study, it is possible that lower levels of PGC1α expression in type 2X and 2B fibers may have rendered these fiber types more susceptible to the immobilization-induced atrophy than type 1 and 2A fibers. Likewise, it is tempting to speculate that decreases in PGC1α expression during mechanical unloading may drive the mTOR-independent atrophic response. Indeed, it has been found that the expression of PGC1α is dramatically reduced in response to immobilization and denervation (102, 103). Therefore, examining molecules that are associated with fiber type-specific expression, such as PGC1α, might be worthy of further investigation for studies that are aimed at identifying the mTOR-independent pathway.

As described above, several lines of evidence indicate that reduced mTOR signaling is not necessary for immobilization-induced decreases in protein synthesis and muscle mass. However, previous

studies have also suggested that enhanced mTOR signaling can mitigate the negative effects of mechanical unloading. For example, it has been shown that the administration of clenbuterol, a β2 adrenergic agonist that activates PKB/mTOR signaling, can alleviate hindlimb suspension-induced losses in muscle mass and that this effect is mediated through a rapamycin-sensitive mechanism (104). Recent studies have also shown that the administration of tomatidine and capsaicin, natural small molecules that stimulate mTOR signaling, can increase muscle mass in immobilized and hindlimb suspended muscles, respectively (105, 106). Finally, the knockdown of Deptor expression, an endogenous inhibitor of both mTORC1 and mTORC2, has been shown to increase the rates of protein synthesis and muscle mass in immobilized muscles (107). The results of our study are in agreement with these findings and provide further support for, and additional mechanistic insight into, the positive role that mTOR signaling can play. Specifically, we have provided evidence which indicates that the immobilization-induced activation of mTOR promotes an increase in eIF4F formation and cap-dependent translation, and that these events, in turn, help to alleviate immobilization-induced decreases in protein synthesis and muscle mass. We have also demonstrated that the positive effects of mTOR signaling can be enhanced when mTOR is further activated by isometric contractions or the overexpression of Rheb. In other words, our results clearly illustrate that the activation of mTOR signaling should be considered as a viable target for therapies that are aimed at preserving muscle mass during periods of mechanical unloading.

The above results clearly demonstrate that the activation of mTOR signaling can positively regulate protein synthesis and muscle mass during mechanical unloading; however, as mentioned in the results, the activation of mTOR can also promote protein degradation through multiple mechanisms (84, 85, 108). Indeed, a recent study showed that the activation of mTOR signaling that occurs during denervation strongly contributed to the increase in catabolic signaling events such as global ubiquitination, whereas its contribution to the increase in anabolic signaling events was relatively small (83). Consistent with the catabolism-favoring effect of mTOR signaling, this study also showed that the denervation-induced activation of mTOR signaling exacerbated the atrophic response (i.e., neurogenic atrophy). Despite this potential role of mTOR activation in promoting protein degradation, our results demonstrated that the

immobilization-induced activation of mTOR signaling contributes only marginally, if any, to the increase in catabolic pathway as opposed to its strong anabolic effect on protein synthesis. Therefore, we have concluded that the anti-atrophic effect of mTOR activation in immobilized muscles is primarily driven through the anabolism-favoring effect of mTOR signaling. It is not known what factors determine whether the activation of mTOR will favor anabolism or catabolism; however, given the importance of its final outcome, investigating the switch factors will be an interesting subject for future studies.

In summary, the results from this study demonstrate that; 1) the activation of mTOR signaling that occurs during immobilization helps to alleviate the immobilization-induced decreases in protein synthesis and muscle mass, and 2) the positive effects of mTOR signaling can be enhanced when mTOR is further activated by stimuli such as isometric contractions or the overexpression of Rheb. Therefore, we conclude that the activation of mTOR signaling positively regulates protein synthesis and muscle mass during immobilization. Furthermore, our findings highlight that the activation of mTOR signaling should be considered as a viable target for therapies that are aimed at preventing atrophy during periods of mechanical unloading. In the future, it will be important to define how mTOR signaling is activated during immobilization and how immobilization elicits the mTOR-independent, but fiber type-dependent, decreases in protein synthesis and muscle size. The resulting knowledge from such investigations should further advance our understanding of the mechanisms through which mechanical unloading regulate muscle mass and may facilitate the development of new therapies for preventing disuse atrophy.

Methods

Materials. - Rapamycin was purchased from LC laboratories (Woburn, MA) and dissolved in DMSO to generate a 5 mg/ml stock solution. Puromycin was purchased from Calbiochem (EMD Millipore, Billerica, MA) and dissolved in diH_2O to generate a 75 mM stock solution. Rabbit anti-$p70^{S6k}$, anti-PKB, anti-phospho-PKB (T308), anti-phospho-S6 (S240/244), anti-S6, anti-4E-BP1, anti-eIF4G, anti-eIF4E, anti-phospho-eIF4E (S209), anti-eEF2, anti-phospho-eEF2 (Thr-56), and anti-GFP antibodies were purchased from Cell Signaling (Danvers, MA). Rabbit anti-phospho $p70^{S6k}$ (T389), and mouse anti-

Ubiquitin antibodies were purchased from Santa Cruz Biotechnologies (Santa Cruz, CA). Rabbit anti-laminin antibody was purchased from Sigma Aldrich. Mouse anti-Rheb antibody was purchased from Abnova (Taipei, Taiwan). Mouse anti-eIF4E and mouse anti-puromycin antibodies were obtained from Dr. Scot Kimball (Pennsylvania State University, PA) and Dr. Philippe Pierre (Centre d'Immunologie de Marseille-Luminy, France), respectively. Mouse control IgG1 antibody was purchased from BioLegend (San Diego, CA). Mouse IgG1 anti-type 2A MHC, mouse IgM anti-type 2B MHC, and mouse IgM anti-type 2X MHC antibodies were purchased from the Developmental Studies Hybridoma Bank (Ames, IA). HRP-conjugated anti-rabbit IgG and HRP-conjugated anti-mouse IgG antibodies were purchased from Vector Laboratories (Burlingame, CA). HRP-conjugated anti-mouse IgG Fc 2a, anti-mouse IgG Fab, DyLight 594-conjugated anti-mouse IgG Fc 2a, Alexa 488-conjugated anti-mouse IgG1, AMCA-conjugated anti-mouse IgM antibodies, and normal goat serum were purchased from Jackson ImmunoResearch Laboratories Inc. (West Grove, PA). Alexa 350-conjugated anti-rabbit IgG antibody was purchased from Invitrogen (Carlsbad, CA).

Plasmid constructs. - pEGFP-C3 (GFP) was purchased from Clontech (Mountain View, CA). GFP-tagged Rheb (GFP-Rheb) was generated by replacing the YFP-tag from YFP-Rheb (109) with the GFP tag from the pEGFP-C3. pRK5-myc-$p70^{S6k}$-glutathione transferase (GST-$p70^{S6k}$) was provided by Dr. Karyn Esser (University of Kentucky, Lexington, KY). The dual-luciferase bicistronic reporter of cap-dependent translation has been previously described (110) and was obtained from Dr. Sunnie Thompson (University of Alabama, Birmingham, AL). All plasmid DNA was grown in DH5α Escherichia coli, purified with an EndoFree plasmid kit (QIAGEN, Valencia, CA), and re-suspended in sterile PBS.

Animals. - Eight- to ten-week-old female FVB/N mice (Jackson Laboratories, Bar Harbor, MA) were used for all experiments. The mice were fed ad libitum in a room maintained at 25°C with a 12-hour:12-hour light:dark cycle, and anaesthetized with an intraperitoneal (IP) injection of ketamine (100 mg/kg) plus xylazine (10 mg/kg) immediately prior to experimental procedures. In the case of isometric contractions, the mice were anaesthetized through inhalation of 1-5 % isoflurane in O_2. At the end of the

experimental procedures, muscles were collected and then the mice were euthanized by cervical dislocation under anesthesia. All animal experiments followed protocols approved by the Institutional Animal Care and Use Committee of the University of Wisconsin-Madison (# V01324).

Immobilization (Figure 2-1A). - To make a splint, a capless 1.5 ml microfuge tube was cut along its short-axis (at 1.2 cm from opening) and the upper cylindrical part was attached to one end of a 3.7 cm-long cut metal paperclip (ACC72585, ACCO Brands, Inc., Lincolnshire, IL) by wrapping them together with the adhesive side of 5 x 1.1 cm Velcro loop (Velcro 90198, Velcro USA, Inc., Manchester, NH) (Step 1). Then, the other end of the cut paperclip was wrapped with the adhesive side of 3 x 1.5 cm Velcro loop to enclose the open paperclip region and was used to secure the dorsum of the mouse foot which will directly contact with the fabric side of the Velcro loop (Step 2). Unilateral mouse hindlimb immobilization was then performed by inserting the right hindlimb into the cylindrical part of the splint and then wrapping the hindfoot and the enclosed end of the paperclip together with another 3 x 1.5 cm Velcro loop tape (Step 3). The immobilized limbs were maintained with the knee in an extended and the ankle in a plantar-flexed position for 3 or 7 days. Hindlimb muscles from mice that were not placed in the splint served as controls.

Isometric contractions. - Unilateral isometric contractions of the dorsiflexor muscles, such as EDL, were performed by stimulating the sciatic nerve of the right hindlimb which was maintained in a full plantar-flexed position throughout the stimulation period. The surgical procedures and the pattern of stimulation were performed as previously described (56). In brief, the sciatic nerve of the right hindlimb was exposed with a small incision and stimulated with 100 Hz, 3–7 V pulses though electrodes that connected the sciatic nerve with a SD9E Grass stimulator (Grass Instruments, Quincy, MA, USA). Each resulting contraction was sustained for 3 seconds and was followed by a 10 seconds rest period. This pattern of stimulation was repeated for a total of 10 sets of six repetitions with a 1 minute rest period between each set. Sham-treated contralateral muscles and sham-treated immobilized muscles served as controls for stimulated muscles in non-immobilized and immobilized animals, respectively.

Skeletal muscle transfection. - Mouse Tibialis Anterior (TA) muscles were transfected by electroporation as previously described (109). In brief, a small incision was made through the skin covering the TA muscle. A total of 30 μg of plasmid DNA solution containing GFP or GFP-Rheb was then injected into proximal and distal ends (6 μl per injection) of the muscle belly with a 27-gauge needle. In some cases (e.g., cotransfections), the DNA solution also contained 2 μg of GST-$p70^{S6k}$ plasmid DNA. After the injections, 2 stainless steel pin electrodes (1-cm gap) connected to an ECM 830 electroporation unit (BTX/Harvard Apparatus, Holliston, MA) were laid on top of the proximal and distal myotendinous junctions. Then, eight 20 ms square-wave electric pulses were delivered onto the muscle at a frequency of 1 Hz with a field strength of 160 V/cm. Following the electroporation procedure, the incisions were closed with Vetbond surgical glue and the animals were allowed to recover for 3 or 7 days.

Rapamycin and Puromycin injections. - Rapamycin solution was prepared by diluting the appropriate volume of the stock solution needed to inject mice with 1.5 mg/kg body weight in 200 μl of PBS, and subsequently administered into the animals via IP injection. Mice that were injected with an equivalent amount of DMSO diluted in 200 μl of PBS served as vehicle controls. For acute administration, these injections were made at 4 hours prior to muscle collection. For chronic administration, the injections were made immediately after the immobilization procedure and repeated every 24 hours for 7 days. For all *in vivo* measurements of protein synthesis with surface sensing of translation (SUnSET) (80), puromycin solution was prepared by diluting the appropriate volume of the stock solution that was needed to inject mice with 0.04 μmol/g body weight in 200 μl of PBS, and subsequently administered into the animals via IP injection at exactly 30 minutes prior to muscle collection.

Sample preparation for Immunoprecipitation and Western blot analysis. - Upon collection, Plantaris, Gastrocnemius, Soleus, EDL and TA muscles were immediately frozen in liquid nitrogen and then stored at - 80°C. The frozen muscles were then homogenized with a Polytron in ice-cold buffer A [40 mM Tris (pH 7.5), 1 mM EDTA, 5 mM EGTA, 0.5% Triton X-100, 25 mM β-glycerolphosphate, 25 mM NaF, 1 mM Na_3VO_4, 10 μg/ml leupeptin, and 1 mM PMSF] and a portion of the whole homogenates were used for Western blot analysis as described below. The remaining portion of the whole homogenates

was pre-cleared by centrifugation at 10,000 g for 10 minutes and the supernatants were used for immunoprecipitation as described below. The protein concentration in the whole homogenates and supernatants was determined with a DC protein assay kit (Bio-Rad, Hercules, CA).

Immunoprecipitation of eIF4E. - Equal amounts of protein from each sample were diluted to the same volume with fresh ice-cold buffer A and then incubated with either mouse anti-eIF4E (1:10) or mouse control IgG antibody for 3 hours at 4°C. During this incubation, Protein A agarose beads (Santa Cruz Biotechnologies, Santa Cruz, CA) were blocked with 1% BSA in PBS for 1 hour at 4°C and then washed 3 times with PBS. The antibody-containing samples were then incubated with 20 µl of the blocked beads at 4°C for 3 hours. Following the incubation, the beads were pelleted by centrifugation at 500 g for 30 seconds and washed 4 times with fresh ice-cold buffer A. After the washes, the beads were boiled in 1x Laemmli buffer for 5 minutes and pelleted again. The supernatants were subjected to Western blot analysis as described below.

Western blot analysis. - Equal amounts of protein from each sample were boiled in 2x Laemmli buffer and subjected to SDS-PAGE, transfer, blocking, and primary and secondary antibody incubations as previously described (111). The resulting membranes were then developed on film or with a Chemi410 camera mounted to a UVP Autochemi system (UVP, Upland, CA) by using regular ECL (Pierce, Rockford, IL) or ECL Prime (GE healthcare, Piscataway, NJ). Once the appropriate image was captured, the membranes were stained with Coomassie Blue to verify equal loading throughout all lanes. Densitometric measurements of each blot were carried out using ImageJ (NIH).

Analysis of cap-dependent translation. - TA muscles were cotransfected with 30 µg of plasmid DNA encoding either GFP or GFP-Rheb and 5 µg of plasmid DNA encoding a dual-luciferase bicistronic reporter of cap-dependent translation. Collected muscles were homogenized with a Polytron in passive lysis buffer (Promega, Madison, WI), and Renilla and firefly luciferase activities were measured with a FLUOstar Optima luminometer (BMG Labtech, Durham, NC) by using the Dual-Luciferase Reporter Assay kit (Promega) as described in the manufacturer's instructions. Renilla luciferase activity was normalized to the firefly luciferase activity in the same sample.

Immunohistochemical analysis of cross-sectional area (CSA), protein synthesis, and S6 phosphorylation. - Upon collection, muscles from control and immobilized animals were submerged individually (for Figure 2-7), or adjacent to one another (for Figure 2-8), in optimal cutting temperature (OCT) compound (Tissue-Tek; Sakura, Torrance, CA) at resting length, and frozen in liquid nitrogen-chilled isopentane. Cross sections (10 μm thick) from the mid-belly of the muscles were obtained with a cryostat and fixed in acetone for 10 minutes at -30°C. For experiments that included GFP-transfected muscles, sections were fixed in acetone containing 8% methanol and 2% paraformaldehyde for the first 1 minute of the total 10 minute fixation period. The sections were then warmed to room temperature for 5 minutes and rehydrated by incubating in PBS for 15 minutes. The rehydrated sections were then incubated for 1 hour in solution A (PBS containing 0.5% BSA and 0.5% Triton X-100) containing either anti-mouse IgG Fab (1:10, for analysis of puromycin-labeled peptides), normal goat serum (1:20, for analyses of P- and T-S6), or none of them (for all conditions not stated above). The sections were then washed with PBS and probed with the indicated primary antibodies dissolved in solution A for 1 hour at room temperature. After washing with PBS, the sections were incubated with the appropriate fluorophore-conjugated secondary antibodies dissolved in solution A for 1 hour at room temperature. After a final washing with PBS, grayscale signals from each secondary antibody were captured with a DS-QiMc camera mounted on an 80i epi-fluorescence microscope (both from Nikon, Tokyo, Japan), and the resulting monochrome images were merged with NIS-Elements D image analysis software (Nikon). CSA and signal intensities were then measured by tracing the periphery of randomly selected fibers in each muscle section. All analyses were performed by investigators that were blinded to the sample identification.

Analysis of total and ribosomal RNA - Frozen muscles were homogenized with an RNAse-free pestle in ice-cold TRIzol (Ambion, Life Technologies,Grand Island, NY) and total RNA was isolated with a PureLink RNA Mini Kit (Ambion) according to manufacturer's instructions. The concentration of isolated RNA was determined with a NanoDrop 2000 spectrometer (Thermo Scientific, Wilmington, DE) and the amount of total RNA was calculated by multiplying the RNA concentration by the total volume of

RNA solution. This value was divided by the muscle weight to obtain µg of total RNA per mg muscle. RNA samples from equivalent amounts of muscle mass were also run on 1% agarose gels to check RNA integrity and measure the ribosomal RNA (rRNA) content. Densitometric measurements of the 28S and 18S rRNA were performed with ImageJ.

Statistical analysis. - All values are expressed as the means (+ s.e.m. in graphs). Statistical significance was determined by using the student's t-test (2-tailed, unpaired) or ANOVA (one-way or two-way) followed by post hoc analysis. Differences between groups were considered significant when $P \leq 0.05$. All statistical analyses were performed on SigmaStat software (San Jose, CA).

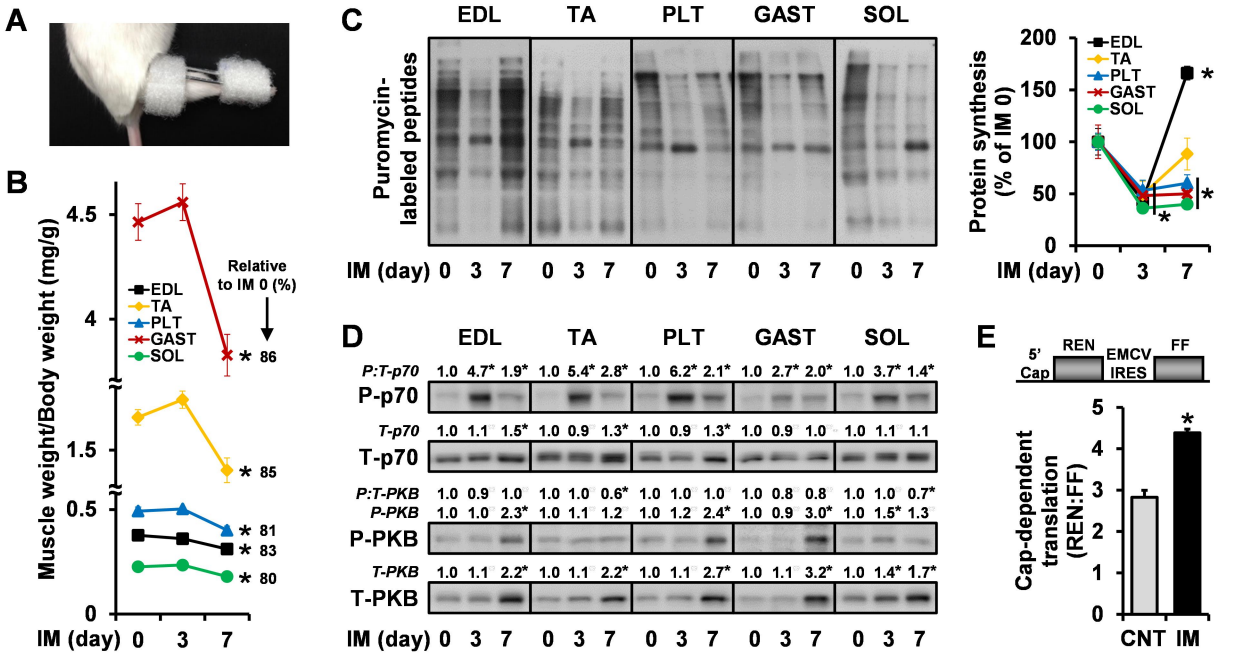

Figure 2-1. Immobilization decreases the global rates of protein synthesis and muscle mass, but activates mTOR signaling and cap-dependent translation. (**A**) Representative image of the caudal end of a mouse that was subjected to unilateral hindlimb immobilization (IM). (**B-D**) Mice were subjected to IM for 3 or 7 days, or a non-immobilized control condition (IM 0), and injected with puromycin at 30 minutes prior to muscle collection for the measurement of protein synthesis by SUnSET. Various lower hindlimb muscles (EDL, extensor digitorum longus; TA, tibialis anterior; PLT, plantaris; GAST, gastrocnemius; SOL, soleus) were weighed to obtain (**B**) the muscle weight to body weight ratio, and then subjected to Western blot analysis for (**C**) puromycin-labeled peptides, (**D**) phosphorylated (P) (T389) and total (T) p70, and P (T308)- and T-PKB. The total amount of puromycin-labeled peptides (i.e., protein synthesis), T-p70, P-PKB, T-PKB, and P:T ratios of p70 and PKB were expressed relative to the values obtained in the muscle-matched IM 0 control groups. (**E**) Mouse TA muscles were cotransfected with GFP, and a dual-luciferase bicistronic reporter of cap-dependent translation, and immediately subjected to IM or the non-immobilized control condition (CNT). At 3 days post transfection, the muscles were collected and luciferase activities produced by cap-dependent translation of *Renilla* luciferase (REN) and cap-independent translation of firefly luciferase (FF) were measured to obtain the REN:FF ratio. All values are presented as the mean (+ s.e.m. in graphs, n = 3-8 muscles per group). * versus the muscle-matched control groups, $P \leq 0.05$.

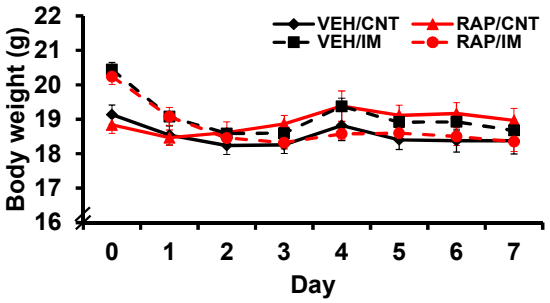

Figure 2-2. Time course for changes in body weight during immobilization. Mice were subjected to unilateral hindlimb immobilization for 7 days (IM), or a non-immobilized control condition (CNT), and received a daily administration of rapamycin (RAP, 1.5mg/kg body weight) or the vehicle (VEH). Note: subsequent CSA analyses needed to be performed on samples from animals that had similar final body weights, therefore, the initial animal body weights in the IM groups were intentionally made higher than that in CNT groups.

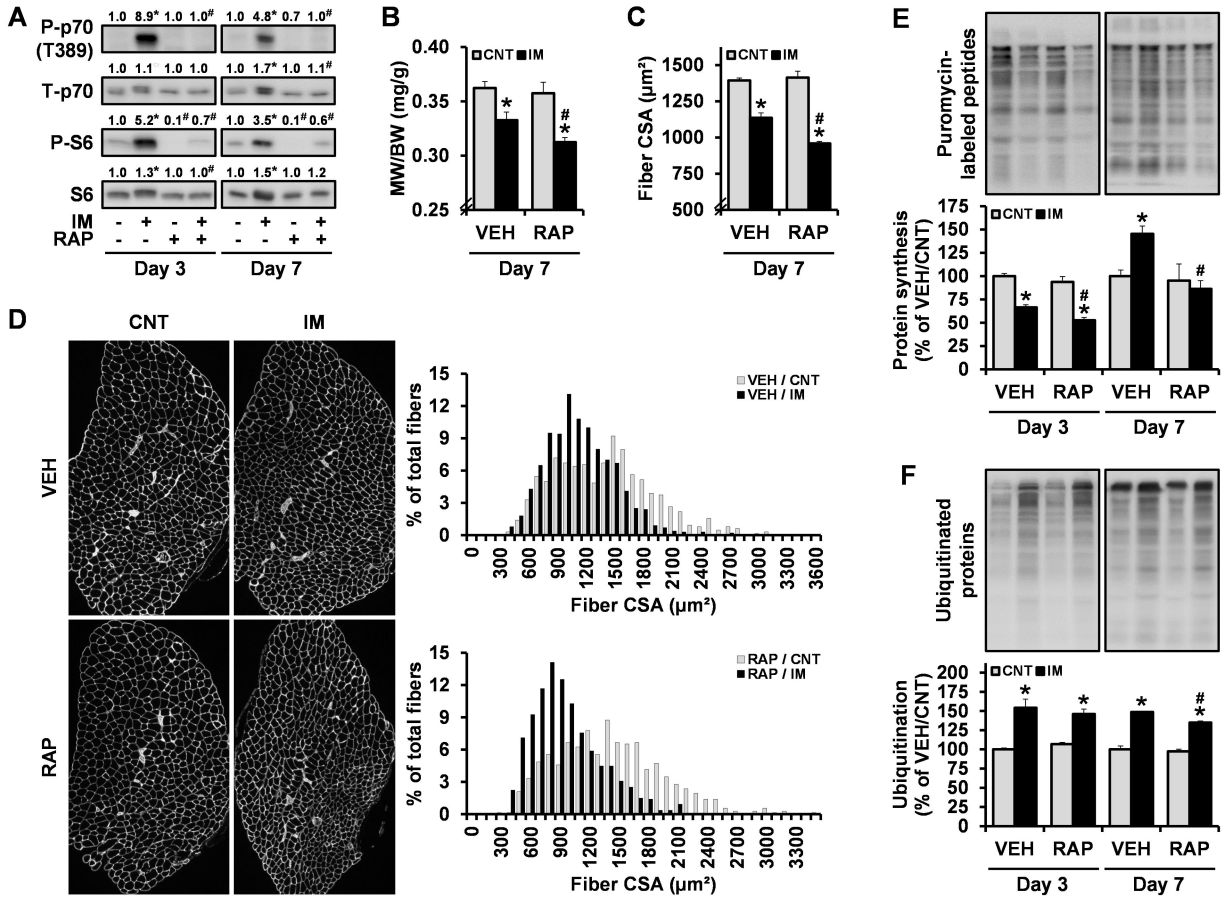

Figure 2-3. Rapamycin exacerbates IM-induced decreases in protein synthesis and muscle mass. Mice were subjected to unilateral hindlimb immobilization for 3 or 7 days (IM+), or a non-immobilized control condition (IM- or CNT), and received an acute (day 3) or chronic (day 7) administration of rapamycin (RAP+) or the vehicle (RAP- or VEH) as described in the Methods. At 30 minutes prior to the collection of the EDL muscles, mice were injected with puromycin. The muscles were (**A**) subjected to Western blot analysis for phosphorylated (P) (T389) and total (T) p70 and P (S240/244)- and T-S6, (**B**) analyzed for the muscle weight (MW) to body weight (BW) ratio, (**C,D**) subjected to immunohistochemistry for laminin to obtain the cross sectional area (CSA) (≥120 fibers per muscle), or (**E,F**) subjected to Western blot analysis for puromycin-labeled peptides (i.e., protein synthesis) and ubiquitinated proteins, respectively. The values in A, E and F were expressed relative to the values obtained in the time-matched IM-/RAP- (A), or CNT/VEH groups (E,F). All values are presented as the mean (+ s.e.m. in graphs, n = 3-12 muscles per group). * versus the time- and drug-matched IM- or CNT groups, # versus the time- and mobility-matched RAP- or VEH groups, $P \leq 0.05$.

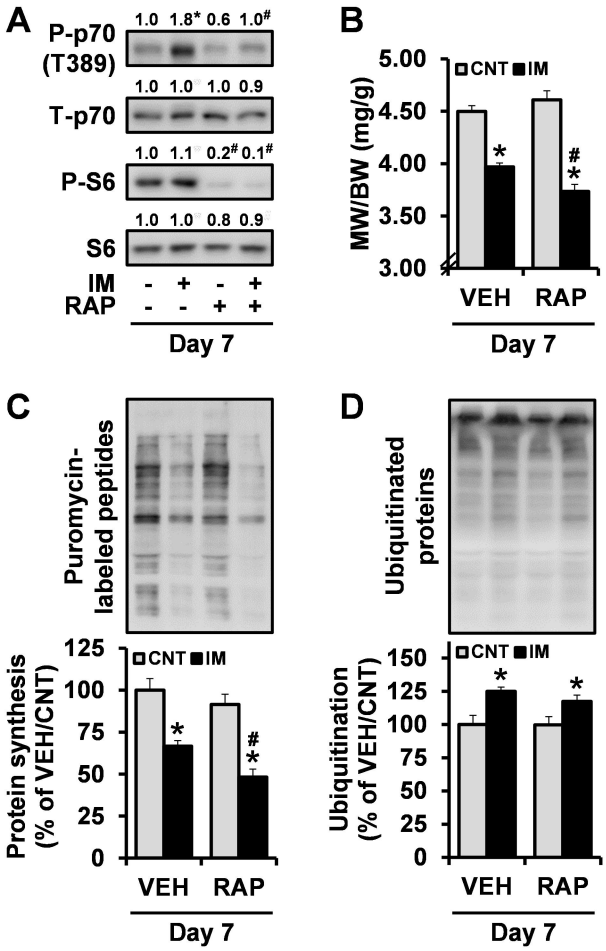

Figure 2-4. Rapamycin exacerbates immobilization-induced decreases in protein synthesis and muscle mass. Mice were subjected to unilateral hindlimb immobilization for 7 days (IM+), or a non-immobilized control condition (IM- or CNT), and received a daily administration of rapamycin (RAP+, 1.5mg/kg body weight) or the vehicle (RAP- or VEH). At 30 minutes prior to the collection of the Gastrocnemius muscles, mice were injected with puromycin. The muscles were (**A**) subjected to Western blot analysis for phosphorylated (P) (T389) and total (T) p70 and P (S240/244)- and T-S6, (**B**) analyzed for the muscle weight (MW) to body weight (BW) ratio, or (**C,D**) subjected to Western blot analysis for puromycin-labeled peptides (i.e., protein synthesis) and ubiquitinated proteins, respectively. The values in A, C and D were expressed relative to the values obtained in the time-matched IM-/RAP- (A), or CNT/VEH groups (C,D). All values are presented as the mean (+ s.e.m. in graphs, n = 4-8 muscles per group). * versus the time- and drug-matched IM- or CNT groups, # versus the time- and mobility-matched RAP- or VEH groups, $P \leq 0.05$.

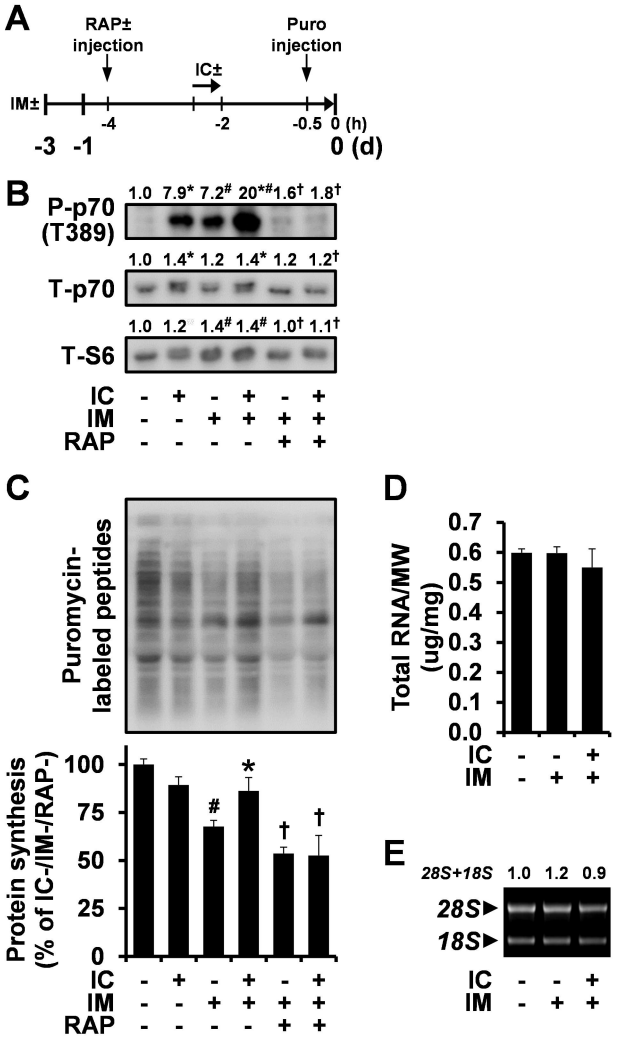

Figure 2-5. In immobilized muscles, isometric contractions enhance mTOR signaling and rescue the decrease in protein synthesis via a rapamycin-sensitive mechanism. (**A-C**) Mice were subjected to unilateral hindlimb immobilization for 3 days (IM+), or a non-immobilized control condition (IM-), and then injected with rapamycin (RAP+) or the vehicle (RAP-) and puromycin (puro) at the indicated time points. Following the RAP-/+ injections, mice were subjected to a bout of isometric contractions (IC+) or the sham condition (IC-). Upon collection, EDL muscles were subjected to Western blot analysis for (**B**) phosphorylated (P) and total (T) p70, T-S6, and (**C**) puromycin-labeled peptides (i.e., protein synthesis). (**D**,**E**) Mice were treated as in (A) except for the injections, and the EDL muscles were analyzed for (**D**) total RNA to muscle weight (MW) ratio and (**E**) 28S+18S rRNA content. The amount of P-p70, T-p70, puromycin-labeled peptides, and 28S+18S rRNA was expressed relative to the values obtained in the IC-/IM-/RAP- groups. All values are presented as the mean (+ s.e.m. in graphs, n = 3-6 muscles per group). * versus the drug- and mobility-matched IC- groups, # versus the contraction-matched IM-/RAP- groups, † versus the contraction-matched IM+/RAP- groups, $P \leq 0.05$.

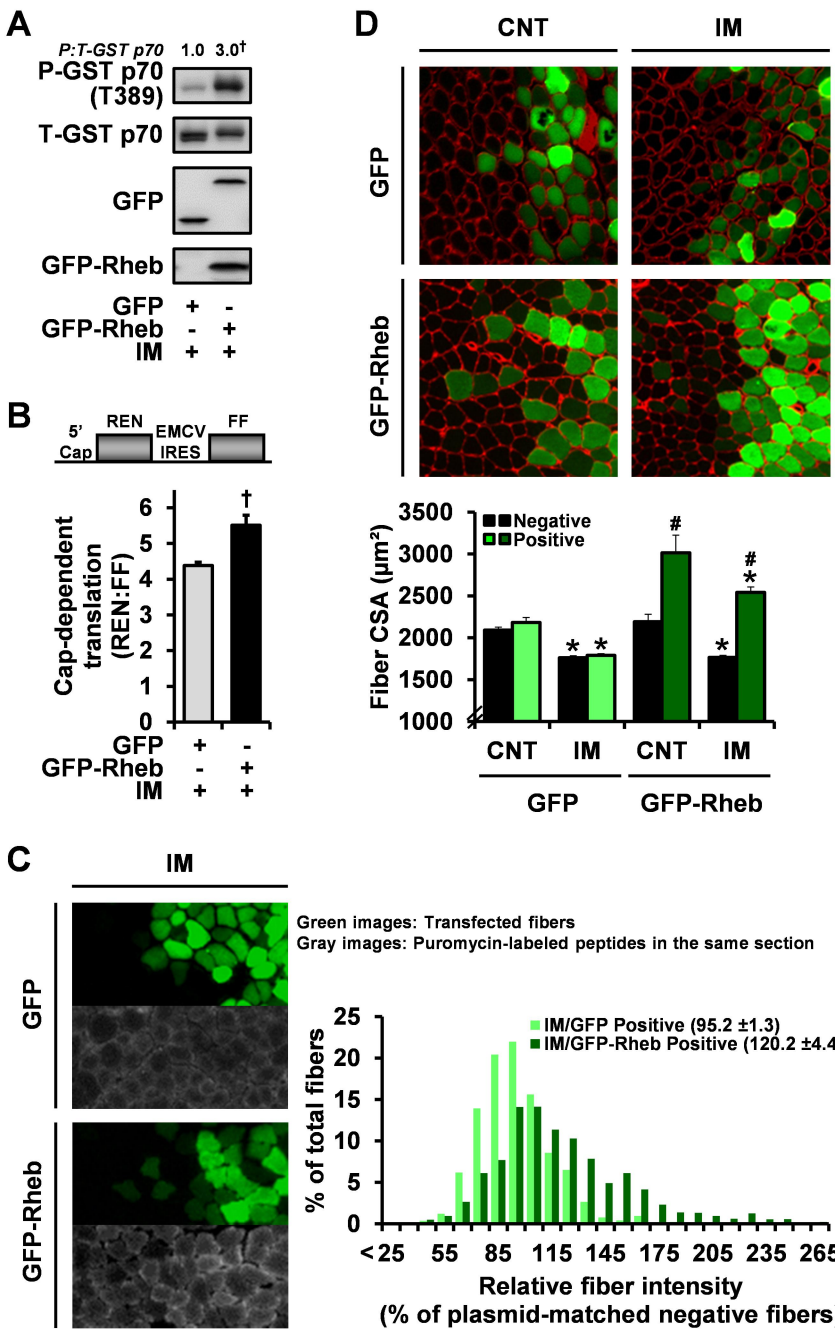

Figure 2-6. In immobilized muscles, Rheb overexpression enhances mTOR signaling, cap-dependent translation, protein synthesis, and rescues the decrease in fiber size. (**A**) Mouse TA muscles were cotransfected with GST-p70 and GFP or GFP-Rheb, and immediately subjected to unilateral hindlimb immobilization (IM). After 3 days, the muscles were collected and subjected to Western blot analysis for phosphorylated (P) and total (T) GST-p70, GFP, and GFP-Rheb. The P:T ratio for GST-p70 was expressed relative to the values obtained in GFP (control) group. (**B**) Mouse TA muscles were cotransfected with a dual-luciferase bicistronic reporter of cap-dependent translation and GFP or GFP-Rheb, and immediately subjected to IM. At 3 days post transfection, the muscles were collected and luciferase activities produced by cap-dependent translation of *Renilla* luciferase (REN) and cap-independent translation of firefly luciferase (FF) were measured to obtain REN:FF ratio. (**C**) Mouse TA muscles were transfected with GFP or GFP-Rheb, and immediately subjected to IM. After 3 days, the mice were injected with puromycin as in Figure 2-1 and the muscles were subjected to immunohistochemistry for GFP and puromycin-labeled peptides. The puromycin staining intensity in transfected (Positive) fibers was expressed relative to the value obtained in non-transfected fibers from the same section and plotted on histograms (≥160 fibers per muscle). (**D**) Mouse TA muscles were transfected with GFP or GFP-Rheb, and immediately subjected to IM or a non-immobilized control condition (CNT). After 7 days, the muscles were collected and subjected to immunohistochemistry for GFP and laminin to obtain the cross sectional area (CSA) of the transfected (Positive) and non-transfected (Negative) fibers within each muscle (≥100 fibers per muscle). All values are presented as the mean (+ s.e.m. in graphs, n = 3-4 muscles per group). † versus GFP groups, * versus the plasmid- and transfection-matched CNT groups, # versus the mobility-matched GFP-Rheb Negative groups as well as the mobility-matched GFP Positive groups, , $P \leq 0.05$.

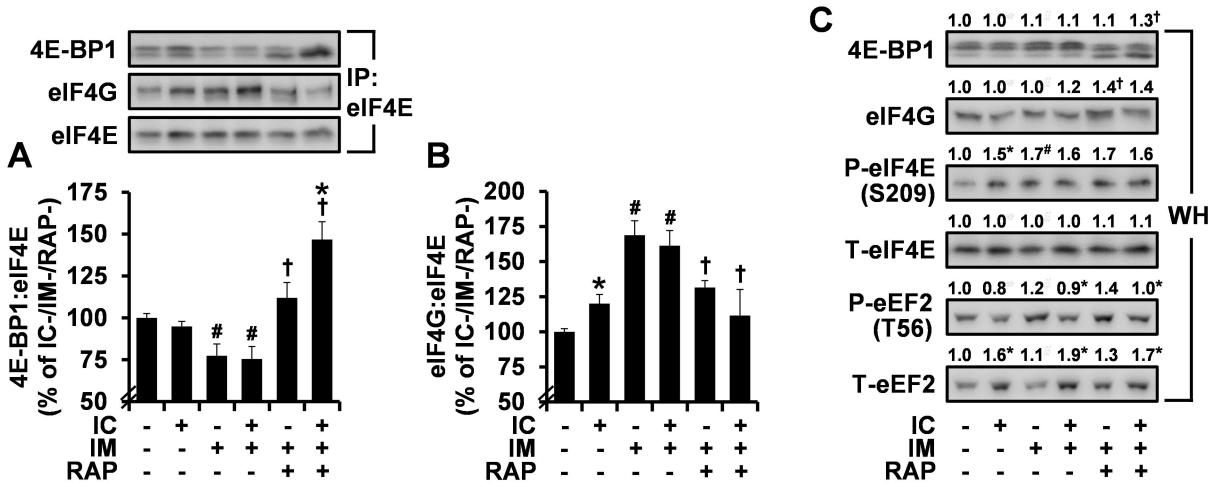

Figure 2-7. eIF4F formation is enhanced by immobilization in a rapamycin-sensitive manner, but not further enhanced by isometric contractions. Mice were treated as in Figure 2-5 and pre-cleared homogenates from EDL muscles were subjected to immunoprecipitation (IP) of eIF4E followed by Western blot analysis for 4E-BP1, eIF4G and eIF4E to obtain the ratio of (**A**) 4E-BP1:eIF4E and (**B**) eIF4G:eIF4E. (**C**) Whole homogenates (WH) were subjected to Western blot analysis for the total (T) and phosphorylated (P) forms of various proteins. All values were expressed relative to the values obtained in IC-/IM-/RAP- group and presented as the mean (+ s.e.m. in graphs, n = 3-6 muscles per group). * versus the drug- and mobility-matched IC- groups, # versus the contraction-matched IM-/RAP- groups, † versus the contraction-matched IM+/RAP- groups, $P \leq 0.05$.

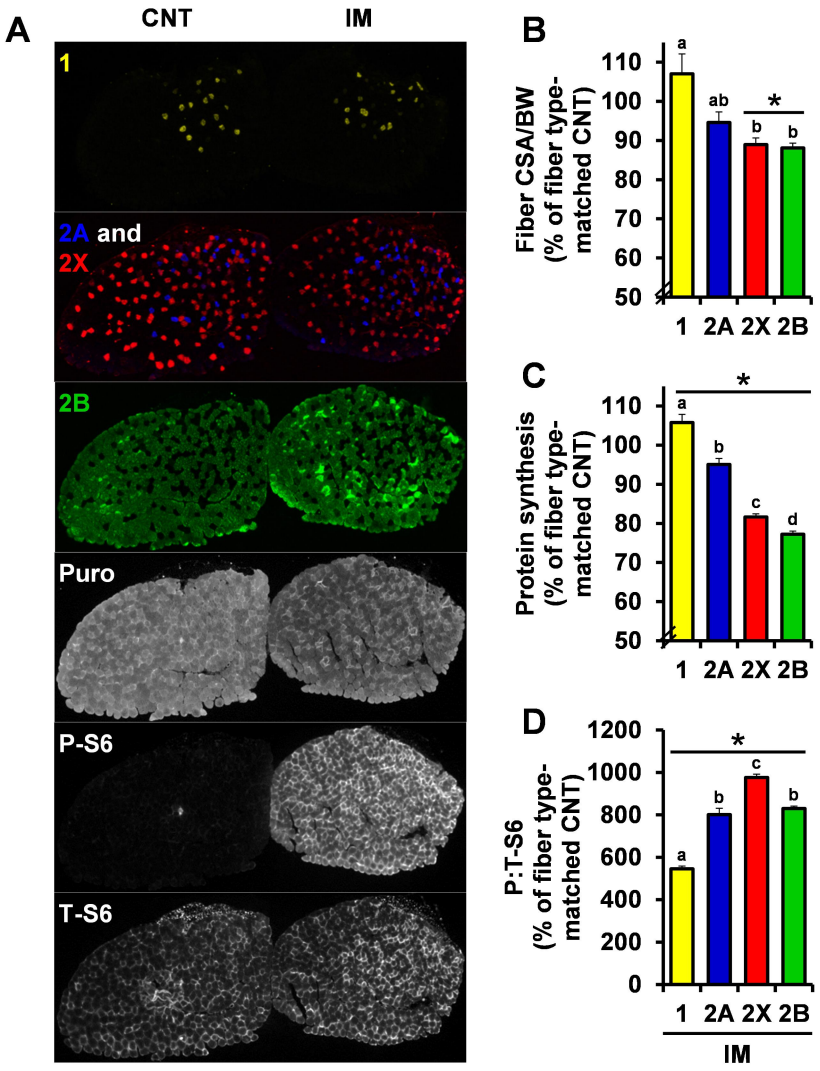

Figure 2-8. Immobilization induces fiber type-dependent decreases in protein synthesis and fiber size that are not associated with the level of mTOR activity. Mice were subjected to unilateral hindlimb immobilization (IM) for 3 days, or a non-immobilized control condition (CNT), and injected with puromycin as in Figure 2-1. (**A**) EDL muscles obtained from CNT and IM mice were frozen adjacent to one another and subjected to immunohistochemistry for different isoforms of myosin heavy chain (MHC; 1, yellow; 2A, blue; 2X, red; 2B, green) and puromycin-labeled peptides, phosphorylated (P)-S6 (S240/244), or total (T)-S6. (**B-D**) Fiber-type specific measurements of (**B**) the fiber cross sectional area (CSA) normalized to body weight (BW), (**C**) the puromycin staining intensity (i.e., protein synthesis), and (**D**) the ratio of P-S6 normalized to T-S6. All values were expressed relative to the values obtained in the fiber type-matched CNT muscles and presented as the mean + s.e.m. (n = 48-360 fibers per group from 4 independent pairs of muscles). * versus the fiber type-matched CNT groups, a - d versus one another, $P \leq 0.05$.

Chapter 3

Mechanical Stimulation Induces mTOR Signaling via an ERK-Independent Mechanism: Implications for a Direct Activation of mTOR by Phosphatidic Acid

Jae-Sung You[1,2], John W. Frey[2], Troy A. Hornberger[1,2]

[1]Program in Cellular and Molecular Biology and [2]Department of Comparative Biosciences in the School of Veterinary Medicine, University of Wisconsin - Madison, WI 53706 USA

Corresponding authors: Troy Alan Hornberger (Address: 2015 Linden Drive, Madison, WI 53706, USA; Phone: 608.695.2847; E-mail: troy.hornberger@wisc.edu),

Author contributions: J.-S.Y. and T.A.H. conceived and designed the experiments. J.-S.Y. and J.W.F. performed the experiments and analyzed the data. J.-S.Y. and T.A.H. wrote the paper.

This chapter was published in: *PLoS One.* 2012;7(10):e47258

and modified slightly to comply with the format of this dissertation

Abstract

Signaling by mTOR is a well-recognized component of the pathway through which mechanical signals regulate protein synthesis and muscle mass. However, the mechanisms involved in the mechanical regulation of mTOR signaling have not been defined. Nevertheless, recent studies suggest that a mechanically-induced increase in phosphatidic acid (PA) may be involved. There is also evidence which suggests that mechanical stimuli, and PA, utilize ERK to induce mTOR signaling. Hence, we reasoned that a mechanically-induced increase in PA might promote mTOR signaling via an ERK-dependent mechanism. To test this, we subjected mouse skeletal muscles to mechanical stimulation in the presence or absence of a MEK/ERK inhibitor, and then measured several commonly used markers of mTOR signaling. Transgenic mice expressing a rapamycin-resistant mutant of mTOR were also used to confirm the validity of these markers. The results demonstrated that mechanically-induced increases in $p70^{s6k}$ T389 and 4E-BP1 S64 phosphorylation, and unexpectedly, a loss in total 4E-BP1, were fully mTOR-dependent signaling events. Furthermore, we determined that mechanical stimulation induced these mTOR-dependent events, and protein synthesis, through an ERK-independent mechanism. Similar to mechanical stimulation, exogenous PA also induced mTOR-dependent signaling via an ERK-independent mechanism. Moreover, PA was able to directly activate mTOR signaling *in vitro*. Combined, these results demonstrate that mechanical stimulation induces mTOR signaling, and protein synthesis, via an ERK-independent mechanism that potentially involves a direct interaction of PA with mTOR. Furthermore, it appears that a decrease in total 4E-BP1 may be part of the mTOR-dependent mechanism through which mechanical stimuli activate protein synthesis.

Introduction

It is well recognized that mechanical signals play a critical role in the regulation of skeletal muscle mass and the maintenance of muscle mass contributes significantly to health and issues associated with the quality of life (7, 112, 113). However, the mechanism(s) via which mechanical signals are converted into the molecular events that regulate muscle mass remain poorly defined. Nevertheless, advances in our knowledge are being made and it is becoming increasingly evident that mechanically-induced changes in muscle mass are largely driven by changes in the rate of protein synthesis (15, 114, 115). Thus, identifying the molecular mechanisms that control mechanically-induced changes in protein synthesis should provide fundamental insight into how mechanical stimuli regulate muscle mass.

One mechanism that has been widely implicated in the regulation of protein synthesis involves signaling through the mammalian target of rapamycin (mTOR) (75). For instance, mTOR-mediated phosphorylation of the eukaryotic initiation factor (eIF) 4E binding protein 1 (4E-BP1) results in the recruitment of elF4G to the 5' end of most mRNAs, and thereby, promotes the initiation of protein synthesis (76, 77). Furthermore, mTOR can phosphorylate, and activate, the p70 ribosomal protein S6 kinase ($p70^{s6k}$). Active $p70^{s6k}$ can, in-turn, promote an increase in the helicase activity of eIF4A, and thus, provide an additional stimulus for the initiation of protein synthesis (78).

mTOR is a Serine/Threonine kinase that is typically found in characteristically distinct multi-protein complexes. For example, the mTOR complex 1 (mTORC1) contains unique accessory proteins such as the regulatory-associated protein of mTOR (Raptor). On the other hand, the mTOR complex 2 (mTORC2) contains a protein called Rictor, but not Raptor. Furthermore, signaling by mTORC1, unlike mTORC2, is highly sensitive to inhibition by the drug rapamycin (116). This is important because numerous studies have shown that rapamycin inhibits not only the mechanical activation of mTOR-dependent signaling events, but also mechanically-induced increases in the rate of protein synthesis and ultimately growth (30-32, 34, 35). Hence, it has become widely concluded that signaling by mTOR (presumably mTORC1) is a key determinant in the mechanical regulation of protein synthesis and muscle

mass; however, the mechanism(s) via which mechanical signals induce mTOR signaling remain vaguely defined.

One mechanism that has been implicated in the mechanical activation of mTOR signaling, but has not yet been directly tested, involves signaling by the extracellular regulated kinase (ERK) (117). For example, previous studies have demonstrated that ERK can induce mTOR signaling via the phosphorylation of proteins such as tuberous sclerosis complex 2 (TSC2) and Raptor (118-120). Previous studies have also shown that mechanical stimuli can induce a rapid and prolonged phosphorylation / activation of ERK, and this occurs concomitantly with the activation of mTOR signaling (30, 117). Furthermore, Miyazaki *et al*. (2011) recently demonstrated that mechanical overload induces an increase in the phosphorylation of TSC2 on the S664 residue, which is a site that can be phosphorylated by ERK, and potentially promotes the activation of mTOR signaling. Combined, all of these studies suggest that signaling through ERK could be an important part of the mechanism via which mechanical signals activate mTOR signaling.

A potential role of ERK is also highlighted by previous studies which suggest that phosphatidic acid (PA) may be involved in the mechanical activation of mTOR signaling. Specifically, work from our lab has shown that mechanical stimuli induce an increase in the concentration of PA (56, 63). Furthermore, several groups have shown that PA can induce the activation of mTOR signaling (56, 65, 121); however, the mechanism(s) via which PA activates mTOR signaling have not been clearly defined. Currently, the most widely accepted mechanism involves direct binding of PA to mTOR (65, 66, 122). Yet, an alternative mechanism has recently been proposed, in which, PA activates mTOR signaling via the induction of signaling through ERK (123). Indeed, a number of studies support this idea. For example, PA can bind and activate Raf which, in-turn, promotes signaling through the mitogen activated protein kinase kinase (MEK) / ERK pathway (124-126). Furthermore, PA can activate signaling through Raf/MEK/ERK via the recruitment of Son of Sevenless to the plasma membrane (127). Therefore, it remains highly possible that a mechanically-induced increase in PA promotes the activation of mTOR signaling via an ERK-dependent mechanism.

Taken together, the aforementioned studies suggest that ERK could play an important role in the mechanical activation of mTOR signaling. However, limitations with the *in-vivo* administration of MEK/ERK inhibitors, such as U0126, have hampered a direct investigation into this potentially important mechanism (117). Therefore, in this study, we attempted to overcome these limitations by employing an *ex-vivo* model of mechanical stimulation in which ERK inhibition was fully effective. Combined, our results demonstrate that the mechanical activation of mTOR signaling, and protein synthesis, occur through an ERK-independent mechanism that potentially involves a direct interaction of PA with mTOR.

Methods

Materials. - 1,2-dioctanoyl-*sn*-glycero-3-phosphate (C8 PA), egg L-*α*-phosphatidic acid (egg PA), and 1-palmitoyl-2-oleoyl-*sn*-glycero-3-phosphocholine (PC) were purchased from Avanti Lipids (Alabaster, AL, USA). For cell stimulation experiments, C8 PA and egg PA were prepared by drying lipids under nitrogen gas and dissolving in PBS with 3 min of water bath sonication at concentration of 0.6 mM and 6 mM respectively. For *in-vitro* stimulation experiments, C8 PA vesicles (50% C8 PA + 50% PC) or PC vesicles (100% PC) were prepared by drying lipids as described above and dissolving in vesicle buffer (150 mM NaCl and 10 mM Tris pH 8.0) with 5 min of water bath sonication at a concentration of 6 mM. U0126 was purchased from Cell Signaling (Danvers, MA, USA) and dissolved in DMSO at concentration of 50 mM or 20 mM before adding to the *ex-vivo* organ culture media or cell culture media, respectively. Rapamycin was purchased from LC laboratories (Woburn, MA, USA) and dissolved in DMSO at a concentration of 150 μM before adding to *ex-vivo* organ culture media. Acetic acid, ethyl acetate, trimethylpentane and trichloroacetic acid were purchased from Fisher Chemical (Fair Lawn, NJ, USA). ^{3}H-Myristic acid and ^{3}H-Phenylalanine were purchased from Perkin Elmer (Waltham, MA, USA). Rabbit anti-phospho-p70^{s6k} (Thr389) and anti-total 4E-BP1 (R-113, used only for Figure 3-4) were purchased from Santa Cruz Biotechnologies (Santa Cruz,CA, USA). Peroxidase-conjugated anti-rabbit IgG (H+L) was purchased from Vector Laboratories (Burlingame, CA, USA). All other antibodies including rabbit anti-phospho-p70^{s6k} (Thr421/Ser424), anti-total p70^{s6k}, anti-phospho-ERK1/2

(Thr202/Tyr204), anti-total ERK1/2, anti-phospho-S6 (Ser240/244), anti-phospho-S6 (Ser235/236), anti-total S6, anti-phopho-4E-BP1 (Thr37/46), anti-phospho-4E-BP1 (Ser65) [note: the Thr37/46 and Ser65 residues in human are equivalent to the Thr36/45 and Ser64 residues in mouse, respectively], anti-total 4E-BP1 (53H11), anti-phospho-PKB (Ser473), and anti-total PKB were purchased from Cell Signaling (Danvers, MA, USA).

Animal care and use. - Eight- to ten-week-old inbred or outbred (Taconic, NY, USA) FVB/N male mice were used for all experiments. For inbred mice, wild type FVB/N mice were bred with hemizygotic FVB/N mice that contain human skeletal actin promoter-driven expression of a FLAG-tagged rapamycin-resistant (Ser2035Thr) mutant of mTOR (128). The offspring were genotyped with tail snips by PCR to identify null (wild type) and hemizygotic (RR-mTOR) mice. The mice were anaesthetized with an intraperitoneal injection of ketamine (100 mg/kg) and xylazine (10 mg/kg) before all surgical procedures. After muscle collection, mice were sacrificed by cervical dislocation under anesthesia. The collected muscles were frozen in liquid nitrogen immediately or after washing when necessary. All animals were housed in a room maintained at 25°C with a 12 h:12 h light–dark cycle and received food and water ad libitum. All methods were approved by the Institutional Animal Care and Use Committee of the University of Wisconsin-Madison under protocol # V01324.

Organ culture and mechanical stimulation. - Mouse extensor digitorum longus (EDL) muscles were placed in an *ex-vivo* organ culture system which consisted of a refined myograph apparatus (Kent Scientific, Torrington, CT) and an organ culture bath as previously described (31). In most experiments, the bath incubation media consisted of Krebs Henseleit Buffer (120 mM NaCl, 4.8 mM KCl, 25 mM NaHCO3, 2.5 mM CaCl2, 1.2 mM KH2PO4, 2 mM MgSO4, and 5 mM HEPES) supplemented with 1X MEM amino acid mixture (Invitrogen, Carlsbad, CA) and 25 mM glucose. For experiments involving the measurement of protein synthesis, high glucose DMEM was used for the incubation media (HyClone, Logan, UT, USA). In all cases, the media was maintained at 37°C with continuous 95% O_2 and 5% CO_2 gassing, and fresh media was added to the bath at 30 min intervals.

For mechanical stimulation, the EDL muscles were connected to the lever arms of a force transducer and micromanipulator, and then placed in the organ culture bath. The length of the EDL muscles were then adjusted until a passive tension of 13.5 mN was obtained (note: preliminary studies demonstrated that the optimal length (*Lo*) of EDL muscles was obtained at 13.5 mN). The muscles were then subjected to intermittent 15% passive stretch as a source of mechanical stimulation or held static at *Lo* as a control condition as previously described (31).

Cell culture. - For stimulation experiments, wild type C2C12 myoblasts were purchased from ATCC (Manassas, VA) and cultured in growth media consisting of high glucose DMEM supplemented with antibiotics and antimycotics (100 μg/ml streptomycin, 100 U/ml penicillin and 0.25 μg/ml amphotericin) and 10% fetal bovine serum (Gibco, Grand Island, NY, USA). These cells were plated on 6-well dishes and grown to confluence. Upon confluence, all cells were serum-starved in the absence of any antibiotics and antimycotics overnight before being subjected to experimental treatments. Cell cultures were maintained at 37°C in a humidified atmosphere of 95% air and 5% CO_2.

Western blot analysis. - Collected muscles were homogenized with a Polytron in an ice-cold lysis buffer [40 mM Tris (pH 7.5), 1 mM EDTA, 5 mM EGTA, 0.5% Triton X-100, 25 mM β-glycerolphosphate, 25 mM NaF, 1 mM Na_3VO_4, 10 μg/ml leupeptin, and 1 mM PMSF] and the whole homogenate was used for analysis. Myoblasts were lysed in the ice-cold buffer described above, centrifuged at 500 *g* for 5 min, and then the supernatant was used for analysis. Protein concentrations were determined with the DC protein assay kit (Bio-Rad, Hercules, CA, USA) and equal amounts of protein from each sample were dissolved in Laemmli buffer before being subjected to SDS-PAGE. Following the electrophoretic separation, proteins were transferred to a PVDF membrane, blocked with 5% milk in TBST (Tris-buffered saline, 1% Tween 20) for 1 h, and probed with rabbit primary antibodies overnight at 4°C. The membranes were then washed for 30 min in TBST and incubated with a peroxidase-conjugated anti-rabbit secondary antibody for 1 h at room temperature. Following 30 min of washing in TBST, the blots were developed on film using ECL [Pierce (Rockford, IL, USA) for Regular ECL and Amersham (Piscataway, NJ, USA) for ECL Plus]. Once the appropriate image was captured, the

membranes were stained with Coomassie Blue to verify equal loading througout all lanes. Densitometric measurements of each blot were carried out using ImageJ (NIH).

Analysis of protein synthesis. - Protein synthesis rates were measured *ex-vivo* as previously described (31). Briefly, EDL muscles were pre-incubated for 30 min and then subjected to 90 min of control or stretch conditions in DMEM. During the final 30 min, the media was switched to fresh DMEM containing 2.7 mM phenylalanine and 10 μCi/ml ^{3}H-phenylalanine for 30 min. An aliquot of the media was saved for determining the specific activity of the phenylalanine (cpm/nmol of phenylalanine) before collecting the muscles. The muscles were then washed three times with ice-cold PBS (pH 7.5) and homogenized in 10% (w/v) trichloroacetic acid (TCA). The TCA homogenates were incubated on ice for 30 min and then centrifuged at 5000 *g* for 5 min. TCA-soluble material was decanted and the TCA-insoluble material was consecutively washed at least five times by repeating resuspension of the pellet in 10% TCA and centrifugation at 5000 *g*. The TCA-insoluble material was then dissolved in 0.15M NaOH at 55°C with frequent vortex-mixing for 1 h. Aliquots of the sample were counted by liquid scintillation spectrometry and used for determination of protein concentration with the DC protein assay kit to yield the specific activity (cpm/mg of protein) of the TCA-insoluble proteins. The rate of protein synthesis was calculated by using the following equation:

$$\text{Rate} = ((A / B) \text{ x incubation time})$$

where A represents the specific activity of the TCA-insoluble material and B the specific activity of the media.

Protein synthesis rates in cells were measured by incubating the cells in DMEM media containing 1.2 mM phenylalanine and 2 μCi/ml ^{3}H-phenylalanine for 30 min. After saving an aliquot of the media for determination of the phenylalanine specific activity, the reaction was terminated by rinsing the culture wells three times with ice-cold PBS and then adding 10% (w/v) TCA to the wells. The cells were

incubated on ice for 30 min and collected to determine the specific activity (cpm/mg of protein) of the TCA-insoluble proteins as described above.

Analysis of phosphatidic acid concentration. - The method for measuring the concentration of PA in skeletal muscles *ex-vivo* has been previously described (56). Briefly, EDL muscles were pre-labeled in the organ culture system with media containing ^{3}H-myristic acid (2.5 μCi/ml) for 2 h and then subjected to experimental treatments before being collected. The muscles were then homogenized in chloroform–methanol 2:1 (v/v) with a polytron, and total lipids were extracted according to Folch *et al.* (1957). The extracted lipids were combined with 10 μg of PA standard and aliquots were used for the measurement of radioactivity in the total lipids or spotted on LK5D silica gel plates for separation of PA by thin layer chromatography (TLC). The plates were developed with a solvent system consisting of ethyl acetate–isooctane–acetic acid–water 13:2:3:10 (v/v). The standard PA spots containing the ^{3}H-labelled PA were visualized by iodine staining and scraped off the TLC plate to count the amount of radioactivity by liquid scintillation spectrometry. Final calculations for [PA] were made by dividing the amount of radioactivity in the PA spot by the amount of radioactivity in the total lipid extract.

***In-vitro* mTOR kinase activity assay. -** Mouse wild type C2C12 myoblasts were cultured as described above. C2C12 myoblasts stably expressing FLAG-tagged mTOR were obtained from Dr. Jie Chen (Department of Cell and Developmental Biology, University of Illinois, Urbana IL) and maintained in DMEM containing 0.2 mg/ml G418 (HyClone). G418 was not included in the media after the cells had been plated for the experiments. Upon confluence, cells were serum-starved overnight and subsequently collected in ice cold CHAPS lysis buffer [40 mM HEPES pH. 7.4, 2 mM EDTA, 0.3% CHAPS, 10 mM sodium pyrophosphate, 10 mM β-glycerophosphate, and 1 tablet of EDTA-free protease inhibitors (Roche) per 25 mL]. Fresh cell lysates were centrifuged at 2500 g for 5 min, and 400 μg of protein from the supernatant was diluted to a volume of 0.5 mL with fresh ice cold CHAPS lysis buffer. Samples were immunoprecipitated for the FLAG tag by incubating with 10 μL of EZview red ANTI-FLAG M2 agarose affinity gel beads (Sigma-Aldrich, St Louis, MO) and gently rocking at 4°C for 3 h. Following the incubation, the beads were pelleted by centrifugation at 500 g for 30 sec and washed 3 times with fresh

ice cold Wash buffer (40 mM HEPES pH. 7.4, 150 mM NaCl, 2 mM EDTA, 0.3% CHAPS, 10 mM sodium pyrophosphate, 10 mM β-glycerophosphate, and 1 tablet of EDTA-free protease inhibitors per 25 ml). The beads were then washed 2 times with Kinase Wash buffer (25 mM HEPES pH 7.4 and 20 mM KCl).

For lipids stimulation, C8 PA or PC vesicles were prepared as described in the *Materials* section. The vesicles were diluted to 150 μM in 1.5-fold concentrated mTOR kinase assay buffer (see below), and 10 μL of this solution was incubated with the immunoprecipitates at 30°C for 15 min. Then, mTOR kinase activity towards purified GST-tagged p70 (79, 129) was initiated by adding 5 μL of 750 μM ATP to the immuoprecipitates which yielded a final mTOR kinase assay buffer that contained (25 mM HEPES pH 7.4,50 mM KCl, 10 mM MgCl2, 250 μM ATP, 50 ng GST-p70, and 100 μM C8 PA or PC vesicles). After 20 min of the reaction, the kinase assay was terminated by the addition of 25 μL of 2X Laemmli Buffer. Samples were boiled for 5 min and then subjected to western blot analysis.

Statistical analysis. - All values are expressed as means (+ SEM in graphs). Statistical significance was determined by using ANOVA, followed by Student–Newman–Keuls *post hoc* analysis. Differences between groups were considered significant when $P \leq 0.05$. All statistical analyses were performed on SigmaStat software (San Jose, CA, USA).

Results

Mechanical stimulation activates mTOR signaling via an ERK-independent mechanism. - As stated in the introduction, there are several lines of evidence which suggest that ERK may play a role in the mechanical activation of mTOR signaling. To test this possibility, we employed an *ex-vivo* organ culture system in which mouse EDL muscles were mechanically stimulated with intermittent passive stretch. In this model, we determined that both 15 and 90 min mechanical stimulation was sufficient to induce an increase in the phosphorylation of ERK1 (T202/Y204). Furthermore, in this system, the MEK/ERK inhibitor U0126 was fully capable of inhibiting signaling through ERK (Figure 3-1).

Combined, these results demonstrated that our *ex-vivo* system would enable us to define the role of ERK in the mechanical activation of mTOR signaling.

Changes in the phosphorylation status of molecules such as $p70^{s6k}$, ribosomal S6 protein (S6), and 4E-BP1, are commonly used as markers of mTOR activity. For example, the T389 residue on $p70^{s6k}$ is a widely accepted mTOR-specific phosphorylation site (130). On the other hand, the T421/S424 residues of $p70^{s6k}$ contain the consensus "S/T-P" sequence which can be phosphorylated by proline-directed kinases such as ERK (131). Therefore, we measured the phosphorylation status of the T389 and T421/S424 residues. Our results indicated that as little as 15 min of mechanical stimulation was sufficient to induce phosphorylation on these sites, and the magnitude of this effect was further amplified with 90 min of mechanical stimulation. Interestingly, when signaling through ERK was inhibited with U0126, the basal levels of T389 and T421/S424 phosphorylation were significantly reduced; however, U0126 did not block the mechanically-induced increase in the phosphorylation of these sites at either time point. Combined, these results indicate that ERK plays a role in maintaining basal levels of T389 and T421/S424 phosphorylation, but it is not necessary for a mechanically-induced increase in the phosphorylation of these sites.

As mentioned above, the phosphorylation status of S6 is also commonly used as a marker of mTOR activity, and previous studies have shown that S6 is predominantly phosphorylated by $p70^{s6k}$ on residues such as S235/236 and S240/244 (86, 132). Furthermore, phosphorylation of the S235/236 residues, unlike the S240/244 residues, can also be mediated by ERK-dependent activation of the p90 ribosomal S6 kinase (RSK) (133, 134). Thus, we were interested in determining if mechanical stimulation would induce an increase in S6 phosphorylation, and if ERK would be necessary for this event. As shown in Figure 3-1, our results indicated that 15 min of mechanical stimulation significantly increased S6 phosphorylation on both the S235/236 and S240/244 residues, and the magnitude of this effect was similarly maintained after 90 min of mechanical stimulation. In the presence of U0126, basal levels of S235/236 and S240/244 phosphorylation were significantly reduced, but U0126 did not block the mechanically-induced increase in the phosphorylation of these residues. Hence, it can be concluded that signaling through ERK plays a

role in maintaining basal levels of S235/236 and S240/244 phosphorylation, but it is not necessary for a mechanically-induced increase in the phosphorylation of these sites.

In order to further clarify the role of ERK in the mechanical activation of mTOR signaling, we measured the phosphorylation status of 4E-BP1. For example, we measured changes in gel mobility as a marker of global changes in 4E-BP1 phosphorylation (135). As shown in Figure 3-1, both 15 and 90 min of mechanical stimulation induced an increase in the appearance of the slower migrating / hyper-phosphorylated γ band, and inhibition of ERK with U0126 did not alter this affect. We also measured the phosphorylation of the T36/45 residues on 4E-BP1. Importantly, numerous studies have shown that mTOR can directly phosphorylate these residues (136, 137), but much to our surprise, neither mechanical stimulation, nor U0126, altered the amount of T36/45 phosphorylation. On the other hand, 15 min of mechanical stimulation induced a significant increase in the phosphorylation of 4E-BP1 on the S64 residue, and the magnitude of this effect was further amplified with 90 min of mechanical stimulation. However, U0126 did not affect the phosphorylation of S64 in either the basal or mechanically-stimulated states. Finally, we also found that mechanical stimulation induced a significant loss in the abundance of total 4E-BP1, and again, inhibition of ERK with U0126 did not alter this effect. Note: a mechanically-induced loss of 4E-BP1 was also detected with an antibody that was raised against a different antigenic peptide (Figure 3-4). Taken together, these results demonstrate that mechanical stimulation induces an increase in 4E-BP1 phosphorylation on sites such as S64, as well as a loss of total 4E-BP1, and signaling through ERK is not necessary for these events.

Validation of mechanically-induced mTOR-dependent signaling events. - As previously noted, changes in the phosphorylation status of molecules, such as $p70^{s6k}$, S6, and 4E-BP1, are commonly used as markers of mTOR activity. However, many of the phosphorylation sites on these molecules can be regulated by both mTOR-dependent and mTOR-independent events (35, 131, 134, 138). Hence, we set out to determine if the markers analyzed were indeed valid markers of mechanically-induced mTOR signaling. To accomplish this, we first used a supramaximal dose of rapamycin (150 nM) to inhibit signaling by mTOR in muscles from wild type mice. As shown in Figure 3-2A, this dose of rapamycin

eliminated the mechanically-induced increase in $p70^{s6k}$ T389 and 4E-BP1 S64 phosphorylation, suggesting that these events occur through an mTOR-dependent mechanism. Interestingly, the mechanically-induced decrease in total 4E-BP1 was also eliminated by rapamycin, which suggests that the loss of 4E-BP1 may be a previously unrecognized mTOR-dependent signaling event. On the other hand, rapamycin did not prevent mechanical stimulation from inducing an increase in the phosphorylation of the $p70^{s6k}$ T421/S424, S6 S235/236 and S6 S240/244 residues. Thus, it can be concluded that rapamycin-insensitive / mTOR-independent mechanism(s) are at least partially responsible for the mechanically-induced phosphorylation of these residues.

Like all pharmacological inhibitors, rapamycin can potentially exert non-specific (mTOR-independent) actions. For example, it has been shown that rapamycin can bind and sequester the FKBP12 protein and this can interfere with the role that FKBP12 plays in the function of the ryanodine receptor and signaling by members of the transforming growth factor-β superfamily (139-141). Thus, we wanted to determine if mTOR was indeed responsible for the inhibitory effects of rapamycin. To accomplish this, we employed transgenic mice that express endogenous wild type mTOR in conjunction with overexpression of a rapamycin-resistant mutant of mTOR (RR-mTOR). Specifically, the RR-mTOR transgene contains a S2035T mutation located within the FKBP12-rapamycin complex binding domain of mTOR. The S2035T mutation prevents the interaction of mTOR with the FKBP12-rapamycin complex, and thereby, confers resistance to the inhibitory effects that rapamycin normally exerts on mTOR signaling (38, 39). As shown in Figure 3-2B, when muscles from RR-mTOR mice were subjected to mechanical stimulation in the presence of rapamycin, the mechanically-induced increase in $p70^{s6k}$ T389 and 4E-BP1 S64 phosphorylation, and the decrease in total 4E-BP1, were all effectively rescued from the inhibitory actions of rapamycin. Therefore, it can be concluded that these events are indeed valid markers of mechanically-induced signaling by mTOR.

Mechanical stimulation induces protein synthesis via an ERK-independent mechanism. - Previous studies have indicated that signaling through mTOR is necessary for a mechanically-induced increase in the rate of protein synthesis, and that the activation of mTOR signaling is sufficient to induce

protein synthesis (30-32, 142). In addition, the results presented above indicate that ERK is not necessary for the mechanical activation of mTOR signaling. Combined, these points suggest that mechanical stimulation should induce an increase in protein synthesis via an ERK-independent mechanism. However, signaling by ERK can also control protein synthesis by regulating mTOR-independent molecules such as RSK and the mitogen-activated protein kinase-interacting S/T kinase (143, 144). Thus, we wanted to determine if signaling through ERK is necessary for a mechanically-induced increase in the rate of protein synthesis. To test this, we subjected muscles to 90 min of mechanical stimulation and then measured rates of protein synthesis during the final 30 min of stimulation. Interestingly, we could not observe a mechanically-induced increase in the rate of protein synthesis when muscles were incubated with the same media [Krebs Henseleit Buffer (KHB) supplemented with amino acids and glucose, see methods] that was used to obtain the signaling data presented in Figures 3-1 and 3-2 (Figure 3-3). However, we have previously demonstrated that mechanical stimulation in our organ culture system induces protein synthesis when muscles are incubated with DMEM media (31). Therefore, we performed our protein synthesis measurements on muscles that were incubated with DMEM. Before doing this, we confirmed that mechanical stimulation induced an ERK-independent activation of mTOR signaling when muscles were incubated with DMEM (Figure 3-4). We then performed our protein synthesis measurements and, consistent with our previous studies, we found that mechanical stimulation induced an increase in the rate of protein synthesis. However, inhibition of ERK with U0126 did not prevent the mechanically-induced increase in protein synthesis (Figure 3-5). Thus, it can be concluded that signaling through ERK is not necessary for a mechanically-induced increase in protein synthesis.

PA induces mTOR signaling via an ERK-independent mechanism. - Previous studies have suggested that a mechanically-induced increase in PA is necessary for the activation of mTOR signaling (56, 63). Furthermore, an increase in PA is capable of inducing the activation of ERK, which could then induce signaling by mTOR (118, 125, 127). Based on these points, we initially envisioned the potential for a mechanism in which a mechanically-induced increase in PA would promote signaling through ERK and this, in-turn, would induce the activation of mTOR signaling. However, our results demonstrated that

the mechanical activation of mTOR signaling occurred through an ERK-independent mechanism. Thus, we reasoned that if PA is actually involved in the mechanical activation of mTOR signaling, then PA should also promote the activation of mTOR signaling via an ERK-independent mechanism. To test this, we first wanted to confirm our previous observation that mechanical stimulation induces an increase in PA. As shown in Figure 3-6A, both 15 and 90 min of mechanical stimulation resulted in a significant increase in ^{3}H-myristic acid labeled PA.

Next, we wanted to determine if PA activates mTOR signaling via an ERK-independent mechanism. Importantly, we have previously confirmed that exogenous PA can induce mTOR signaling in C2C12 myoblasts (56). Thus, to accomplish our goal, we stimulated C2C12 myoblasts with different species of exogenous PA (C8 PA and Egg PA) in the presence or absence of U0126. It should be noted that at least some of exogenous PA can be hydrolyzed into lysophosphatidic acid (LPA) by the phospholipase A present in the cell culture media, and this could promote additional LPA receptor-mediated activation of ERK (123). Consistent with this possibility, we found that treatment with both species of exogenous PA induced a much more robust increase in ERK phosphorylation than what was observed with mechanical stimulation (Figure 3-6B). Furthermore, the robust activation of ERK by C8 PA was found to be necessary for C8 PA to induce an increase in protein synthesis (Figure 3-7). However, inhibition of ERK with U0126 did not prevent the ability of PA to induce the markers of mechanically-induced mTOR signaling, such as p70^{s6k} T389 and 4E-BP1 S64 phosphorylation, or the loss of total 4EBP1 (Figure 3-6B). These results indicate that, in C2C12 myoblasts, exogenous PA induces mTOR-dependent signaling events via an ERK-independent mechanism.

PA can directly activate mTOR signaling *in-vitro*. - Our observation that PA induces mTOR signaling via an ERK-independent mechanism prompted us to explore the possibility that PA might directly activate mTOR signaling (65, 66, 122). To test this, we employed wild type C2C12 myoblasts and C2C12 myoblasts that stably express FLAG-tagged wild type mTOR (145). Lysates from these cells were first subjected to immunoprecipitation against the FLAG tag, and as shown in Figure 3-8, only the immunoprecipitates from the FLAG-mTOR myoblasts contained mTOR. Next, the immunoprecipitates

were incubated with lipid vesicles composed of 50% C8 PA and 50% PC, or 100% PC as a control condition. The immunoprecipitates were then subjected to an *in-vitro* mTOR kinase activity assay in which $p70^{s6k}$ T389 phosphorylation was used as a readout of mTOR activity (129). The results demonstrated that PA can induce an increase in $p70^{s6k}$ T389 phosphorylation, and this only occurred in the immunoprecipitates obtained from the FLAG-mTOR cells. This is an important point because it established that the PA-induced increase in $p70^{s6k}$ T389 phosphorylation required the presence of mTOR and, therefore, did not result from the presence of a non-specific kinase that was pulled down during the immunoprecipitation procedure. Thus, it can be concluded that PA is capable of directly activating mTOR signaling *in-vitro*.

Discussion

In this study we employed an *ex-vivo* passive stretch model of mechanical stimulation to determine if signaling through ERK is necessary for the mechanical activation of mTOR signaling and protein synthesis. Based on the results, it can be concluded that ERK's contribution to these events, if any, is very limited. However, we also found that the basal level of mTOR signaling was severely impaired by ERK inhibition, which suggests that ERK is indeed a potent regulator of mTOR signaling in skeletal muscle. Hence, the seemingly negligible role of ERK in the mechanical activation of mTOR signaling is likely due, at least in part, to the relatively small increase in signaling through ERK that was induced by our model of mechanical stimulation (≈ 2-fold). However, a more robust increase in signaling through ERK has been observed with other types of mechanical stimulation. For example, Martineau and Gardiner 2001, demonstrated that concentric, isometric, and eccentric contractions produce a 3-, 4-, and 5-fold increase in signaling through ERK, respectively (146). Therefore, we cannot fully exclude the possibility that ERK may contribute to the activation of mTOR signaling, and protein synthesis, in other models of mechanical stimulation as previously suggested by Miyazaki *et al.,* 2011 (117). Nevertheless, our results do clearly reveal that mechanical stimuli can induce mTOR signaling, and protein synthesis, through an ERK-independent mechanism.

To date, numerous studies have attempted to identify the molecular mechanisms that are involved in the mechanical activation of mTOR signaling (50, 67). Based on these studies, it has been concluded that mechanical stimuli activate mTOR signaling through a unique mechanism that does not require typical candidates such as phosphoinositide 3-kinase, protein kinase B, exogenous nutrients, protein kinase C, phosphoinositide-specific phospholipase C, or changes in intracellular calcium (31, 56, 62, 63). On the other hand, several lines of evidence suggest that PA may be involved (56, 63). For example, the results of this study demonstrate that; i) mechanical stimuli can induce an increase in PA, ii) stimulating cells with PA is sufficient to induce mTOR signaling, and iii) PA can directly activate mTOR signaling *in-vitro*. Furthermore, like mechanical stimuli, we found that PA induces mTOR signaling through an ERK-independent mechanism. All of these observations are consistent with a model in which mechanical stimuli induce an increase in PA, and the newly formed PA then binds and activates mTOR. Although intriguing, additional studies will be needed to test the validity of this concept.

In this study, we also used RR-mTOR mice to identify valid markers of mechanically-induced mTOR signaling. For example, the RR-mTOR mice enabled us to demonstrate that a mechanically-induced increase in $p70^{s6k}$ T389 phosphorylation is fully dependent on mTOR. Conversely, we found that other commonly used markers of mTOR signaling, such as S6 S235/236 and S6 S240/244 phosphorylation, were at least partially induced via a rapamycin-insensitive / mTOR-independent mechanism. Consistent with these results, another recent study also demonstrated that rapamycin does not block mechanical overload-induced increases in S6 S235/236 and S6 S240/244 phosphorylation (117). This is particularly interesting because a previous study with $p70^{s6k1}$ and $p70^{s6k2}$ double knockout mice demonstrated that S6 S240/244 phosphorylation requires $p70^{s6k}$ activity (133). Thus, our results might indicate that mechanical stimulation induces a partially rapamycin-resistant activation of $p70^{s6k}$, the activation of unrecognized S6 kinase(s), or an inhibition of S6 phosphatases. Furthermore, our observations illustrate that caution should be used when interpreting changes in S6 S235/236 or S6 S240/244 phosphorylation as markers of mTOR signaling.

The RR-mTOR mice also enabled us to demonstrate that mTOR is necessary for mechanical stimulation to induce an increase in 4E-BP1 S64 phosphorylation, and a decrease in total 4E-BP1. However, much to our surprise, mechanical stimulation did not alter 4E-BP1 T36/45 phosphorylation. This observation was surprising because numerous studies have shown that, when activated, the rapamycin-sensitive mTORC1 can directly phosphorylate both $p70^{s6k}$ T389 and 4E-BP1 T36/45 residues (37, 147). Furthermore, an extensively large number of studies have shown that the classical agonists of mTORC1 signaling (e.g. growth factors and nutrients) induce an increase in both $p70^{s6k}$ T389 and 4E-BP1 T36/45 phosphorylation (129, 148, 149). Hence, observing a robust increase in $p70^{s6k}$ T389 phosphorylation, in conjunction with no change in 4E-BP1 T36/45 phosphorylation, was highly unexpected. Although the reason for this disparity is not known, a recent study by Yip et al. 2010 may have revealed some important clues. Specifically, Yip et al. demonstrated that rapamycin inhibits the ability of immunopurified mTOR to phosphorylate $p70^{s6k}$ T389 and 4E-BP1 T36/45 (37). Furthermore, the presence of raptor was found to be necessary for mTOR to phosphorylate 4E-BP1 T36/45. However, contrary to previous assumptions, the presence of raptor was not necessary for mTOR to phosphorylate $p70^{s6k}$ T389. Yet, in the absence of raptor, the ability of mTOR to phosphorylate $p70^{s6k}$ T389 was still sensitive to inhibition by rapamycin. In other words, it appears that there is a rapamycin-sensitive pool of mTOR that does not involve the classical raptor-associated mTORC1 complex. Similar to the results we observed with mechanical stimulation, this uncharacterized rapamycin-sensitive pool of mTOR can phosphorylate $p70^{s6k}$ T389, but not 4E-BP1 T36/45. Thus, it is very tempting to speculate that mechanical stimuli activate a unique rapamycin-sensitive pool of mTOR that is distinct from mTORC1.

As mentioned in the introduction, signaling through mTOR has been widely implicated in the regulation of protein synthesis. For example, the mTOR kinase inhibitor (Torin 1) induces a greater than 60% reduction in the rate of protein synthesis when added to wild-type mouse embryonic fibroblasts (MEF). However, Torin 1 has essentially no effect on the rate of protein synthesis when added to MEFs that are deficient of 4E-BP1 and 4E-BP2 (150). Based on these observations, it has been concluded that the 4E-BPs play a key role in the mechanism through which mTOR controls protein synthesis.

In general, mTOR is thought to control the function of the 4E-BPs by inducing changes in the phosphorylation state of the protein. For example, mTOR can directly phosphorylate the 36/45 residues of 4E-BP1, and phosphorylation on these residues allows 4E-BP1 to become further phosphorylated on residues such as S64 (137, 151). When hyperphosphorylated, 4E-BP1 dissociates from eIF4E and this, in-turn, promotes the formation of the eIF4F complex and ultimately the initiation of protein synthesis (76, 77). In addition to controlling 4E-BP1 phosphorylation, there is also emerging evidence which suggests that mTOR can regulate the abundance of 4E-BP1. For example, inducible knockout of mTOR in the adult myocardium results in an increase in total 4E-BP1 (152). Furthermore, HSV-1 infection has been shown to induce a decrease in total 4E-BP1, and this effect can be prevented by rapamycin (153). Presumably, a decrease in total 4E-BP1, and hyperphosphorylation of 4E-BP1, would result in functionally equivalent effects on protein synthesis (i.e. enhanced eIF4F complex formation). Thus, we were intrigued by our results which demonstrated that mechanical stimulation induces an mTOR-dependent decrease in total 4E-BP1. Specifically, previous studies have indicated that signaling through mTOR is necessary for a mechanically-induced increase in protein synthesis but the mechanisms through which mTOR exerts this effect have not been defined. Based on our results, it would appear that a mechanically-induced decrease in total 4E-BP1 could be part of this mechanism. Furthermore, we have measured total 4E-BP1 levels in muscles that were subjected to *in-vivo* eccentric contractions as described in (56), and again, we observed a decrease in total 4E-BP1 levels (data not shown). Based on these observations, it would appear that a mechanically-induced decrease in the total 4E-BP1 levels is a conserved event. Hence, in the future, it will be important to determine if the loss of total 4E-BP1 plays a significant role in the mechanism through which mechanical stimuli induce an increase in protein synthesis.

In summary, the results from this study demonstrate that mechanical stimulation induces mTOR signaling, and protein synthesis, via an ERK-independent mechanism that potentially involves a direct interaction of PA with mTOR. Since signaling through mTOR is necessary for a mechanically-induced increase in protein synthesis, and ultimately growth, these findings should help advance our

understanding of how mechanical signals are converted into the molecular events that regulate skeletal muscle mass.

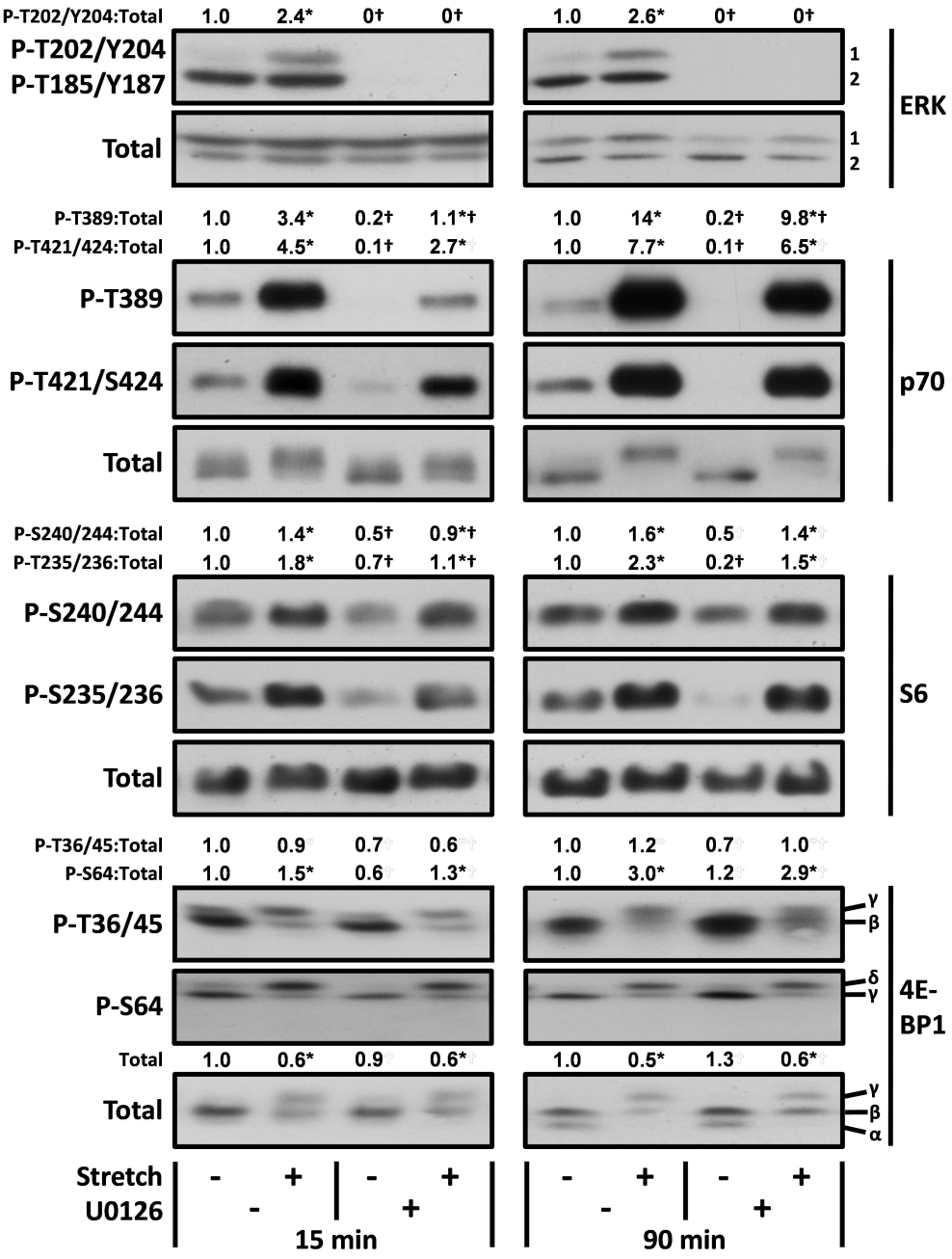

Figure 3-1. Mechanical stimulation activates mTOR signaling via an ERK-independent mechanism. EDL muscles were held at optimal length (*Lo*) in an *ex-vivo* organ culture system and pre-incubated with 50 μM U0126 (U0126 +) or the vehicle (U0126 -, DMSO) for 30 min. The muscles were then subjected to 15 or 90 min of intermittent 15% stretch or held static at *Lo* as a control condition. Muscles were collected at the end of the 15 or 90 min interval and subjected to western blot analysis for phosphorylated (P) and total ERK, p70, S6, and 4E-BP1. The total amount, and phospho:total ratios, of each protein were measured and then expressed relative to the values obtained in the time-matched vehicle control samples (U0126 -, Stretch -). All values are presented as the mean (n = 3-6 per group). * Significantly different from the drug-matched control group, † Significantly different from the stimulation-matched vehicle group, P ratios,

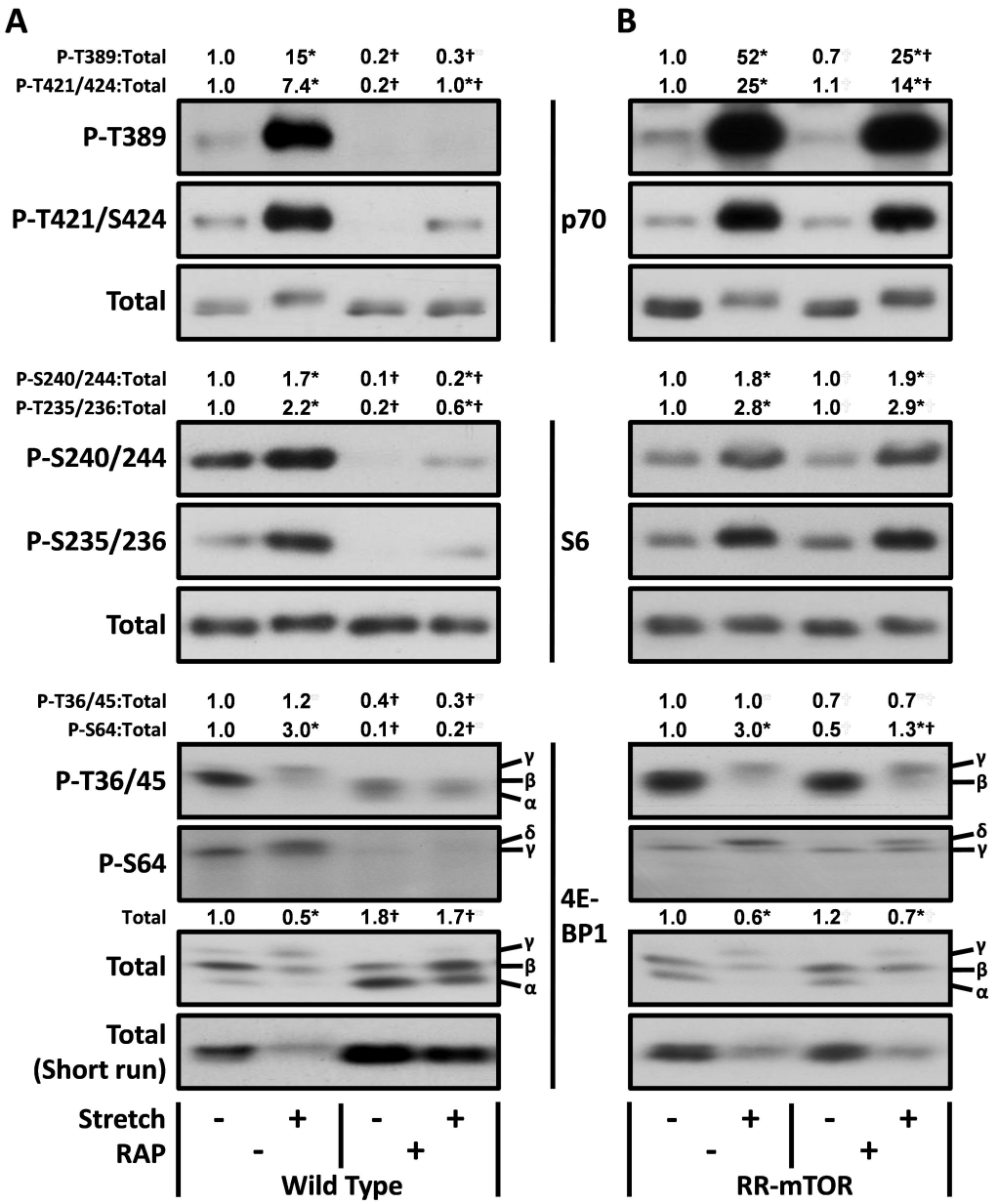

Figure 3-2. Validation of mTOR-dependent signaling events that are induced by mechanical stimulation. (**A**) EDL muscles from wild type mice, and (**B**) transgenic mice with muscle specific expression of a rapamycin-resistant mutant of mTOR (RR-mTOR), were held at *Lo* and pre-incubated with 150 nM rapamycin (RAP +) or the vehicle (RAP -, DMSO) for 30 min. The muscles were then subjected to 90 min of stretch or control conditions followed by western blot analysis for phosphorylated (P) and total p70, S6, and 4E-BP1. The total amount, and phospho:total ratios, of each protein were measured and then expressed relative to the values obtained in the genotype-matched vehicle control samples (RAP -, Stretch -). Note: total 4E-BP1 gels were also run under conditions that minimize the gel mobility shift (short-run). All values are presented as the mean (n = 3-5 per group). * Significantly different from the drug-matched control group, † Significantly different from the stimulation-matched vehicle group, P differe

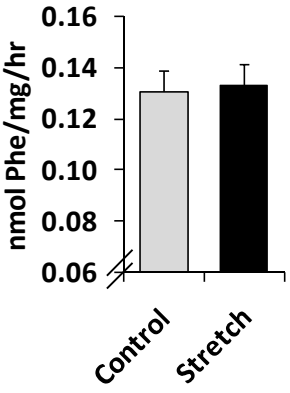

Figure 3-3. Mechanical stimulation does not increase protein synthesis in muscles incubated with KHB media. EDL muscles were held at *Lo* and pre-incubated for 30 min with KHB media containing 0.1% DMSO, 1X MEM amino acids and 25 mM glucose. The muscles were then subjected to 90 min of stretch or control conditions, and protein synthesis rates were measured during the final 30 min. All values are presented as the mean + SEM (n = 4-6 per group).

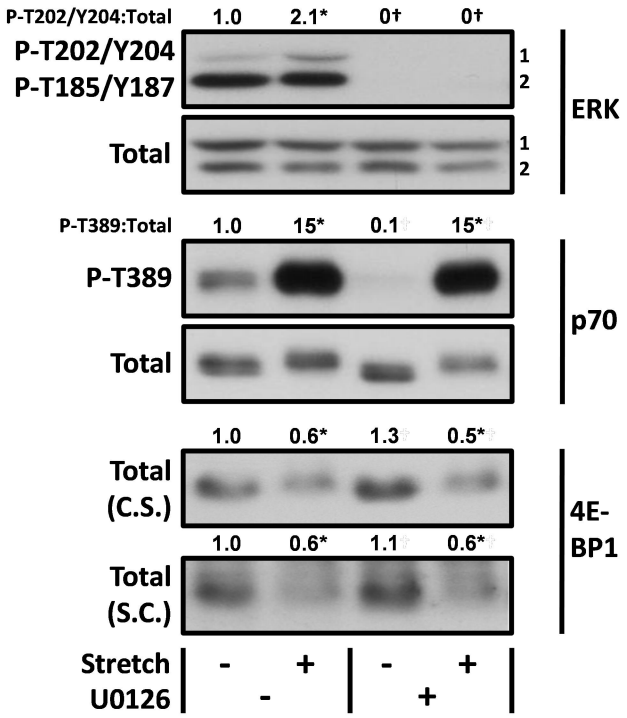

Figure 3-4. Mechanical stimulation activates mTOR signaling via an ERK-independent mechanism in DMEM media. EDL muscles were held at *Lo* and pre-incubated with DMEM media containing 50 μM U0126 (U0126 +) or the vehicle (U0126 -, DMSO) for 30 min. The muscles were then subjected to 90 min of stretch or control conditions. Muscles were collected at the end of the 90 min interval and subjected to western blot analysis for phosphorylated (P) and total ERK, p70 and total 4EBP1. The total amount, and phospho:total ratios, of each protein were measured and then expressed relative to the values obtained in the vehicle control samples (U0126 -, Stretch -). Note: total 4E-BP1 was measured with two different antibodies, i) a monoclonal antibody from Cell Signaling that was raised against a peptide surrounding the Ser112 residues (C.S.), and ii) a polyclonal antibody from Santa Cruz that was raised against full length 4E-BP1 as the antigenic peptide (S.C.). All values are presented as the mean (n = 3-5 per group). * Significantly different from the drug-matched control group, † Significantly different from the stimulation-matched vehicle group, P Patios,

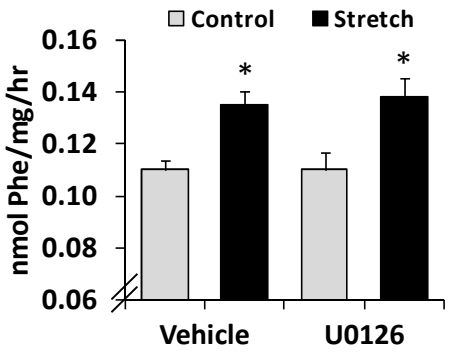

Figure 3-5. Mechanical stimulation induces an increase in protein synthesis via an ERK-independent mechanism. EDL muscles were held at *Lo* and pre-incubated with 50 μM U0126 or the vehicle (DMSO) for 30 min. The muscles were then subjected to 90 min of stretch or control conditions, and protein synthesis rates were measured during the final 30 min. All values are presented as the mean + SEM (n = 4-7 per group). * Significantly different from the drug-matched control group, P U0126

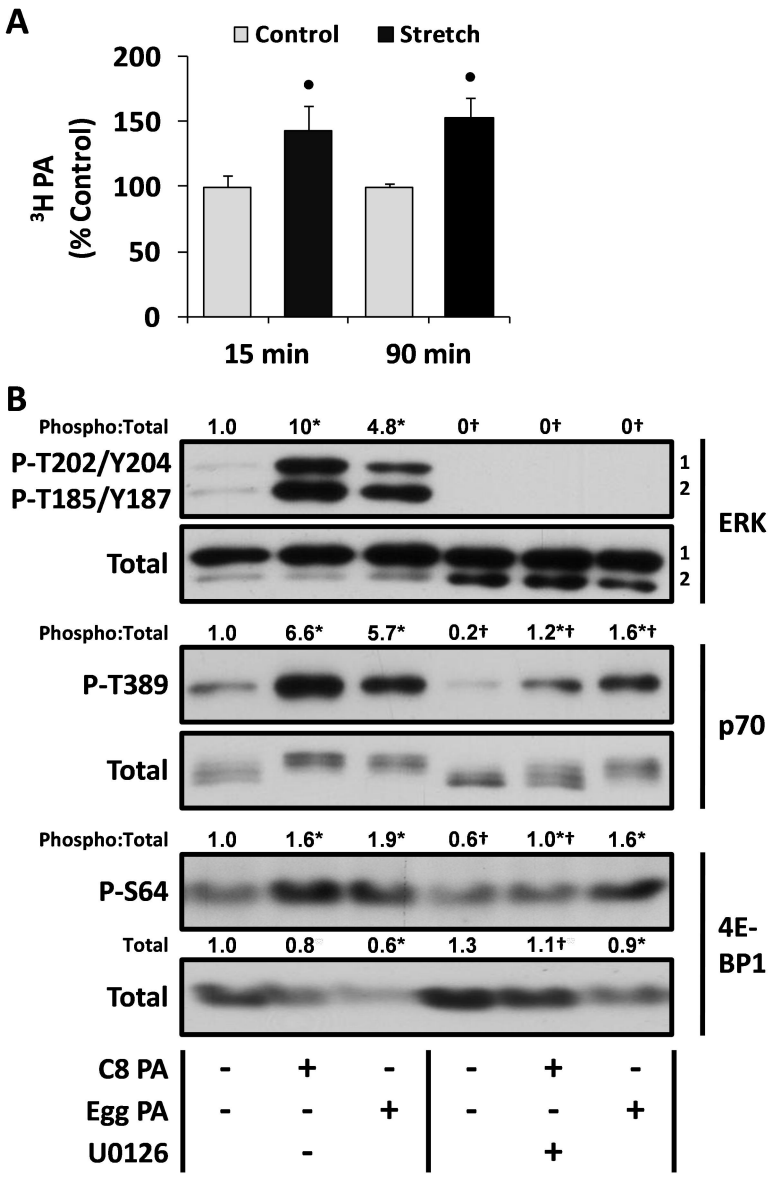

Figure 3-6. Exogenous phosphatidic acid activates mTOR signaling via an ERK-independent mechanism. (**A**) EDL muscles were held at *Lo* and pre-labeled with [^{3}H]-myristic acid for 2 h. The muscles were then subjected to 15 or 90 min of stretch or control conditions. Muscles were collected at the end of the 15 or 90 min interval, and the amount of ^{3}H-labeled PA (^{3}H PA) was measured and then expressed as a percentage of time-matched control values. The values are presented as the mean + SEM (n = 4-7 per group). • Significantly different from the time-matched control group. (**B**) C2C12 myoblasts were serum-starved overnight and then pre-incubated with 50 μM U0126 (U0126 +) or the vehicle (U0126 -, DMSO) for 30 min, followed by 20 min stimulation with 30 μM C8 PA, 300 μM Egg PA or the vehicle (Control, PBS). The samples were then subjected to western blot analysis for phosphorylated (P) and total ERK, p70, and 4E-BP1. The total amount, and phospho:total ratios, of each protein were measured and then expressed relative to the values obtained in the vehicle control samples (U0126 -, PBS). All values are presented as the mean and were obtained from three independent experiments (n = 3-5 per group). * Significantly different from the drug-matched control group, † Significantly different from the stimulation-matched vehicle group, P ratios,

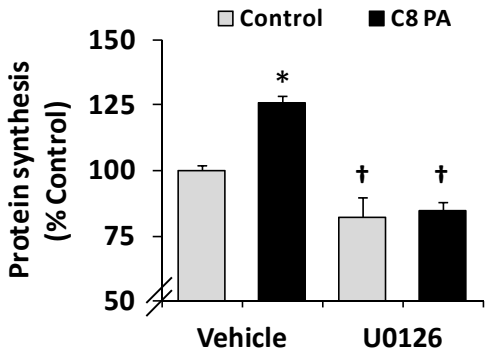

Figure 3-7. Exogenous phosphatidic acid induces protein synthesis via an ERK-dependent mechanism. C2C12 myoblasts were serum-starved overnight and then pre-incubated with 50 μM U0126 or the vehicle (DMSO) for 30 min, followed by 60 min stimulation with 30 μM C8 PA or the vehicle (PBS). Protein synthesis rates were measured during the final 30 min and expressed as a percentage of the vehicle control values. All values are presented as the mean + SEM and were obtained from five independent experiments (n = 9-11 per group). * Significantly different from the drug-matched control group. † Significantly different from the stimulation-matched vehicle group, P C8 PA

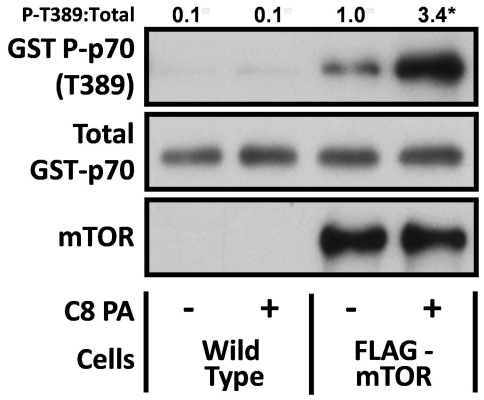

Figure 3-8. Phosphatidic acid directly promotes mTOR kinase activity *in-vitro*. Wild type C2C12 myoblasts and C2C12 myoblasts stably expressing FLAG-tagged mTOR (FLAG-mTOR) were serum starved overnight, collected, and then the cell lysates were subjected to immunoprecipitation against the FLAG epitope. The immunoprecipitates were incubated for 15 min with either 150 μM C8 PA vesicles (50% C8 PA + 50% PC) or 150 μM phosphatidylcholine (PC) vesicles (100% PC) as a control condition. mTOR kinase activity was then assayed with GST-p70 as a substrate. The resulting samples were subjected to western blot analysis, and the phospho:total ratios for GST-p70 were expressed relative to the values obtained in the PC treated FLAG-mTOR group. All values are presented as the mean and were obtained from at least three independent experiments (n = 5-8 per group). * Significantly different from the cell type-matched control group, P ratios

Chapter 4

The Role of DGKζ and Phosphatidic Acid in the Mechanical Activation of mTOR Signaling and Skeletal Muscle Hypertrophy

Jae-Sung You[1,2], Hannah C. Lincoln[2], Chan-Ran Kim[2], John W. Frey[2], Craig A. Goodman[2], Xiao-Ping Zhong[3,4], and Troy A. Hornberger[1,2]

[1]Program in Cellular and Molecular Biology and [2]Department of Comparative Biosciences in the School of Veterinary Medicine, University of Wisconsin - Madison, WI 53706

[3]Division of Allergy and Immunology, Department of Pediatrics, and [4]Department of Immunology, Duke University Medical Center, Durham, NC 27710.

Corresponding authors: Troy Alan Hornberger (Address: 2015 Linden Drive, Madison, WI 53706, USA; Phone: 608.695.2847; E-mail: troy.hornberger@wisc.edu),

Author contributions: J.-S.Y. and T.A.H. conceived and designed the experiments. J.-S.Y., H.C.L., C.-R.K, J.W.F., and C.A.G. performed the experiments and analyzed the data. X.-P.Z. provided animals. J.-S.Y. and T.A.H. wrote the paper.

This chapter was published in: *Journal of Biological Chemistry*. 2014 Jan 17;289(3):1551-63 and modified slightly to comply with the format of this dissertation

Abstract

The activation of mTOR signaling is essential for mechanically-induced changes in skeletal muscle mass, and previous studies have suggested that mechanical stimuli activate mTOR signaling through a phospholipase D (PLD)-dependent increase in the concentration of phosphatidic acid ([PA]). Consistent with this conclusion, we obtained evidence which further suggests that mechanical stimuli utilize PA as a direct upstream activator of mTOR signaling. Unexpectedly though, we found that the activation of PLD is not necessary for the mechanically-induced increases in [PA] or mTOR signaling. Motivated by this observation, we performed experiments that were aimed at identifying the enzyme(s) that promote the increase in [PA]. These experiments revealed that mechanical stimulation increases the concentration of diacylglycerol (DAG) and the activity of DAG kinases (DGKs) in membranous structures. Furthermore, using knockout mice, we determined that the zeta isoform of DGK (DGKζ) is necessary for the mechanically-induced increase in [PA]. We also determined that DGKζ significantly contributes to the mechanical activation of mTOR signaling and this is likely driven by an enhanced binding of PA to mTOR. Lastly, we found that the overexpression of DGKζ is sufficient to induce muscle fiber hypertrophy through an mTOR-dependent mechanism and this event requires DGKζ kinase activity (i.e. the synthesis of PA). Combined, these results indicate that DGKζ, but not PLD, plays an important role in mechanically-induced increases in [PA] and mTOR signaling. Furthermore, this study suggests that DGKζ could be a fundamental component of the mechanism(s) through which mechanical stimuli regulate skeletal muscle mass.

Introduction

Mechanical stimuli play a critical role in the regulation of skeletal muscle mass and the maintenance of muscle mass contributes significantly to health and issues associated with quality of life (15, 20). However, the mechanism(s) via which mechanical stimuli are converted into the molecular events that regulate muscle mass remain poorly defined. Nevertheless, advancements in our understanding are being made and it is becoming increasingly evident that a protein kinase called the mammalian [or mechanistic] target of rapamycin (mTOR) is a key determinant in the mechanical regulation of muscle mass. For example, many studies have demonstrated that mechanical stimulation leads to the activation of mTOR signaling, and its inhibition with the drug rapamycin prevents mechanically-induced increases in muscle mass (35, 67, 154). Furthermore, it has been shown that the activation of mTOR signaling is sufficient to induce an increase in muscle fiber size (i.e. hypertrophy) (79). These observations are important because they provide the cornerstone (i.e. mTOR signaling) for investigations that are aimed at developing pharmacological treatments that can mimic the effects of mechanical stimuli on muscle mass. However, in order to develop such treatments, we will first need to understand how mechanical stimuli regulate mTOR signaling.

Based on previous studies, it has been concluded that mechanical stimuli activate mTOR signaling through a unique mechanism that does not require typical candidates such as PI3K, protein kinase B, ERK, exogenous nutrients, or intracellular calcium (31, 56, 62, 63, 111). However, the identity of the unique mechanism remains unknown (67). Nonetheless, an emerging body of evidence suggests that phosphatidic acid (PA) may play a key role in this process. For instance, various forms of mechanical stimuli can promote an increase in the intracellular concentration of PA ([PA]) (56, 63, 64). Furthermore, just like mechanical stimulation, PA can activate mTOR signaling via a PI3K- and ERK-independent mechanism (56, 111). It has also been shown that PA can bind to the FKBP12-rapamycin binding (FRB) domain of mTOR, and it can directly activate mTOR kinase activity *in-vitro* (65, 66, 111). Based on these points, it has been proposed that a mechanically-induced increase in [PA] could lead to an enhanced

binding of PA to mTOR and, in-turn, facilitate the activation of mTOR signaling and ultimately muscle growth.

The potential role of PA in the mechanical activation of mTOR signaling was first exposed in 2006 when it was shown that: (i) mechanical stretch induces a transient increase in the activity of phospholipase D (PLD), (ii) the use of 1-butanol to inhibit the synthesis of PA by PLD completely prevented the mechanically-induced increase in [PA] and mTOR signaling, and (iii) mTOR signaling in mechanically-stimulated muscles exhibited resistance to the inhibitory effects of rapamycin (63). With regards to this last point, it is important to consider that rapamycin forms a complex with the FKBP12 protein and, like PA, this complex can bind to the FRB domain in mTOR (an event that is responsible for the inhibitory effects of rapamycin on mTOR signaling) (36, 37). Furthermore, it has been suggested that PA and the rapamycin-FKBP12 complex can compete with each other for binding to the FRB domain and, due to this competition, an enhanced binding of PA to the FRB domain would be expected to induce resistance to the inhibitory effects of rapamycin (155, 156). For these reasons, it has been concluded that the rapamycin resistance that is observed in mechanically-stimulated muscles indicates that mechanical stimulation promotes an enhanced binding of PA to mTOR.

A potential role of PA in the mechanical activation of mTOR signaling was further explored in a subsequent study which employed a bout of eccentric contractions as the source of mechanical stimulation (56). Again, it was determined that 1-butanol prevents the mechanical activation of mTOR signaling. Thus, the results from this study provided further support for the conclusion that a PLD-dependent increase in [PA] is necessary for the mechanical activation of mTOR signaling. However, more recent studies have shown that many of the biological effects of 1-butanol cannot be attributed to the inhibition of the synthesis of PA by PLD (157-159). Moreover, the time course of the mechanically-induced increase in PLD activity does not adequately correspond with the increase in [PA], and hence, it has been argued that a mechanically-induced increase in PLD activity may not fully explain how mechanical stimuli promote an increase in [PA] (67). In other words, the potential role of PLD and/or [PA] in the mechanical activation of mTOR signaling remains a subject of debate. Therefore, the initial

aim of the current study was to re-evaluate the role that PLD plays in controlling the mechanically-induced changes in [PA] and mTOR signaling. Surprisingly, our results demonstrated that changes in PLD activity are not required for these events. Instead, we obtained evidence which indicates that the zeta isoform of diacylglycerol kinase (DGKζ), an enzyme that synthesizes PA via the phosphorylation of diacylglycerol (DAG), is largely responsible for the mechanically-induced increase in [PA] and significantly contributes to the mechanical activation of mTOR signaling. Furthermore, we determined that the overexpression of DGKζ is sufficient to induce hypertrophy, and this effect occurs through a rapamycin-sensitive mechanism that requires DGKζ kinase activity (i.e. the synthesis of PA). Combined, these results highlight a novel role for DGKζ, but not PLD, in the mechanical activation of PA-mTOR signaling and reveal new insights into the potential mechanism(s) through which mechanical stimuli ultimately regulate muscle mass.

Methods

Materials. - Phosphatidic acid (1,2-dioctanoyl-sn-glycero-3-phosphate, C8 PA), phosphatidylcholine (1-palmitoyl-2-oleoyl-sn-glycero-3-phosphocholine, PC), diacylglycerol (1-2-dioleoyl-sn-glycerol, DAG), and phosphatidylbutanol (1,2-dioleoyl-sn-glycero-3-phosphobutanol, PtdBut), were purchased from Avanti Lipids (Alabaster, AL, USA). Phosphatidylserine (1,2-dipalmitoyl-sn-glycero-3-phosphoserine, PS) were purchased from Echelon Biosciences (Salt Lake City, UT, USA). [^{3}H]Myristic acid and [γ-^{32}P]ATP were purchased from Perkin Elmer (Waltham, MA, USA).

Rapamycin was purchased from LC laboratories (Woburn, MA, USA). 5-fluoro-2-indolyl des-chlorohalopemide (FIPI) was purchased from Sigma Aldrich (St Louis, MO, USA). 12-O-tetradecanoylphorbol-13-acetate (TPA) and R59949 was purchased from Enzo Life Sciences (Farmingdale, NY, USA). These drugs were all dissolved in DMSO to make stock solutions.

Rabbit anti- ribosomal S6 Kinase (p70^{S6k}), anti-phospho ERK1/2 (Thr202/Tyr204), anti-ERK1/2, anti-regulatory-associated protein of mTOR (Raptor), anti-mTOR, anti-GFP, and anti- lactate dehydrogenase (LDH) antibodies were purchased from Cell Signaling (Danvers, MA, USA). Rabbit anti-

phospho $p70^{S6k}$ (Thr389), goat anti-DGKζ, and FITC-conjugated goat anti-rat IgG antibodies were purchased from Santa Cruz Biotechnologies (Santa Cruz, CA, USA). Mouse anti-Na^+/K^+-ATPase antibody was purchased from Developmental Studies Hybridoma Bank (Iowa City, IA, USA). Rat anti-HA antibody was purchased from Roche (Madison, WI, USA). Rabbit anti-laminin antibody was purchased from Sigma Aldrich. HRP-conjugated anti-rabbit IgG antibody was purchased from Vector Laboratories (Burlingame, CA, USA). HRP-conjugated anti-mouse IgG, HRP-conjugated anti-rat IgG, and DyLight 594-conjugated anti-Rabbit IgG antibodies were purchased from Jackson ImmunoResearch Laboratories Inc. (West Grove, PA, USA).

Plasmid constructs and purification. - pEGFP-C3 (GFP) was purchased from Clontech (Mountain View, CA, USA). pRK5-myc-$p70^{S6k}$-glutathione transferase (GST-$p70^{S6k}$) was kindly provided by Dr. Karyn Esser (University of Kentucky, Lexington, KY, USA). YFP-tagged Ras homologue enriched in brain (YFP-Rheb) was obtained from Dr. Kun-Liang Guan (University of California San Diego, La Jolla, CA, USA). pHA3-DGKζ with three tandem N-terminal HA epitope tags (HA-WT-DGKζ) was a generous gift from Dr. Matthew Topham (University of Utah, Salt Lake City, UT, USA). pHA3-kinase dead DGKζ (HA-KD-DGKζ) was generated from the pHA3-DGKζ via a guanine-to-adenosine change (160) at nucleotide 1756 of DGKζ (NCBI Reference Sequence NM_001105540.1) using a QuickChange Lightning Mutagenesis kit (Agilent Technologies, Inc., Santa Clara, CA, USA). All plasmid DNA was grown in DH5α Escherichia coli, purified with an Endofree plasmid kit (QIAGEN, Valencia, CA, USA), and re-suspended in sterile PBS.

Animals. - Wild type FVB/N and C57BL/6 mice were purchased from Charles River Laboratories (Wilmington, MA, USA), Taconic (Hudson, NY, USA), or Jackson Laboratories (Bar Harbor, MA, USA). $DGK\zeta^{-/-}$ C57BL/6 mice have been described previously (161) and were kindly provided by Dr. Xiaoping Zhong (Duke University, Durham, NC, USA). All animals were housed in a room maintained at 25°C with a 12 h:12 h light:dark cycle and received food and water ad libitum. Eight- to ten-week-old animals were used for all experiments and they were anaesthetized with an intraperitoneal injection of ketamine (100 mg/kg) and xylazine (10 mg/kg) before all surgical procedures. After muscle collection, mice were

sacrificed by cervical dislocation under anesthesia. For all non-histochemical analyses, the muscles were immediately frozen in liquid nitrogen at the end of the experimental procedures. All methods were approved by the Institutional Animal Care and Use Committee of the University of Wisconsin-Madison under protocol # V01324.

Ex-vivo mechanical stimulation. - Mouse extensor digitorum longus (EDL) muscles were mechanically-stimulated in an ex-vivo organ culture system which consisted of a refined myograph apparatus (Kent Scientific, Torrington, CT, USA) and an organ culture bath as previously described (31). Briefly, the proximal and distal tendons of EDL muscles were connected to a micromanipulator and the lever arm of a force transducer, respectively. Then, the length of the muscle was adjusted until a passive tension of 13.5 mN was obtained (note: preliminary studies demonstrated that the optimal length (Lo) of EDL muscles was obtained at 13.5 mN). The muscles were then subjected to intermittent 15% passive stretch as a source of mechanical stimulation or held static at Lo as a control condition. The bath incubation media consisted of Krebs Henseleit Buffer (120 mM NaCl, 4.8 mM KCl, 25 mM NaHCO3, 2.5 mM CaCl2, 1.2 mM KH2PO4, 2 mM MgSO4, and 5 mM HEPES) supplemented with 1X MEM amino acid mixture (Invitrogen, Carlsbad, CA, USA) and 25 mM glucose. The media was maintained at 37°C with continuous 95% O_2 and 5% CO_2 gassing, and it was exchanged with fresh media at 30 min intervals.

Skeletal muscle transfection and rapamycin injections. - Mouse tibialis anterior (TA) muscles were transfected by electroporation as previously described (79). In brief, a small incision was made through the skin covering the TA muscle. A total of 30 - 50 μg of plasmid DNA (GFP, HA-WT-DGKζ, or HA-KD-DGKζ) solution was then injected into the proximal (6 μl) and distal (6 μl) ends of the muscle belly with a 27-gauge needle. After the injections, 2 stainless steel pin electrodes (1-cm gap) connected to an ECM 830 electroporation unit (BTX/Harvard Apparatus, Holliston, MA, USA) were laid on top of the proximal and distal myotendinous junctions. Then, eight 20-ms square-wave electric pulses at a frequency of 1 Hz were delivered onto the muscle with a field strength of 160 V/cm. Following the electroporation procedure, incisions were closed with Vetbond surgical glue and the animals were allowed to recover for

3 or 7 days. In some experiments, vehicle or rapamycin solution was administered into the animals via intraperitoneal injections immediately following the electroporation procedure. Rapamycin solution was prepared by dissolving the appropriate volume of the stock solution (in DMSO) that was needed to inject mice with 1.5 or 4.5 mg/kg body weight in 200 µl of PBS. For the vehicle control solution, an equivalent amount of DMSO was dissolved in 200 µl of PBS. These injections were repeated every 24 h.

Cell culture and transfection. - C2C12 myoblasts were cultured in growth media consisting of high glucose DMEM (HyClone, Logan, UT, USA) supplemented with antibiotics and antimycotics (100 µg/ml streptomycin, 100 U/ml penicillin, and 0.25 µg/ml amphotericin) and 10% fetal bovine serum (Gibco, Grand Island, NY, USA). For mTOR kinase activity assay, C2C12 myoblasts stably expressing FLAG-tagged mTOR (FLAG-mTOR) were obtained from Dr. Jie Chen (University of Illinois, Urbana, IL) and were cultured in the growth media that was further supplemented with 0.2 mg/ml G418 (HyClone). For stimulation experiments, the growing myoblasts were plated on 6-well dishes at 40-60% confluence. During this time, if needed, cells were co-transfected with 2 µg of GFP, HA-WT-DGKζ, or HA-KD-DGKζ, and 0.2 µg of GST-$p70^{S6k}$ constructs by using Lipofectamine 2000 (Life Technologies, Inc., Grand Island, NY, USA) according to the manufacturer's instructions. The following day, the cells were serum-starved in the absence of any antibiotics and antimycotics before being subjected to experimental treatments. Cell cultures were maintained at 37°C in a humidified atmosphere of 95% air and 5% CO_2.

Fractionation. - Frozen muscles were homogenized with a Polytron homogenizer in ice-cold fractionation buffer [20 mM Tris (pH 7.5), 250 mM sucrose, 1 mM EDTA, 1 mM EGTA, 1 mM DTT, 50 mM NaF, 1 mM Na_3VO_4, 1 mM PMSF, and 20 µg/ml each leupeptin, pepstatin, aprotinin, and soybean trypsin inhibitor] and the homogenates were pre-cleared by centrifugation at 1000 g (4°C) for 10 min. The pre-cleared supernatants (whole lysate) were further centrifuged at 100,000 g (4°C) for 1 h to separate the soluble supernatants (cytosolic fraction) and insoluble pellets (crude membrane fraction) as previously described (162). The membrane pellets were washed once and re-suspended in the ice-cold fractionation buffer for DGK activity assay or Laemmli buffer for western blot analysis. The protein concentration in each whole lysate sample was determined with the DC protein assay kit (Bio-Rad, Hercules, CA, USA)

and used to control the loading amounts of cytosolic and/or membrane protein in the DGK activity assay and western blot analysis.

In-vitro DGK activity assay. - DGK activity was measured by the standard otylglucoside(OG)/PS-mixed micelle assay as previously described (163). In brief, OG/PS-mixed micelles were prepared by re-suspending dried DAG and PS in 5x OG buffer (275mM OG, 1mM DTPA) with vortexing and sonication. Then, the reaction was initiated by adding 10 µl of each diluted sample into 90 µl of reaction mixture (20 µl of mixed micelles added to 70 µl of reaction buffer), which yielded a final concentration of [55 mM OG, 0.25 mM DAG (0.87 mol% in micelles), 1 mM PS, 50 mM imidazole (pH 6.6), 50 mM NaCl, 12.5 mM $MgCl_2$, 1 mM EGTA, 0.2 mM DTPA, 1 mM DTT, 500 µM ATP, and 1 µCi [γ-^{32}P]ATP]. Following a 30 min incubation at 25°C, the reaction was terminated by the addition of 0.45 ml chloroform-methanol 1:2 (v/v) and 0.15 ml of 1% perchloric acid. After vortexing, 0.15 ml of chloroform and 0.15 ml of 1% perchloric acid were added to the mixture and vortexed again. The mixture was centrifuged at 2000 g for 5 min and the lower organic phase was washed twice with 1% perchloric acid. [γ-^{32}P]PA in the organic phase was separated on LK5D silica gel plates by TLC with a solvent system consisting of ethyl acetate–isooctane–acetic acid–water 13:2:3:10 (v/v) as previously described (63). The amount of [γ-^{32}P]PA was then visualized and quantified with a Strom Phosphoimager (Molecular Dynamics, Sunnyvale, CA, USA).

In-vitro mTOR kinase activity assay. - Growing C2C12 myoblasts stably expressing FLAG-mTOR were plated and then maintained in G418-free growth media. Upon confluence, the cells were serum-starved overnight and then collected in either ice cold CHAPS lysis buffer [40 mM HEPES (pH 7.4), 2 mM EDTA, 0.3% CHAPS, 10 mM sodium pyrophosphate, 10 mM β-glycerophosphate, and 1 tablet of EDTA-free protease inhibitors (Roche) per 25 mL] or Triton X-100 lysis buffer [40 mM Tris (pH 7.5), 1 mM EDTA, 5 mM EGTA, 0.5% Triton X-100, 25 mM β-glycerolphosphate, 25 mM NaF, 1 mM Na_3VO_4, 10 µg/ml leupeptin, and 1 mM PMSF]. Fresh cell lysates were centrifuged at 2500 g for 5 min, and 100-150 µg of protein from the supernatant was immunoprecipitated for the FLAG tag by incubating with 10 µl of EZview red ANTI-FLAG M2 agarose affinity gel beads (Sigma-Aldrich) at 4°C

for 2 h. Following the incubation, the beads were pelleted by centrifugation at 500 g for 30 s and washed with fresh ice cold wash buffer [40 mM HEPES (pH 7.4), 150 mM NaCl, 2 mM EDTA, 0.3% CHAPS, 10 mM sodium pyrophosphate, 10 mM β-glycerophosphate, and 1 tablet of EDTA-free protease inhibitors per 25 ml] three times and kinase wash buffer [25 mM HEPES (pH 7.4) and 20 mM KCl] two times.

For lipid stimulations, C8 PA vesicles (50% C8 PA + 50% PC) or PC vesicles (100% PC) were prepared by drying lipids under nitrogen gas and dissolving in vesicle buffer [150 mM NaCl and 10 mM Tris (pH 8.0)] with 5 min of sonication at a concentration of 6 mM. The lipid vesicles were then diluted to 150 μM in 1.5x reaction buffer (see below), and 10 μl of this solution was incubated with the immunoprecipitates at 30°C for 15 min. The mTOR kinase reaction towards purified GST-$p70^{S6k}$ (111) was initiated by adding 5 μl of 750 μM ATP into the immuoprecipitates, which yields a final mTOR kinase assay buffer that contains [25 mM HEPES (pH 7.4), 50 mM KCl, 10 mM MgCl2, 250 μM ATP, 50 ng GST-$p70^{S6k}$, and 100 μM C8 PA or PC vesicles]. Following 20 min of incubation, the reaction was terminated by the addition of 25 μl of 2x Laemmli Buffer. Samples were boiled for 5 min and subjected to western blot analysis as described below.

Western blot analysis. - Frozen muscles were homogenized in the ice-cold Triton X-100 lysis buffer and the whole homogenates were used for analysis. Myoblasts were lysed in the ice-cold Triton X-100 buffer, centrifuged at 500 g (4°C) for 5 min, and the supernatant was used for further analyses. The protein concentration in each sample was determined with the DC protein assay kit.

Equal amounts of protein from each sample were dissolved in 2x Laemmli buffer before being subjected to SDS-PAGE. Following the electrophoretic separation, proteins were transferred to a PVDF membrane, blocked with 5% milk in TBST (TBS with 1% Tween 20) for 1 h, and probed with the indicated primary antibodies overnight at 4°C. The membranes were then washed for 30 min in TBST and incubated with the appropriate HRP-conjugated secondary antibodies for 45 min at room temperature. Following 30 min of washing in TBST, the blots were incubated in regular ECL (Pierce, Rockford, IL, USA) or ECL Prime (GE healthcare, Piscataway, NJ, USA) for 5 min at room temperature. Images of the blots were either captured on film or with a Chemi410 camera mounted to a UVP Autochemi system

(UVP, Upland, CA, USA). Once the appropriate image was captured, the membranes were stained with Coomassie Blue to verify equal loading throughout all lanes. Densitometric measurements of each blot were carried out using ImageJ (NIH).

Immunohistochemical analysis. - Transfected muscles were subjected to immunohistochemistry as previously described (79). Briefly, collected muscles were incubated in PBS containing 4% paraformaldehyde with gentle rocking at 4°C for 30 min. The muscles were then submerged in optimal cutting temperature compound (Tissue-Tek; Sakura, Torrance, CA, USA) at resting length and frozen in liquid nitrogen-chilled isopentane. Cross sections (10 μm in thickness) from the midbelly of the muscle were obtained with a cryostat and fixed in −20°C acetone for 10 min. Sections were warmed to room temperature for 5 min and then rehydrated with cool steam vapors followed by a 15 min incubation in PBS. Note: in experiments that did not include GFP-transfected muscles, the above paraformaldehyde and steam vapor treatments were omitted as in (164). The rehydrated sections were then incubated in solution A (PBS containing 0.5% BSA and 0.5% Triton X-100) for 20 min and probed with the indicated primary antibodies dissolved in solution A for 45 min at room temperature. Sections were washed with PBS and then incubated with the appropriate fluorophore-conjugated secondary antibodies dissolved in solution A for 1 h at room temperature. Finally, the sections were washed with PBS and images of the different fluorophores were captured with a DS-QiMc camera on an 80i epi-fluorescence microscope (both from Nikon, Tokyo, Japan). The monochrome images were merged with NIS-Elements D image analysis software (Nikon) and the average cross-sectional area (CSA) of 35-120 randomly selected fibers per sample was measured by tracing the periphery of individual fibers along the laminin stain. All analyses were performed by investigators that were unaware of the sample identification.

Analysis of PLD activity and lipid concentrations. - PLD activity, [PA], and [DAG], in skeletal muscles ex-vivo, were measured with modifications of previously described methods (63). Briefly, EDL muscles were pre-labeled in the organ culture system with media containing [^{3}H]myristic acid (2.5 μCi/ml) for 2 h and then subjected to experimental treatments. For the measurement of PLD activity, the PLD-mediated transphosphatidylation reaction was initiated by incubating the muscles with fresh media

containing 0.5% 1-butanol during the final 15 min of the treatments. The muscles were homogenized with a Polytron in chloroform–methanol 2:1 (v/v), and total lipids were extracted according to Folch et al. (1957). The extracted lipids were combined with 10 μg of PtdBut, PA, or DAG standards and then subjected to TLC as described in the DGK activity assay section. The solvent system consisted of ethyl acetate–isooctane–acetic acid–water 13:2:3:10 (v/v) for separation of PtdBut and PA, or hexane-diethyl ether-acetic acid 50:50:1 (v/v) for separation of DAG. The standard PtdBut, PA, or DAG spots, containing the ^{3}H-labelled PtdBut, PA, or DAG, respectively, was visualized by iodine staining and scraped off the TLC plate to count the amount of radioactivity by liquid scintillation spectrometry (LSS). An aliquot of the extracted lipids was also subjected to the LSS to count radioactivity in the total lipids. Final calculations for PLD activity, [PA], and [DAG], were made by dividing the amount of radioactivity in the Ptdbut, PA, or DAG spot, by the amount of radioactivity in the total lipid extract.

For analysis of PLD activity and [PA] in cells, myoblasts were pre-labeled in serum-free media containing [^{3}H]myristic acid (2.5 μCi/ml) overnight and then washed twice with fresh serum-free media. After an additional 2 h incubation in serum-free media, the cells were subjected to experimental treatments in the presence (for PLD activity) or absence (for [PA]) of 0.3% 1-butanol during the final 15 min of the treatments. The cells were collected in chloroform–methanol 2:1 (v/v) and then processed as described above.

Statistical analysis. - All values are expressed as means (+ SEM in graphs). Statistical significance was determined by using the student's t-test (2-tailed, unpaired) or ANOVA (one-way or two-way) followed by Student–Newman–Keuls post hoc analysis. Differences between groups were considered significant when $P \leq 0.05$. All statistical analyses were performed on SigmaStat software (San Jose, CA, USA).

Results

Evidence that PA can function as a direct upstream activator of mTOR signaling in response to mechanical stimulation. - In this study, we employed the same ex-vivo model of mechanical

stimulation that was previously used to expose the potential role of PLD and PA in the mechanical activation of mTOR signaling (63). With this model, it has been shown that mechanical stimulation induces an increase in [PA] and rapamycin-sensitive mTOR signaling (63, 111); however, whether the increase in [PA] is driven through a rapamycin-sensitive mechanism has not been addressed. This is an important question because recent studies have revealed that rapamycin-sensitive mTOR can phosphorylate and inhibit the activity of the phosphatidic acid phosphatase called Lipin 1 (165, 166). Thus, it remained possible that the mechanically-induced increase in [PA] could be driven through a pathway that lies downstream, rather than upstream, to the activation of rapamycin-sensitive mTOR. Therefore, to test this, we subjected muscles to mechanical stimulation in the presence or absence of rapamycin and then examined the muscles for changes in mTOR signaling and [PA]. As expected, rapamycin eliminated the mechanical activation of rapamycin-sensitive mTOR signaling as revealed by changes in the phosphorylation of $p70^{S6k}$ on the T389 residue (130) (Figure 4-1A). However, rapamycin did not affect the mechanically-induced increase in [PA] (Figure 4-1B). Based on these results, it can be concluded that the mechanically-induced increase in [PA] is driven through a pathway that lies upstream and/or parallel to the activation of the rapamycin-sensitive elements of mTOR signaling.

mTOR is typically found in multi-protein complexes such as the mTOR complex 1 (mTORC1) and the mTOR complex 2 (mTORC2). mTORC1 is defined by the presence of a protein called Raptor, whereas mTORC2 contains a protein called the rapamycin-insensitive companion of mTOR (Rictor), but not Raptor. Previous studies have suggested that signaling by mTORC1, but not mTORC2, is responsible for controlling the rapamycin-sensitive phosphorylation of substrates such as $p70^{S6k}$(T389) (116). However, more recent studies have shown that mTOR, in the absence of Raptor, can also regulate $p70^{S6k}$(T389) phosphorylation through a rapamycin-sensitive mechanism (37). In other words, it appears that there is an uncharacterized rapamycin-sensitive pool of mTOR that does not involve the classic mTORC1. Furthermore, it was recently proposed that mechanical stimuli might specifically regulate this uncharacterized pool of mTOR rather than mTORC1 (111). Based on this possibility, we wanted to determine if PA could activate mTOR signaling in the absence of Raptor. To test this, we collected

C2C12 myoblasts that stably express FLAG-mTOR in CHAPS lysis buffer, to preserve the mTOR/Raptor interaction, or Triton X-100 lysis buffer, to dissociate the mTOR/Raptor interaction. mTOR from the different lysis conditions was then immunoprecipitated and incubated with lipid vesicles composed of 50% C8 PA and 50% PC, or 100% PC as a control condition. The immunoprecipitates were then subjected to an in-vitro mTOR kinase activity assay with $p70^{S6k}$ as a substrate. In this experiment, we confirmed an enhanced mTOR kinase activity in the absence of Raptor as previously demonstrated (Figure 4-1C) (167). Importantly, the results also demonstrated that PA can induce an increase in mTOR kinase activity and that Raptor is not required for this effect (Figure 4-1C). Combined, the results presented in Figure 4-1 establish that a mechanically-induced increase in [PA] could function as a direct upstream activator of mTOR signaling.

Changes in PLD activity are not required for a mechanically-induced increase in [PA] or mTOR signaling. - To re-examine the role of PLD in the mechanical regulation of [PA] and mTOR signaling, we first performed measurements of PLD activity in muscles that were pre-labeled with [^{3}H]myristic acid which preferentially labels the PLD substrate PC (168). In contrast to the previous study that used [^{3}H]arachidonic acid for labeling (63), our results indicated that mechanical stimulation does not alter the activity of PLD towards [^{3}H]myristic acid-labeled substrates (Figure 4-2A). However, mechanical stimulation was still able to induce an increase in the concentration of [^{3}H]myristic acid-labeled PA (Figure 4-2E). This observation suggested that changes in PLD activity are not required for a mechanically-induced increase in [PA].

To further determine if changes in PLD activity are required for a mechanically-induced increase in [PA], we employed FIPI, which is known to be a more potent and specific inhibitor of PLD than 1-butanol (157). With this compound, we first performed a dose-response analysis in C2C12 myoblasts to identify the minimal concentration of FIPI that was needed to fully inhibit an agonist-induced increase in PLD activity. When TPA was used as a PLD agonist, it was determined that 100 nM FIPI could completely prevent the TPA-induced increase in both PLD activity and [PA] (Figure 4-2, B and C). We also determined that 100 nM FIPI could completely block the TPA-induced increase in PLD activity

when muscles were incubated in the ex-vivo organ culture system (Figure 4-2D).

Having established that 100 nM FIPI could block agonist-induced changes in PLD activity, we next set out to determine if FIPI would impair the ability of mechanical stimuli to induce an increase in [PA] and mTOR signaling. As shown in Figure 4-2E, the increase in [PA] induced by both 15 and 90 min of mechanical stimulation was not impaired when muscles were treated with FIPI. Furthermore, FIPI did not alter the ability of mechanical stimuli to induce an increase in mTOR signaling (Figure 4-2F). When combined, these results demonstrate that mechanical stimuli induce an increase in [PA] and mTOR signaling via a PLD-independent mechanism.

Mechanical stimulation increases [DAG] and membrane DGK activity. - Our finding that changes in PLD activity are not required for a mechanically-induced increase in [PA] inspired us to search for other enzyme(s) that could contribute to this event. During this search, we realized that several forms of mechanical stimuli, including contractions and stretch, have been reported to induce a rapid increase in the intracellular concentration of DAG [DAG] (64, 169). Based on these reports, we envisioned the potential for a mechanism in which mechanical stimulation induces an accumulation of DAG and this, in turn, would provide an enhanced level of substrate for the DGKs. Since the DGKs can synthesize PA via the phosphorylation of DAG, the net result of the DAG accumulation would be an enhanced synthesis of PA. To begin testing this possibility, we first wanted to determine if our model of mechanical stimulation also promotes an increase in [DAG]. As shown in Figure 4-3A, [DAG], just like [PA], was significantly elevated after both 15 min and 90 min of mechanical stimulation. Next, we asked if the elevated levels of [DAG] are associated with an increase in DGK activity. Interestingly, we found that mechanical stimulation induced a biphasic increase in membranous DGK activity (Figure 4-3, B and C). However, the activity of DGK in whole muscle lysates was not increased by mechanical stimulation (Figure 4-3D). Thus, it appears that mechanical stimulation causes a pool of DGK to translocate to membranous structures and/or allosterically activates membrane-associated DGK.

R59949 does not inhibit the mechanically-induced increase in [PA] or the activation of mTOR signaling. - The aforementioned findings prompted us to further explore the potential role of the DGKs in

the mechanical regulation of [PA] and mTOR signaling. To begin this analysis, we first took advantage of the DGK inhibitor R59949. Before describing our results, it is important to mention that the DGK family of enzymes is composed of at least 10 different isoforms and currently available inhibitors of DGK (R59949 and its weaker analogue R59902) preferentially inhibit only the α, β, γ, and θ isoforms of DGK (170, 171). Consistent with these points, we found that R59949 (100 μM) induces a partial, but significant, inhibition of basal DGK activity (Figure 4-4A). However, R59949 did not inhibit the mechanically-induced increase in [PA] or mTOR signaling (Figure 4-4, B and C). Based on these results, we have concluded that the α, β, γ, and θ isoforms of DGK are not necessary for a mechanically-induced increase in [PA] and mTOR signaling.

The mechanically-induced increase in [PA] and mTOR signaling is impaired in muscles from DGKζ $^{-/-}$ mice. - Previous studies have shown that the δ, ε and ζ isoforms of DGK are highly expressed in skeletal muscle (172). Of these isoforms, we became particularly interested in DGKζ because this isoform is resistant to the inhibitory effects of R59949 and, in HEK 293 cells, it has been reported that the synthesis of PA by DGKζ contributes to the serum-induced activation of mTOR signaling (170, 173). Moreover, we were able to further validate this latter point in C2C12 myoblasts by demonstrating that the overexpression of DGKζ enhances the serum-induced activation of mTOR signaling and this effect requires the kinase activity of DGKζ (i.e. the synthesis of PA) (Figure 4-5). To the best of our knowledge, DGKζ is the only isoform of DGK that has been shown to exert a regulatory effect on mTOR signaling. Therefore, we set out to perform a series of experiments that were specifically aimed at addressing the role of DGKζ in the mechanical regulation of [PA] and mTOR signaling. To accomplish this, we employed muscles from homozygous DGKζ knockout (DGKζ$^{-/-}$) mice. As originally described (161), DGKζ$^{-/-}$ mice were viable, fertile, and had a normal appearance. Furthermore, our initial analysis of the muscles from DGKζ$^{-/-}$ mice did not reveal any overt abnormality in phenotypes such as muscle weight to body weight ratio, muscle fiber type distributions, and histological appearance (data not shown).

Previous studies have suggested that the loss of DGKs can result in an accumulation of DAG and a concomitant elevation in the PKC-ERK signaling pathway (163, 173, 174). Consistent with these reports,

we found that EDL muscles from DGKζ$^{-/-}$ mice exhibit elevated basal levels of [DAG] (140% of control, $P < 0.0001$) and ERK phosphorylation (Figure 4-6A). Since signaling through ERK has been widely implicated in the activation of mTOR signaling, we were not surprised to find that the DGKζ$^{-/-}$ muscles also exhibit elevated basal levels of mTOR signaling under both in-vivo and ex-vivo conditions (Figure 4-6, A and C). Combined, these results indicate that muscles from DGKζ$^{-/-}$ mice display the expected molecular phenotypes.

To address the role of DGKζ in the mechanical regulation of [PA] and mTOR signaling, EDL muscles from WT and DGKζ$^{-/-}$ mice were subjected to mechanical stimulation and examined for changes in [PA] and mTOR signaling. Intriguingly, we found that the mechanically-induced increase in [PA] was almost completely abolished in the muscles from DGKζ$^{-/-}$ mice (Figure 4-6B). Furthermore, the mechanical activation of mTOR signaling was also significantly impaired in the DGKζ$^{-/-}$ muscles (Figure 4-6, C and D). Finally, when mechanically-stimulated muscles from WT and DGKζ$^{-/-}$ mice were treated with increasing doses of rapamycin (0-20 nM), it was determined that mTOR signaling in the DGKζ$^{-/-}$ muscles was significantly more sensitive to the inhibitory effects of rapamycin (Figure 4-6E). As mentioned in the introduction, mTOR signaling in mechanically-stimulated muscles exhibits resistance to the inhibitory effects of rapamycin, and this is most likely driven by an enhanced binding of PA to the FRB domain in mTOR. Thus, the results from these experiments not only demonstrate that DGKζ is largely responsible for the mechanically-induced increase in [PA], but also suggest that the DGKζ-dependent increase in [PA] leads to an enhanced binding of PA to mTOR and, in-turn, the activation of mTOR signaling.

Overexpression of DGKζ induces hypertrophy through a kinase-dependent and rapamycin-sensitive mechanism. - Previous studies have shown that signaling through mTOR is necessary for a mechanically-induced hypertrophic response, and that the activation of mTOR signaling is sufficient to induce hypertrophy (35, 79). Thus, we wanted to know if an enhanced synthesis of PA by DGKζ could also promote a hypertrophic response. To address this question, we transfected TA muscles with plasmid DNA encoding WT-DGKζ, a kinase-dead mutant of DGKζ (KD-DGKζ), or GFP as a control condition.

As expected, the overexpression of WT-DGKζ, but not KD-DGKζ, led to an enhanced synthesis of PA as assessed by an in-vitro DGK activity assay (Figure 4-7C). Furthermore, the examination of CSA revealed that the WT-DGKζ-transfected fibers were 33% larger than non-transfected fibers of the same muscles, whereas the CSA of fibers transfected with KD-DGKζ or GFP was not altered (Figure 4-7, A and B). Based on these results, it can be concluded that the overexpression of DGKζ is sufficient to induce hypertrophy and this effect requires the kinase activity of DGKζ (i.e. the synthesis of PA).

Next, we wanted to determine if DGKζ induces hypertrophy through an mTOR-dependent mechanism. To this end, mouse TA muscles were transfected with WT-DGKζ, or Rheb as a positive control. Immediately following transfection, the mice were subjected to daily injections of rapamycin or the solvent vehicle as a control condition. As shown in Figure 4-7, D and E, a daily dose of 1.5 mg/kg rapamycin prevented the robust hypertrophic response that is induced by the overexpression of Rheb. However, the same dose of rapamycin did not significantly inhibit the hypertrophic effect of WT-DGKζ (Figure 4-7, D and E). This result was not entirely surprising because the fibers transfected with WT-DGKζ would presumably have higher levels of [PA] which, in-turn, would be expected to confer resistance to the inhibitory effects of rapamycin. Therefore, we performed an additional experiment in which the mice were injected with a higher dose of rapamycin (4.5 mg/kg/day). In this case, the results demonstrated that the DGKζ-induced hypertrophic response was significantly inhibited (Figure 4-7, D and E). Thus, it appears that the DGKζ-induced hypertrophic response is driven, at least in part, through an mTOR-dependent mechanism. Furthermore, just like the mechanical activation of mTOR signaling, the DGKζ-induced hypertrophic response is partially resistant to the inhibitory effects of rapamycin which suggests that it is mediated by an enhanced binding of PA to mTOR.

Discussion

How mechanical stimuli are converted into the molecular events that regulate skeletal muscle mass has been one of the long-standing questions in the field of muscle biology. Accordingly, several hypotheses have been proposed to explain this phenomenon, and one that has attracted increasing interest

predicts that a mechanically-induced increase in [PA] leads to an enhanced binding of PA to mTOR and, in-turn, promotes the activation of mTOR signaling and ultimately muscle growth (67). In this study, we have obtained several novel lines of evidence which support this hypothesis by identifying that: i) mechanical stimulation induces an increase in [PA] via a DGKζ-dependent mechanism, ii) loss of DGKζ impairs mechanically-induced increases in both mTOR signaling and a sign of enhanced PA-mTOR binding, and iii) overexpression of DGKζ promotes fiber hypertrophy through a mTOR-dependent mechanism that requires the ability of DGKζ to synthesize PA.

In the early 2000's, a potential role for PLD and PA in the regulation of mTOR signaling was unveiled by studies that used primary alcohols (e.g. 1-butanol) to inhibit the PLD-catalyzed synthesis of PA. For example, these studies concluded that the PLD-dependent synthesis of PA is necessary for the serum- and phenylephrine-induced activation of mTOR signaling (156, 175). Based on these studies, it was subsequently hypothesized that the mechanical activation of mTOR signaling might also be mediated by the PLD-dependent synthesis of PA. Indeed, this appeared to be confirmed when it was demonstrated that 1-butanol can prevent mechanically-induced increases in both [PA] and mTOR signaling (63). However, the involvement of PLD in these events became uncertain when it was shown that a newly developed PLD-specific inhibitor (FIPI) did not affect many of the biological processes that are inhibited by 1-butanol (157, 158). Moreover, a recent study has also shown that several ethanol (a two-carbon primary alcohol)-sensitive events were not observed when more reliable techniques, such as a genetic deletion of PLD, were employed (159). Consistent with the concerns raised by these studies, we found that, although FIPI could block agonist-induced changes in PLD activity, it did not prevent the mechanically-induced increase in [PA] or mTOR signaling. Therefore, we have concluded that the previously reported effects of 1-butanol on mechanically-induced changes in [PA] and mTOR signaling were most likely due to off-target / PLD-independent events.

Despite the wide use of primary alcohols, there have been many studies that did not rely solely on primary alcohols to modulate PLD activity, and these studies still demonstrate that PLD can play an important role for the regulation of mTOR signaling. For example, using shRNA-mediated knockdown of

PLD1, it has been shown that an increase in PLD1 activity is required for the activation of mTOR signaling that occurs during myoblast differentiation and in response to amino acid stimulation (148, 176). A more recent study has also found that modulations of PLD1 expression are sufficient to induce changes in both mTOR signaling and the size of L6 myotubes (177). Interestingly, this study also determined that, like DGKζ, overexpression of PLD1 is sufficient to induce hypertrophy in-vivo. Although the link between the regulation of PLD and muscle mass under physiologically relevant conditions is still not known, these results provide fundamental support for the conclusion that an elevation in [PA] can induce the activation of mTOR signaling and ultimately hypertrophy of skeletal muscle.

Our finding that DGKζ contributes to the mechanical activation of PA-mTOR signaling is novel; however, the mechanism through which mechanical stimuli use DGKζ to promote an increase in [PA] and mTOR signaling remains unknown. Nevertheless, recent progress in mTOR biology may have revealed some important clues. Specifically, it has been demonstrated that mTOR can colocalize with late endosomal / lysosomal structures (LEL) where its direct activators, such as Rheb, reside (148, 162, 178, 179). Furthermore, it has been shown that forced targeting of mTOR to the LEL is sufficient to activate mTOR signaling, indicating that the LEL is a key integration site for the regulation of mTOR signaling (178, 180). More recently, it was also shown that the LEL is highly enriched with PA and that mechanical stimulation leads to an increase in the colocalization of mTOR with the LEL (162, 181). This latter observation is of particular interest because it suggests that mechanical stimulation could induce an enhanced binding of PA to mTOR, at least in part, by increasing the association of mTOR with the PA-enriched LEL.

Based on the information mentioned above, it is tempting to suggest that DGKζ could regulate PA-mTOR signaling by directly controlling the level of PA at the LEL. In support of this possibility, it has been reported that DGKζ is able to physically interact with β-arrestins and sorting nexin 27 (SNX27), both of which are found on early endosomal structures (182, 183). Since early endosomes can transform into LEL, the recruitment of DGKζ into early endosomes by β-arrestins and/or SNX27 might ultimately contribute to an enrichment of PA at the newly formed LEL. Interestingly, it has been shown that

mechanical stretching of bladder tissues results in a very rapid and robust increase in the endocytosis of the apical membrane which is then delivered to LEL for degradation (49). Since endocytosis transports β-arrestins and its associated proteins (e.g. DGKζ) to early endosomes, it is possible that mechanical stimulation induces an enhanced targeting of DGKζ to early endosomes, and ultimately the LEL, by promoting endocytosis (48). Consistent with this possibility, we have recently shown that mechanical stimulation induces an increase in the number of LEL (184). Furthermore, in the current study we found that mechanical stimulation promotes an increase in membranous DGK activity which might reflect an enhanced localization of DGKζ with the early endosomes / LEL. If correct, such an event would be expected to promote an increase in [PA] at the LEL and, in-turn, an enhanced binding of PA to mTOR and ultimately the activation of mTOR signaling. Clearly, this hypothesis is quite speculative and the exact mechanism(s) via which DGKζ contributes to the mechanical activation of PA-mTOR signaling remains to be defined. Nonetheless, examining the potential role of the LEL in this process appears to be an area that is worthy of further investigation.

Another novel finding in this study is that overexpression of DGKζ induces fiber hypertrophy via a mechanism that requires its kinase activity. The requirement of kinase activity is noteworthy because it suggests that the DGKζ-induced hypertrophy was mediated by an increase in the synthesis of PA. As shown in previous studies, an enhanced synthesis of PA can trigger mTOR-dependent (rapamycin-sensitive) cellular responses, but these responses tend to be resistant to the inhibitory effects of rapamycin (63, 185). For instance, PLD activity / [PA] is frequently elevated in human breast cancer cells and the growth rate of these cells becomes partially resistant to rapamycin in a manner that is correlated with the higher levels of PLD activity (185). Therefore, our observation that overexpression of DGKζ induces hypertrophy through an mTOR-dependent (rapamycin-sensitive), but partially rapamycin-resistant mechanism, further suggest that the hypertrophic effect of DGKζ is exerted through an increase in [PA] which, in-turn, would lead to an enhanced binding of PA to mTOR and the subsequent activation of mTOR-dependent growth regulatory events.

Previous studies have demonstrated that signaling through mTOR is necessary for a mechanically-

induced hypertrophic response and that the activation of mTOR signaling is sufficient to induce hypertrophy (35, 79, 154). Thus, the results of this study strongly suggest that DGKζ could also play a role in the molecular process through which mechanical stimuli regulate skeletal muscle mass. Consistent with this possibility, a recent clinical study found that subjects who displayed the greatest degree of myofiber hypertrophy in response to heavy resistance exercise also had the highest pre-training levels of skeletal muscle DGKζ transcript expression (186). Additional evidence implicating DGKζ in mechanically-induced hypertrophy is that DGKζ can regulate several stages of skeletal myogenesis including myoblast differentiation and fusion, a process that has been widely implicated in the regulation of mechanically-induced hypertrophy (187-189). Since the process of myogenesis is also largely controlled by mTOR signaling, it is possible that DGKζ could regulate mechanically-induced hypertrophy via the control of mTOR-dependent myogenesis (190). Combined, several pieces of evidence suggest that DGKζ could be a key component of the mechanism(s) through which mechanical stimuli induce hypertrophy, and addressing this possibility will be an essential topic for future studies.

In summary, the results from this study indicate that DGKζ contributes to the mechanical activation of PA-mTOR signaling and induces hypertrophy via an mTOR-dependent mechanism that requires the ability of DGKζ to synthesize PA. In the future, it will be important to determine how DGKζ contributes to the mechanical activation of PA-mTOR signaling and to define the role of DGKζ in mechanically-induced hypertrophy in-vivo. The resulting knowledge will further advance our understanding of the mechanism(s) through which mechanical stimuli regulate skeletal muscle mass and may ultimately lead to the development of therapies that can prevent the loss of muscle mass during conditions such as aging, diseases, and inactivity.

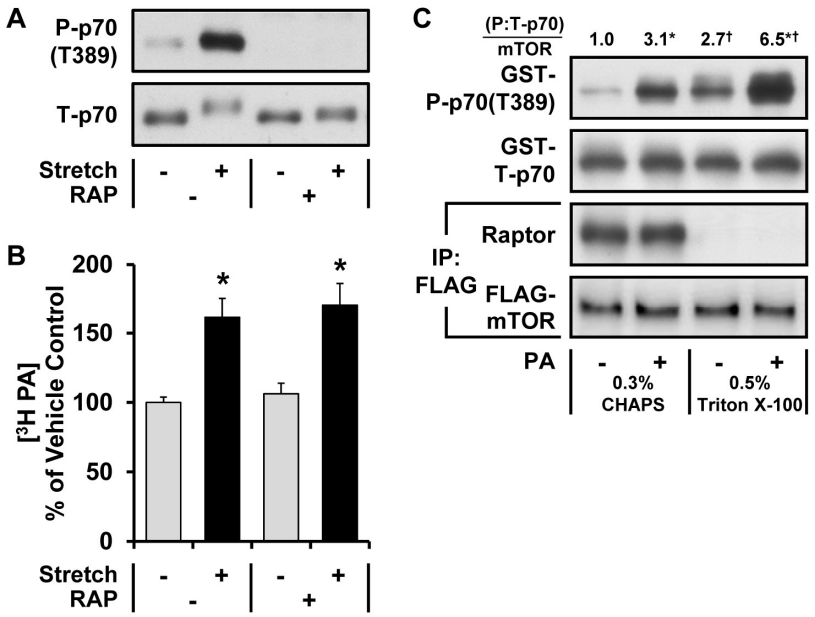

Figure 4-1. Evidence that PA can function as a direct upstream activator of mTOR signaling in response to mechanical stimulation. (**A** and **B**) Mouse EDL muscles were held at *Lo* in an *ex-vivo* organ culture system and treated as follows. (**A**) Pre-incubated with 150 nM rapamycin (RAP +) or the vehicle (RAP -, DMSO) for 30 min and then subjected to 90 min of a stretch (Stretch +) or control condition (Stretch -), followed by western blot analysis for phosphorylated (P) and total (T) p70. (**B**) Pre-labeled with [^{3}H]myristic acid for 2 h. During the final 30 min of the pre-labeling, the muscles were incubated with rapamycin or the vehicle as in A and then subjected to 90 min of the stretch or control conditions. The concentration of ^{3}H-labeled PA ([^{3}H PA]) was measured and expressed as a percentage of values obtained in the vehicle control samples. (**C**) C2C12 myoblasts stably expressing FLAG-mTOR were serum starved overnight and collected in either CHAPS or Triton X-100 lysis buffer. The lysates were subjected to immunoprecipitation (IP) for the FLAG epitope, and then the immunoprecipitates were incubated for 15 min with 150 μM PA vesicles (PA +) or 150 μM PC vesicles as a control condition (PA -). The kinase activity of mTOR was then assayed with GST-p70 as a substrate. The resulting samples were subjected to western blot analysis for the indicated proteins, and the P:T ratios of GST-p70 were divided by the amount of mTOR in each reaction. These values were then expressed as a ratio of the values obtained in the PC treated samples collected in CHAPS lysis buffer. The values were obtained from four independent experiments. All values are presented as the mean (+ SEM in graphs, n = 3-11 per group). * Significantly different from the drug- (B) or lysis buffer- (C) matched control group, † Significantly different from the stimulation-matched CHAPS group, $P \leq 0.05$.

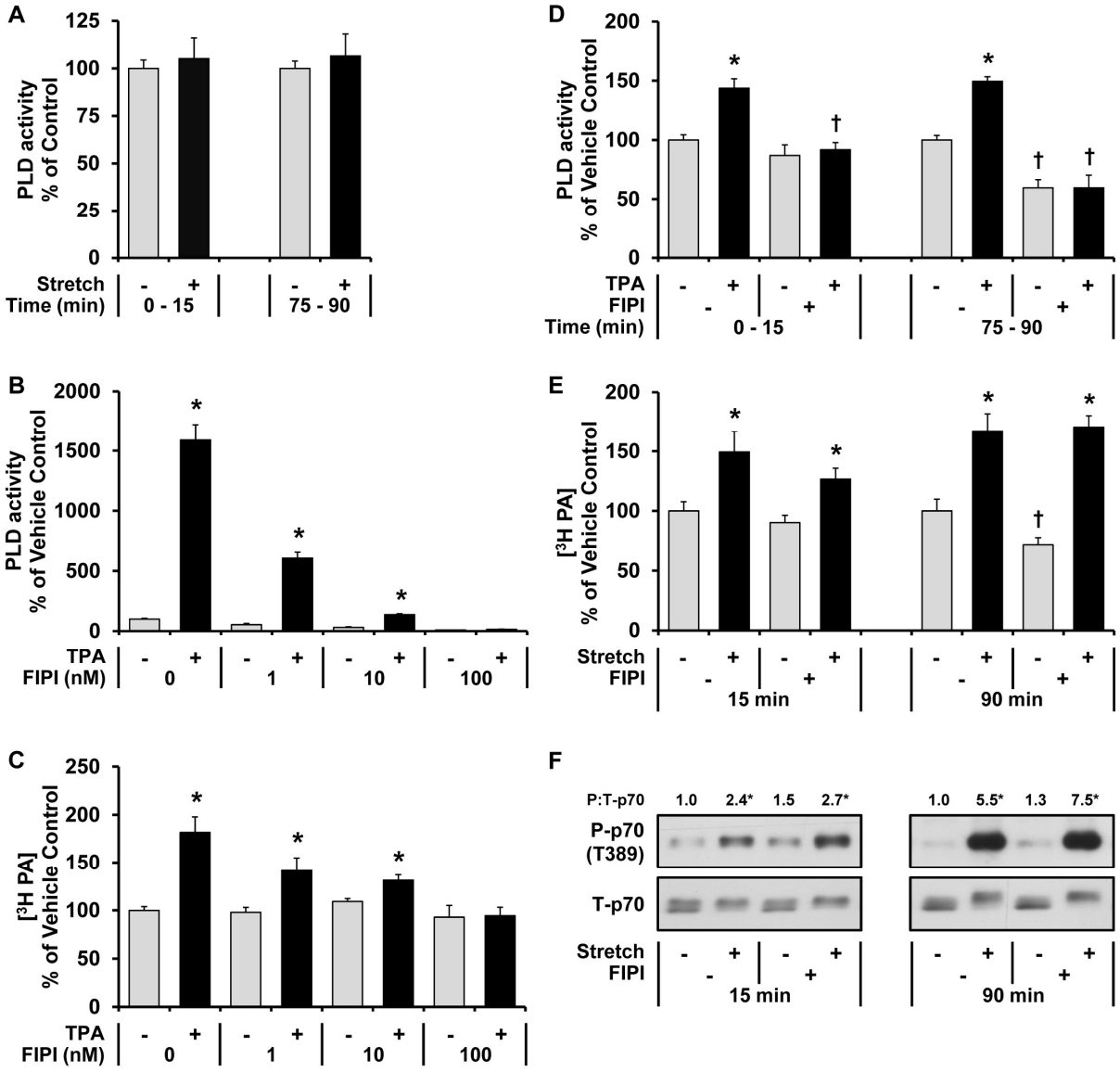

Figure 4-2. Changes in PLD activity are not required for a mechanically-induced increase in [PA] or mTOR signaling. (**A**) Mouse EDL muscles were held at *Lo* in an *ex-vivo* organ culture system, pre-labeled with [^{3}H]myristic acid for 2 h, and then subjected to 15 or 90 min of a stretch (Stretch +) or control condition (Stretch -). PLD activity was measured throughout a 15 min period and expressed as a percentage of the values obtained in the time-matched control samples. (**B** and **C**) C2C12 myoblasts were pre-labeled in serum-free media containing [^{3}H]myristic acid overnight. After being washed with fresh media, the cells were pre-incubated with 1, 10, or 100 nM FIPI or the vehicle (FIPI 0, DMSO) for 30 min and then stimulated with 100 nM TPA (TPA +) or the vehicle as a control condition (TPA -, DMSO) for 15 min in the presence (B) or absence (C) of 0.3% 1-butanol. The cells were collected, and PLD activity (B), or the concentration of ^{3}H-labeled PA ([^{3}H PA]) (C), was measured and expressed as a percentage of the values obtained in the vehicle control samples. The values were obtained from five independent experiments. (**D**-**F**) Mouse EDL muscles were held at *Lo* in an *ex-vivo* organ culture system and treated as follows. (**D** and **E**) Pre-labeled with [^{3}H]myristic acid for 2 h. During the final 30 min of pre-labeling, the muscles were incubated with 100 nM FIPI (FIPI +) or the vehicle (FIPI -, DMSO). The muscles were then subjected to 15 or 90 min of stimulation with 1 μM TPA (TPA +) or the vehicle as a control

condition (TPA -, DMSO) (D), or subjected to 15 or 90 min of the stretch or control conditions (E). PLD activity (D), or the concentration of ^{3}H-labeled PA ([^{3}H PA]) (E), was measured and expressed as a percentage of values obtained in the time-matched vehicle control samples. (**F**) Pre-incubated with FIPI or the vehicle as described above and then subjected to 15 or 90 min of the stretch or control conditions, followed by western blot analysis for phosphorylated (P) and total (T) p70. The P:T ratios of p70 were expressed relative to the values obtained in the time-matched vehicle control samples. All values are presented as the mean (+ SEM in graphs, n = 3-8 per group). * Significantly different from the time- and drug-matched control group, † Significantly different from the time- and stimulation-matched vehicle group, $P \leq 0.05$.

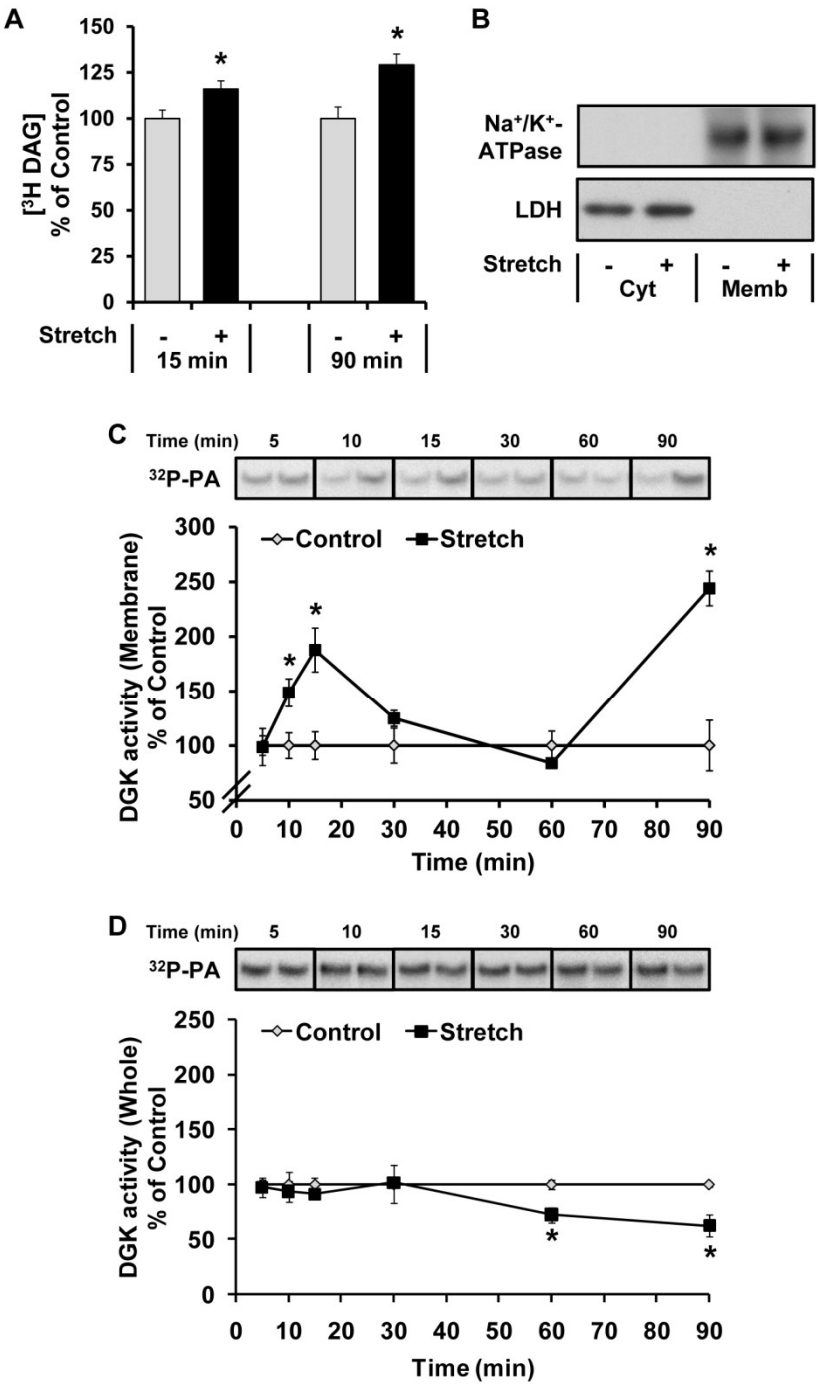

Figure 4-3. Mechanical stimulation increases [DAG] and membrane DGK activity. Mouse EDL muscles were held at *Lo* in an *ex-vivo* organ culture system and treated as follows. (**A**) Pre-labeled with [^{3}H]myristic acid for 2 h and then subjected to 15 or 90 min of a stretch (Stretch +) or control condition (Stretch -). The concentration of ^{3}H-labeled DAG ([^{3}H DAG]) was measured and expressed as a percentage of values obtained in the control samples. (**B**) Subjected to 15 min of the stretch or control conditions and then separated into cytosolic (Cyt) and membrane (Memb) fractions. The different fractions were then subjected to western blot analysis for Na^+/K^+-ATPase and LDH. (**C** and **D**) Subjected to 5 - 90 min of the stretch or control conditions, and then DGK activity (^{32}P-PA) in the membrane fraction (C) and whole lysates (D) was measured and expressed as a percentage of the values obtained in the time-matched control samples. All values are presented as the mean + SEM (n = 3-4 per group). * Significantly different from the time-matched control group, $P \leq 0.05$.

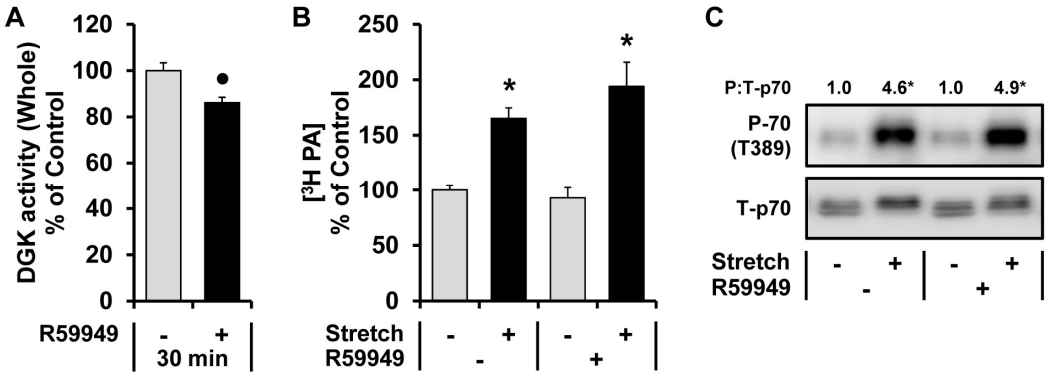

Figure 4-4. R59949 does not inhibit the mechanically-induced increase in [PA] or the activation of mTOR signaling. Mouse EDL muscles were held at *Lo* in an *ex-vivo* organ culture system and treated as follows. (**A**) Incubated with 100 μM R59949 (R59949 +) or the vehicle (R59949 -, DMSO) for 30 min. DGK activity from the whole lysates was measured and expressed as a percentage of values obtained in the vehicle control samples. (**B**) Pre-labeled with [^{3}H]myristic acid for 2 h. During the final 30 min of the pre-labeling, the muscles were incubated with R59949 or the vehicle as described in A. The muscles were then subjected to 90 min of the stretch (Stretch +) or control conditions (Stretch -), and the concentration of ^{3}H-labeled PA ([^{3}H PA]) was measured and expressed as a percentage of values obtained in the vehicle control samples. (**C**) Pre-incubated with R59949 or the vehicle as described in A and then subjected to 90 min of the stretch or control conditions, followed by western blot analysis for phosphorylated (P) and total (T) p70. The P:T ratios of p70 were expressed relative to the values obtained in the vehicle control samples. All values are presented as the mean (+ SEM in graphs, n = 3-8 per group). • Significantly different from the vehicle group, * Significantly different from the drug-matched control group, $P \leq 0.05$.

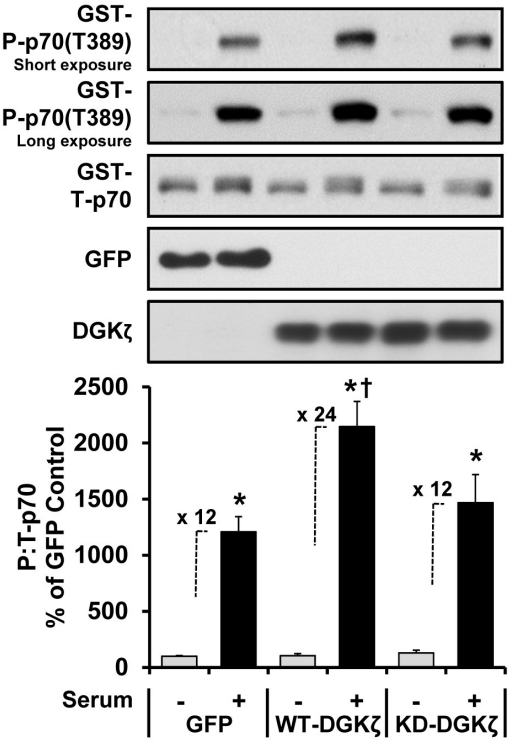

Figure 4-5. Overexpression of DGKζ enhances the serum-induced activation of mTOR signaling in a kinase activity-dependent manner. C2C12 myoblasts were co-transfected with plasmid DNA encoding GFP, wild type DGKζ (HA-WT-DGKζ), or kinase dead DGKζ (HA-KD-DGKζ), and GST-p70. The following day, the cells were serum-starved overnight and then stimulated with 20% fetal bovine serum (Serum +) for 30 min. The cells were collected and then subjected to western blot analysis for the indicated proteins. The phospho (P): total (T) ratios of GST-p70 were then expressed as a percentage of the values obtained in the GFP non-stimulated (control, Serum -) samples. Values are presented as the mean + SEM and were obtained from five independent experiments (n = 5-9 per group). * Significantly different from the plasmid-matched control group, † Significantly different from the stimulation-matched GFP group, $P \leq 0.05$.

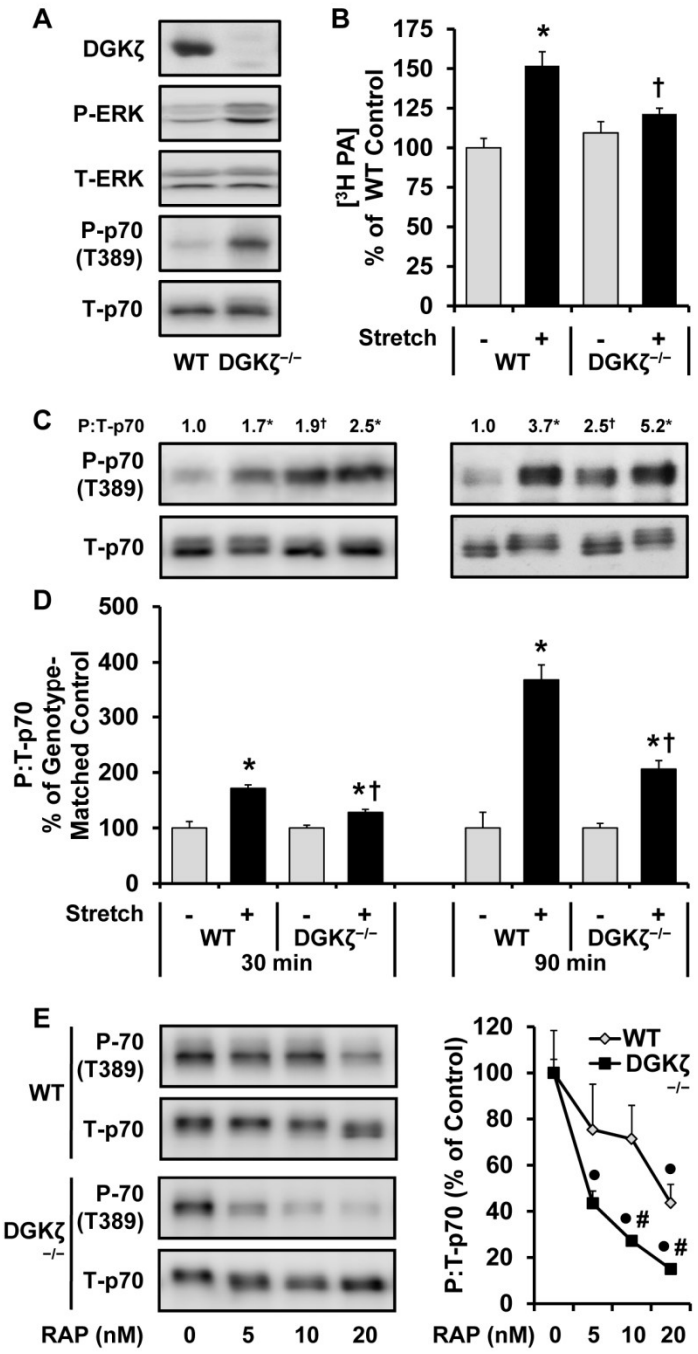

Figure 4-6. The mechanically-induced increase in [PA] and the activation of mTOR signaling is impaired in muscles from DGKζ$^{-/-}$ mice. (**A**) EDL muscles from WT and DGKζ$^{-/-}$ mice were collected and subjected to western blot analysis for the indicated proteins. (**B**-**E**) EDL muscles from WT and DGKζ$^{-/-}$ mice were held at *Lo* in an *ex-vivo* organ culture system and treated as follows. (**B**) Pre-labeled with [^{3}H]myristic acid for 2 h and then subjected to 90 min of the stretch (Stretch +) or control conditions (Stretch -). The concentration of ^{3}H-labeled PA ([^{3}H PA]) was measured and expressed as a percentage of values obtained in WT control samples. (**C** and **D**) Subjected to 30 or 90 min of the stretch or control conditions, followed by western blot analysis for phosphorylated (P) and total (T) p70. The P:T ratios of p70 were expressed relative to the values obtained in the time-matched WT control samples (C) or expressed as a percentage of the time- and genotype-matched control samples (D). (**E**) Pre-incubated with 5, 10, or 20 nM rapamycin (RAP) or the vehicle (RAP 0, DMSO) for 30 min and then subjected to 90 min of stretch, followed by western blot analysis for P- and T-p70. The P:T ratios of p70 were expressed as a percentage of values obtained in the genotype-matched vehicle samples. All values are presented as the mean (+ SEM in graphs, n = 3-9 per group). * Significantly different from the time- and genotype-matched control group, † Significantly different from the time- and stimulation-matched WT group, • Significantly different from the genotype-matched vehicle group, # Significantly different from the drug-matched WT group, $P \leq 0.05$.

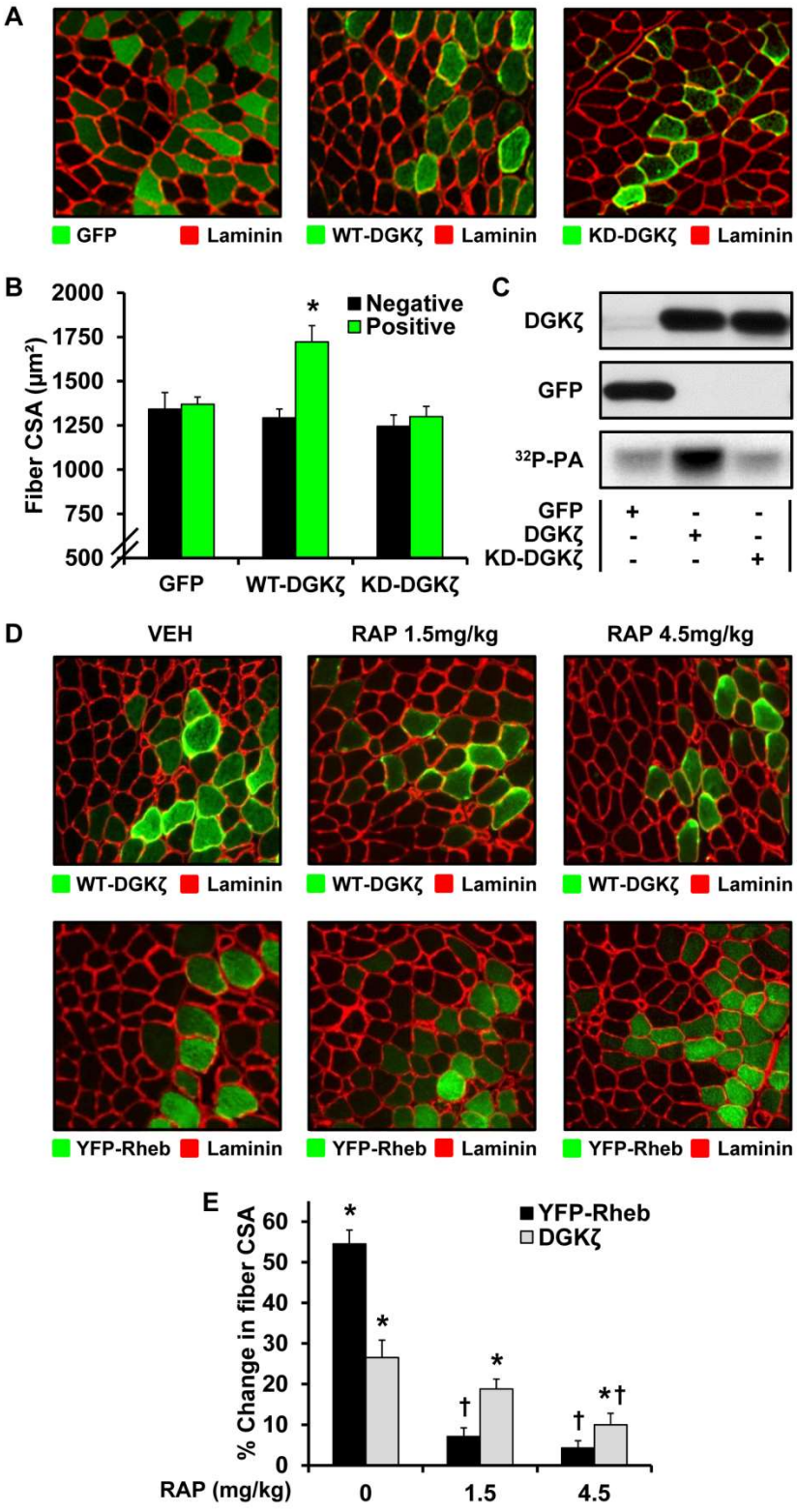

Figure 4-7. Overexpression of DGKζ induces hypertrophy through a kinase-dependent and rapamycin-sensitive mechanism. (**A-C**) Mouse TA muscles were transfected with plasmid DNA encoding GFP, HA-WT-DGKζ, or HA-KD-DGKζ. (**A**) The muscles were collected at 7 days post transfection and cross-sections from the midbelly of the muscles were subjected to immunohistochemistry for GFP and laminin, or HA and laminin. (**B**) CSA of the transfected fibers (Positive) and non-transfected fibers (Negative) within each of the GFP-, HA-WT-DGKζ-, and HA-KD-DGKζ-transfected muscles. (**C**) Muscles were collected at 3 days post transfection, and whole lysates were subjected to a DGK activity assay (^{32}P-PA) or western blot analysis for the indicated proteins. (**D** and **E**) Mouse TA muscles were transfected with plasmid DNA encoding HA-WT-DGKζ or YFP-Rheb. Immediately after transfection, the mice were subjected to a regime of daily 1.5 or 4.5 mg/kg rapamycin (RAP) or vehicle (RAP 0, DMSO) injections. (**D**) The muscles were collected at 7 days post transfection and cross-sections from the midbelly of the muscles were subjected to immunohistochemistry for HA and laminin, or YFP and laminin. (**E**) The CSA of the transfected fibers and non-transfected fibers within each of the HA-WT-DGKζ- and YFP-Rheb-transfected muscles was determined and then the percent difference between the averaged CSA of the transfected fibers and non-transfected fibers of each muscle was calculated. All values are presented as the mean + SEM (n = 3-8 muscles per group, 35-120 fibers per muscle). * Significantly different from the drug- and plasmid-matched non-transfected fibers, † Significantly different from the plasmid-matched vehicle group, $P \leq 0.05$.

Chapter 5

DGKζ Positively Regulates Skeletal Muscle Remodeling by Suppressing the Ubiquitin-Proteasome-System

Jae-Sung You[1,2], Matthew S. Dooley[2], Chan-Ran Kim[2], Craig A. Goodman[2],

Troy A. Hornberger[1,2]

[1]Program in Cellular and Molecular Biology and [2]Department of Comparative Biosciences in the School of Veterinary Medicine, University of Wisconsin - Madison, WI 53706

Corresponding authors: Troy Alan Hornberger (Address: 2015 Linden Drive, Madison, WI 53706, USA; Phone: 608.695.2847; E-mail: troy.hornberger@wisc.edu), and Jae-Sung You (Address: 2015 Linden Drive, Madison, WI 53706, USA; Phone: 608.609.2669; E-mail: jyou4@wisc.edu)

Author contributions: J.-S.Y. and T.A.H. conceived and designed the experiments. J.-S.Y., M.S.D., C.-R.K, and C.A.G. performed the experiments and analyzed the data. J.-S.Y. and T.A.H. wrote the paper.

This chapter was submitted to: *Journal of Clinical Investigation*

and modified slightly to comply with the format of this dissertation

Abstract

Skeletal muscle undergoes dynamic remodeling in response to a variety of stimuli and the resulting changes in muscle mass can profoundly influence health and issues associated with quality of life; however, the molecular mechanisms that regulate remodeling are poorly understood. Here, we identify diacylglycerol kinase ζ (DGKζ) as a critical component of the mechanism that regulates muscle fiber size during remodeling. In response to mechanical overload, DGKζ expression is elevated and required for rapid fiber hypertrophy. Mechanistically, DGKζ not only contributes to the activation of mTOR signaling and protein synthesis, but it also attenuates the induction of proteasome-dependent protein degradation and the ubiquitin-proteasome-system (UPS), including global ubiquitination and muscle-specific E3 ubiquitin ligases. We also identify that nuclear DGKζ is a potent inhibitor of the FoxO and NF-κB transcription factors which promotes the induction of the UPS. In response to denervation, DGKζ expression is also increased and its presence mitigates the induction of fiber atrophy as well as the activation of FoxO, NF-κB and the UPS. Likewise, the overexpression of DGKζ prevents the atrophy that occurs during denervation and food deprivation. Therefore, as a positive regulator of muscle remodeling, DGKζ represents a novel therapeutic target for the prevention of muscle wasting.

Introduction

Skeletal muscle is capable of changing its protein content and size (i.e., remodeling) in response to a variety of factors including physical activity, nutritional status, nerve injuries, diseases, and aging (10, 15). Comprising approximately 45% of total body mass, this highly plastic tissue not only serves as the motor that drives locomotion, but it also plays a critical role in whole-body metabolism (e.g., glucose homeostasis). Hence, changes in skeletal muscle mass have a great impact on our health and quality of life, and the failure to maintain muscle mass is one of the leading risk factors for morbidity and mortality (7, 9, 12, 68).

During remodeling, changes in skeletal muscle mass are driven by the balance between the rate of protein synthesis and the rate of protein degradation. As such, a net positive balance leads to muscle growth (i.e., hypertrophic remodeling), whereas a net negative balance leads to muscle loss (i.e., atrophic remodeling). According to previous studies, the regulation of protein synthesis and protein degradation is largely driven by a rapamycin-sensitive protein kinase called mTOR and the ubiquitin-proteasome-system (UPS), respectively (191). Signaling by mTOR regulates protein synthesis primarily through the phosphorylation of its substrates such as eukaryotic initiation factor (eIF) 4E binding protein 1 (4E-BP1) and p70 ribosomal protein S6 kinase ($p70^{S6k}$) (76-78). Specifically, phosphorylated 4E-BP1 dissociates from eIF4E, allowing eIF4E to associate with eIF4G and thereby promoting eIF4F complex formation and cap-dependent initiation of translation. On the other hand, the UPS regulates protein degradation primarily though the E3-ligase-mediated ubiquitination of protein substrates that are targeted to the 26S proteasome complex (192). For example, in skeletal muscle, the ubiquitination of myofibrillar proteins is mediated by a range of E3 ligases including the muscle-specific E3 ubiquitin ligases that are commonly upregulated in a variety of remodeling conditions, such as muscle atrophy F-box (MAFbx) and muscle RING finger 1 (MuRF1) (193). Given the important roles of mTOR signaling and the UPS in determining muscle protein turnover, unraveling the molecular mechanisms that regulate these two processes should facilitate the development of therapies that can preserve and/or increase muscle mass.

One of the most widely established conditions for promoting an increase in mTOR signaling, protein synthesis, and skeletal muscle mass is mechanical loading (i.e., resistance exercise) (67). Accordingly, various models of mechanical loading have been employed to identify the molecular targets that are responsible for these anabolic events. For instance, using an *ex vivo* passive stretch model, we recently concluded that diacylglycerol kinase ζ (DGKζ) plays an important role in the mechanical activation of mTOR signaling by promoting the synthesis of the mTOR agonist phosphatidic acid (PA) from diacylglycerol (DAG) (109, 111, 194). Moreover, we and others have shown that supplementation with PA, as well as the overexpression of DGKζ, is sufficient to promote an increase in protein synthesis and fiber size, respectively (109, 111, 195). Consistently, a recent clinical study found that the extent of resistance exercise-induced muscle hypertrophy is positively associated with pre-training levels of skeletal muscle DGKζ mRNA expression (186). Based on these points, it is plausible that DGKζ positively regulates mTOR signaling, protein synthesis and fiber size during mechanically-induced skeletal muscle remodeling; however, this possibility has not been directly explored. Therefore, the initial goal of this study was to examine the role of DGKζ in the activation of mTOR signaling, protein synthesis, and muscle growth during mechanical overload (OV), a commonly employed animal model of resistance exercise. Surprisingly, however, our results revealed that DGKζ not only functions as a positive regulator of mTOR signaling and protein synthesis, but also act as a negative regulator of the UPS and protein degradation. Our results also demonstrate that increased expression of DGKζ can mitigate various types of fiber atrophy, thus identifying DGKζ as a potential therapeutic target for the prevention of muscle wasting.

Results

During OV, DGKζ is predominantly increased among DGK isoforms and is required for rapid muscle growth. - Previous *ex vivo* studies have implicated the DGKζ-dependent synthesis of PA in the mechanical activation of mTOR signaling (109, 111). To assess the possible involvement of this mechanism in an *in vivo* model, rats were subjected to 7 days of OV (note: rats were employed in this

experiment because they could provide the amount of tissue needed for the *in vivo* measurement of total PA). The results showed that OV induced muscle growth, increased the levels of DAG and PA, and activated mTOR signaling (as revealed by the phosphorylation of $p70^{S6k}$ on T389) (Figure 5-1, A-D). Furthermore, the increase in DAG-PA-mTOR signaling was associated with an increase in total DGK activity as well as membrane-associated DGKζ activity (Figure 5-1, E and F). Together, these data suggest that a DGKζ-dependent synthesis of PA from DAG could contribute to the OV-induced activation of mTOR signaling.

Interestingly, in this set of experiments, we also found that total DGK activity increased in both whole homogenate and cytosolic fractions (Figure 5-1, E). Thus, we envisioned that OV not only induces membrane translocation of DGKζ, but it also increases its protein expression. Consistent with this possibility, the ζ isoform, but not δ or ε isoforms of DGK, substantially increased in response to OV in mice (Figure 5-2A) (note: DGKζ has two splice variants in mice with DGKζ1 expression being predominant over DGKζ2 in skeletal muscle). The increase in DGKζ protein was also accompanied by a similar increase in DGKζ activity (Figure 5-2B). Although δ, ε, and ζ isoforms of DGK are highly expressed in skeletal muscle, there are still many other isoforms of DGK whose expression could also have increased in response to OV (172). In an attempt to determine the extent to which these other DGK isoforms may have increased, we measured total DGK activity from whole homogenates that were pre-treated with R59949 which preferentially inhibits the α, β, γ, and θ isoforms of DGK (170, 171). The results revealed that R59949-sensitive DGK isoforms accounted for only a small portion (~13%) of the OV-induced increase in total DGK activity (Figure 5-2, C and E). On the other hand, when we measured total DGK activity from whole homogenates in which DGKζ was immunodepleted, it was revealed that DGKζ alone accounted for more than half (~60%) of the OV-induced increase in total DGK activity (Figure 5-2, D and E). Similar results were also obtained when we compared total DGK activity in muscles from WT and DGKζ knockout (DGKζ KO) mice (Figure 5-3). Combined, these results indicate that, among all the DGK isoforms, OV predominantly increases DGKζ expression.

In order to determine the role of DGKζ in OV-induced skeletal muscle growth, we first measured muscle mass in WT and DGKζ KO mice at various time points following the onset of OV. The results showed that DGKζ KO mice not only exhibit smaller basal muscle mass, but more importantly, they also had an impaired OV-induced increase in muscle mass (Figure 5-4 and Figure 5-2F). The impaired increase in muscle mass was not due to artifacts, such as reduced edema, because the accumulation of total protein by OV was also impaired in DGKζ KO muscles (Figure 5-2G). In addition to individual muscle fiber hypertrophy, an increase in muscle mass during OV can also be achieved by an increase in the number of muscle fibers (i.e., hyperplasia) (35). However, muscle hyperplasia, as indicated by the total number of fibers per muscle cross-section, was not altered in the DGKζ KO mice, suggesting that the impaired increase in muscle mass was likely due to a reduction in fiber hypertrophy (Figure 5-2, H and M). Therefore, we compared the cross-sectional area (CSA) of different muscle fiber types over the course of OV. As previously reported, OV induced fiber type-dependent increases in the CSA of WT muscles (94). Specifically, the CSA of non-type 2b fibers increased as early as 3 days after the onset of OV while the CSA of type 2b fibers was not significantly altered at any time point during the 14 days of OV; however, in DGKζ KO muscles, the rapid increase in CSA of non-type 2b fibers (type 2a and 2x fibers) was severely blunted, and the CSA of type 2b fibers was actually reduced at 7 days (Figure 5-2, I, J, and M, and Figure 5-4, A-C). Despite the dysregulation of protein content and fiber size in DGKζ KO muscles during OV, the muscles still showed a normal increase in the number of myonuclei per fiber, a result which is in line with the recently reported dispensable role of myonuclear accretion in OV-induced hypertrophy (Figure 5-2, K, L, and N) (196). Taken together, these results demonstrate that DGKζ is necessary for rapid non-type 2b fiber hypertrophy, and the maintenance of type 2b fiber size, thereby contributing to the growth that occurs during OV.

DGKζ contributes to the activation of protein synthesis and mTOR signaling, and attenuates the activation of UPS-dependent protein degradation during the early period of OV. - During OV, the rates of both protein synthesis and protein degradation increase as muscles undergo the process of remodeling; however, because the increase in protein synthesis exceeds that of protein degradation,

overloaded skeletal muscles eventually increase their mass via the accretion of new proteins (117). In order to begin interrogating the mechanisms through which DGKζ contribute to the OV-induced protein accumulation and muscle growth, we measured several anabolic and catabolic cellular events at 2 days post OV. We selected this time point because we expected that disruptions in protein metabolism would occur prior to the impaired hypertrophic response that we observed at 3 days in the DGKζ KO muscles (Figure 5-2H). At this early time point, we observed that OV only increased the protein level of the low-abundant form of DGKζ (DGKζ2), while the mRNA level of DGKζ increased robustly (splice variant non-specific) (Figure 5-6, A and B). Nevertheless, we found that the OV-induced increase in protein synthesis was considerably attenuated in DGKζ KO muscles (Figure 5-6C). Consistently, the magnitude of OV-induced activation of mTOR signaling was also significantly blunted in DGKζ KO muscles, as indicated by the phosphorylation of p70 (T389) and 4E-BP1 (T36/45), and the association of eIF4E with 4E-BP1 or eIF4G (Figure 5-6D and Figure 5-7). Therefore, these results demonstrate that DGKζ contributes to the activation of protein synthesis and mTOR signaling during the early period of OV.

The attenuated activation of anabolic events by DGKζ KO is noteworthy, but, to our surprise, we also found that the OV-induced increase in the rate of protein degradation was markedly augmented in DGKζ KO muscles (Figure 5-6E). This is an interesting observation because the accelerated increase in protein degradation, in addition to the blunted increase in protein synthesis, further explains why DGKζ KO muscles showed an impaired net accumulation of protein and muscle growth.

The degradation rate of most proteins in mammalian cells is determined through their rate of ubiquitination by E3 ubiquitin ligases and subsequent degradation by 26S proteasome (192). Consistently, we found that the OV-induced increase in the rate of protein degradation, and its augmentation by DGKζ KO, were completely abolished by the proteasome inhibitor, MG132 (Figure 5-6E). Furthermore, when we measured levels of global ubiquitination, and the protein levels of two critical muscle-specific E3 ubiquitin ligases, MAFbx and MuRF1, it was found that, not only were all of these components in the UPS up-regulated by OV, but their increases were also augmented in DGKζ KO muscles (Figure 5-6, F and G) (similar results were also obtained at 1 day post OV, data not shown). Moreover, unlike other

translation factors, the protein level of eIF3f, a target of MAFbx (197), was increased only in WT muscles, supporting the functionality of the relatively large increase in the expression of MAFbx in DGKζ KO muscles (Figure 5-6G). Taken together, these results demonstrate that, during the early period of OV, the presence of DGKζ attenuates the increase in E3 ligase expression, global ubiquitination, and UPS-mediated protein degradation.

DGKζ negatively regulates FoxO and NF-κB activity independent of its kinase activity. - The results from OV experiments unexpectedly revealed that DGKζ can attenuate protein degradation by suppressing key components of the UPS in skeletal muscle (e.g., MAFbx and MuRF1). Among the best characterized transcription factors that can activate *MAFbx* and *MuRF1* genes are FoxO and NF-κB (193). Thus, we wanted to determine if DGKζ exerts an inhibitory function on the activity of these two transcription factors. To this end, we overexpressed DGKζ or GFP as a control, along with FoxO or NF-κB response element reporters in tibialis anterior (TA) muscles of WT and DGKζ KO mice. The results showed that the overexpression of WT-DGKζ was able to inhibit FoxO and, to a lesser extent, NF-κB transcriptional activity, while the activity of FoxO was slightly enhanced in the muscles from DGKζ KO mice (Figure 5-8, A and B). Interestingly, we also found that the inhibitory effects of DGKζ were independent of its kinase activity as a kinase-dead mutant form of DGKζ (KD-DGKζ) was still able to inhibit FoxO and NF-κB reporter activity (Figure 5-8, A and B). Similar results were also obtained when we examined the promoter activities of FoxO and NF-κB target genes including *MAFbx* and *MuRF1* (Figure 5-8C and Figure 5-9). Intrigued by these observations, we wondered if DGKζ can also inhibit the atrophy-promoting effects of FoxO and NF-κB. As previously reported (102, 198), the overexpression of constitutively active (ca) FoxO3a, or ca IκB kinase β (caIKKβ; which activates NF-κB), induced a significant reduction in muscle fiber size, as well as a robust increase in their corresponding reporter activities (Figure 5-8, D-F). However, these changes were all prevented when either WT-DGKζ or KD-DGKζ were co-overexpressed with caFoxO3a or caIKKβ (Figure 5-8, D-F). Therefore, these results identify a novel kinase-independent function of DGKζ that can negatively regulate FoxO and NF-κB activity and their pro-atrophic actions.

Having established the inhibitory role of DGKζ on FoxO and NF-κB activity in resting TA muscles, we then wanted to determine if DGKζ exhibited the same effect in muscles that had been subjected to OV. To this end, we transfected FoxO or NF-κB reporters into plantaris (PLT) muscles and measured their activities at 2 days post OV. The results showed that OV induced a noticeable decrease in the activity of both FoxO and NF-κB, but, interestingly, the decrease in FoxO activity was completely lost is muscles from DGKζ KO mice (Figure 5-8, G and H). When combined, these results demonstrate that, during OV, DGKζ inhibits FoxO activity which, in turn, could contribute to muscle growth by suppressing the expression of FoxO targets such as MAFbx and MuRF1.

The nuclear-localization signal of DGKζ is required for the inhibition of FoxO and NF-κB activity. - Next, we wanted to gain insights into the mechanism through which DGKζ could inhibit FoxO and NF-κB activity. The best established mode of FoxO regulation is through control of its nuclear/cytoplasmic localization. For example, FoxO is excluded from the nucleus when phosphorylated by PKB, but upon dephosphorylation, it translocates into the nucleus and becomes transcriptionally active (199). Thus, we first asked if DGKζ inhibits FoxO nuclear localization. To address this question, we overexpressed wild-type (wt) FoxO3a or caFoxO3a (three PKB phosphorylation sites mutated) with or without co-overexpression of WT-DGKζ or KD-DGKζ in TA muscles. Consistent with the original report in cultured cells (199), our fractionation data confirmed that caFoxO3a had an enhanced nuclear to cytoplasmic ratio compared to wtFoxO3a; however, the results also showed that neither WT-DGKζ nor KD-DGKζ inhibited this event (Figure 5-10A). Based on this observation, and the fact that DGKζ can also localize to the nucleus [(160) and figure 5-10A], we hypothesized that FoxO activity is inhibited by DGKζ inside the nucleus. To test this, we overexpressed a nuclear-localization signal (NLS) mutated form of DGKζ (ΔNLS-DGKζ) in TA muscles. As expected, ΔNLS-DGKζ exhibited reduced nuclear localization (Figure 5-10B) and, quite strikingly, it did not exert any inhibitory effect on FoxO activity (Figure 5-10C). A similar effect of the NLS mutation was also observed for NF-κB activity (Figure 5-10D). Together, these results indicate that nuclear localization of DGKζ is necessary for its inhibitory effects on FoxO and NF-κB activity.

As mentioned above, the protein levels of DGKζ were not robustly altered at 2 days post OV (i.e., no increase in DGKζ1, the predominantly expressed variant form of DGKζ), yet the presence of DGKζ exerted a significant effect on the OV-induced changes in FoxO activity and the expression of FoxO target genes (e.g., MAFbx and MuRF1). These results, combined with the role of nuclear DGKζ, suggest that enhanced nuclear translocation of DGKζ might occur during the early period of OV. Consistent with this prediction, we found that the nuclear localization of endogenous DGKζ1 was enhanced after 2 days of OV (Figure 5-10E). Therefore, these results suggest that, in addition to the regulation of DGKζ expression, enhanced nuclear translocation of DGKζ could be another key regulatory mechanism by which DGKζ inhibits FoxO activity, UPS expression, and protein degradation during OV.

DGKζ inhibits the activation of FoxO/NF-κB/ubiquitin pathway and muscle atrophy during denervation and food deprivation. - In this study, we uncovered a novel inhibitory role of DGKζ on UPS-mediated protein degradation and FoxO transcriptional activity that is associated with its growth-promoting effect after the onset of OV. Because UPS-mediated protein degradation and FoxO activity are typically up-regulated during atrophic conditions (191), we next wanted to explore if the role of DGKζ can be extended to the prevention of muscle atrophy. In particular, we became interested in the role of DGKζ in denervation-induced muscle atrophy because previous studies have shown that denervation-induced atrophy is mediated, at least in part, by MAFbx, MuRF1, and/or FoxOs (200, 201). Furthermore, we have found that denervation, just like OV, leads to an increase in DGKζ mRNA and DGKζ protein levels in fast-twitch muscles but not in slow-twitch soleus (SOL) muscles (Figure 5-11, A and B). Based on this finding, we envisioned that this increase in DGKζ expression could play a role in mitigating the atrophic effect of denervation. Indeed, when we measured changes in muscle mass following 7 days of denervation, we found that the denervation-induced decrease in muscle mass was exacerbated in all of the lower hindlimb muscles of DGKζ KO mice except for the SOL (Figure 5-11C). Similar results were also obtained when we measured fiber CSA in TA and PLT muscles, confirming that DGKζ mitigates denervation-induced fiber atrophy (Figure 5-11D). Next, we tested if the anti-atrophic effect of DGKζ is associated with its inhibitory function on the UPS and FoxO activity. The results showed that the

denervation-induced activation of global ubiquitination, MAFbx expression, FoxO, and even NF-κB, were augmented by DGKζ KO in TA muscles, and therefore confirmed that DGKζ can inhibit the UPS and FoxO activity during denervation (Figure 5-11, E-G). Moreover, these effects were not observed in the SOL which is consistent with the lack of an effect of DGKζ KO on the denervation-induced decrease in SOL muscle mass (Figure 5-11E). Furthermore, the augmented activities of FoxO and NF-κB in DGKζ KO muscles were substantially reduced when either WT-DGKζ or KD-DGKζ were re-expressed in those muscles (Figure 5-11, F and G). Therefore, when combined, our results indicate that DGKζ mitigates the denervation-induced activation of the FoxO/NF-κB/UPS pathway and the concomitant induction of atrophy.

The lack of an effect of DGKζ KO in SOL muscles was consistent with the minimal denervation-induced increase in DGKζ expression and therefore suggested that the anti-atrophic effect of DGKζ may be dose-dependent. This possibility led us to hypothesize that a further increase in DGKζ expression during denervation would exert a more profound anti-atrophic effect and restore fiber size. To test this hypothesis, we overexpressed DGKζ in TA muscles at the time of denervation. The results showed that the overexpression of either WT-DGKζ or KD-DGKζ, but not LacZ, could prevent the loss of fiber size that occurs during denervation (Figure 5-11H).

Based on the above results, we wondered whether the overexpression of DGKζ could also prevent other types of muscle atrophy. To this end, we employed a food deprivation model that has previously been shown to induce muscle atrophy though a mechanism requiring FoxO or NF-κB activity (201, 202). In this model, we first found that the food deprivation-induced loss of muscle mass, as well as increases in the components of the UPS, were not affected by DGKζ KO, and, similar to the SOL during denervation, this was associated with no increase in the protein levels of DGKζ1 (Figure 5-12, A-C). However, when we overexpressed either WT-DGKζ or KD-DGKζ, the food deprivation-induced loss of fiber size was completely prevented (Figure 5-12D). Furthermore, the anti-atrophic effect of DGKζ during food deprivation was associated with its ability to inhibit both FoxO and NF-κB transcriptional

activity (Figure 5-12, E and F). Collectively, these results demonstrate the potential for increasing the level of DGKζ expression as a therapeutic strategy to combat the loss of muscle mass.

Discussion

Skeletal muscle is a highly plastic tissue that can rapidly adapt to environmental changes by remodeling its size. Unfortunately, many of these environmental changes (e.g., physical inactivity, nutritional imbalance, etc.) lead to skeletal muscle atrophy during which the rate of protein degradation exceeds that of protein synthesis (10). On the other hand, mechanical loading induces muscle hypertrophy by promoting an increase in the balance between the rates of protein synthesis and protein degradation (15). Accordingly, a plethora of studies have attempted to understand the molecular mechanisms that mediate the effects of mechanical loading in hopes of identifying therapeutic target(s) for preventing muscle atrophy; however, these mechanisms remain vaguely defined. In this study, we identify DGKζ as an essential cellular component for promoting hypertrophic remodeling. Specifically, during OV, DGKζ not only helps to promote an increase in protein synthesis, but it also attenuates protein degradation by suppressing the activation of the UPS. We also show that the inhibitory effects of DGKζ on the UPS can be extended to atrophic conditions, thus demonstrating its therapeutic potential for the prevention of muscle wasting.

A fundamental question for understanding the mechanisms of load-induced skeletal muscle hypertrophy is how mechanical loading activates protein synthesis and induces a net increase in protein balance. Although an answer to the question is still not clear, advances in our knowledge are being made and it is becoming increasingly evident that the nutrient-sensing mTOR signaling pathway is an integral part of the process. For example, many studies have demonstrated that various forms of mechanical loading activate mTOR signaling, and that nutrient insufficiency or inhibition of the mTOR signaling by rapamycin, limits the mechanical load-induced increase in the rates of protein synthesis and muscle growth (30-35, 203). Furthermore, it has been shown that the activation of mTOR signaling is sufficient to increase the rates of protein synthesis and muscle fiber size (79, 80). Accordingly, several hypotheses

have been proposed to explain how mechanical loading activates mTOR signaling, and one that has recently emerged involves the activation of mTOR by a DGKζ-dependent increase in PA (109, 111). However, this hypothesis has not been explored in an *in vivo* model of mechanical loading. In this study, by employing OV, we have obtained several lines of evidence that support this hypothesis: 1) OV induces an increase in both PA, and its precursor, DAG, 2) OV induces an increase in the expression and membrane activity of DGKζ, and 3) DGKζ KO impairs the OV-induced activation of mTOR signaling, protein synthesis, and muscle growth. Despite this evidence, however, we realized that the impairment of the OV-induced mTOR signaling was only partial, and relatively modest compared to the changes in protein synthesis. Thus, this result suggests that, in addition to DGKζ and PA, other mechanisms are also involved in the OV-induced activation mTOR signaling, and that DGKζ KO inhibits the OV-induced activation of protein synthesis, at least in part, through an mTOR-independent mechanism. With regard to the latter point, the mTOR-independent mechanism may be explained by our observation that DGKζ KO completely blunted the OV-induced increase in eIF3f expression, a critical component in mRNA translation (197, 204). In any case, expanding our understanding of the mechanisms responsible for the mechanical load-induced increase in mTOR signaling and protein synthesis will provide fundamental insights into how mechanical loading promotes muscle growth.

The UPS can ensure the quality of intracellular proteins in cells by the selective degradation of misfolded and/or damaged proteins that may arise from various stress conditions such as mechanical loading (205). Thus, the activation of UPS-dependent protein degradation may be considered as essential for mechanical load-induced hypertrophic remodeling. Indeed, many studies have reported that mechanical loading increases protein degradation, as well as key components of the UPS including muscle-specific E3-ligases (e.g., MAFbx, and MuRF1) and protein ubiquitination (117, 192, 203, 206). Furthermore, our data indicate that the OV-induced increase in the rate of protein degradation is entirely UPS-dependent. However, an excessive activation of the UPS and protein degradation would eliminate the increase in the balance between the rates of protein synthesis and protein degradation that is needed for muscle growth. Thus, the rates of protein degradation following mechanical loading must be tightly

regulated in order for skeletal muscle to obtain an efficient accumulation of intact and functional proteins. In light of this fundamental point, it is surprising that very little is known about the mechanisms through which skeletal muscle accomplishes this regulation. In this study, we shed light on this process by identifying a novel role of DGKζ in preventing an excessive increase in the UPS-dependent protein degradation during OV. Furthermore, we have provided evidence that this function of DGKζ involves the inhibition of FoxO transcriptional activity which is critical for the expression of MAFbx and MuRF1 (193). Lastly, our results suggest that the inhibitory function of DGKζ on FoxO activity is likely mediated by increased protein expression and/or nuclear translocation of DGKζ during OV. Taken together, our findings have unveiled a novel mechanism in which skeletal muscle utilizes DGKζ to control FoxO signaling and UPS-mediated protein degradation, and thereby, help to support the hypertrophic remodeling that occurs in response to mechanical loading.

Similar to the hypertrophic remodeling, a rapid and robust activation of the UPS frequently occurs during atrophic conditions, and this inevitably contributes to the development of muscle wasting. For example, studies employing proteasome inhibitors, or mice lacking MAFbx or MuRF1, have indicated that various types of muscle atrophy occur, at least in part, through a proteasome-, MAFbx-, and/or MuRF1-dependent mechanism (193, 207, 208). In addition to the UPS, the activation of FoxO and NF-κB has also been shown to contribute to muscle wasting. For instance, by using muscle-specific deletion of FoxO genes, Milan et al. recently demonstrated that the activation of FoxO plays a critical role in denervation- and fasting-induced muscle atrophy, as well as the induction of genes that regulate the UPS, such as MAFbx and MuRF1 (201). Furthermore, several previous studies have demonstrated that the activation of NF-κB also plays a critical role in denervation- and fasting-induced muscle atrophy (202, 209, 210). Together, it seems clear that suppressing the activation of the UPS and/or FoxO and NF-κB is a potential strategy for the prevention of muscle wasting. Therefore, it is important to reiterate our results which indicate that increased expression of DGKζ can inhibit muscle atrophy during denervation and fasting, and that this effect is associated with inhibition of the UPS and the transcriptional activity of

FoxO and NF-κB. Based on these points, it would appear that targeting DGKζ may be a viable strategy for therapies that are aimed at preventing the loss of muscle mass.

In summary, the results from this study have exposed a novel mechanism by which skeletal muscle positively regulates fiber size during physiological remodeling. We determined that DGKζ is a critical component of this mechanism, and unexpectedly found that DGKζ can control catabolic pathways involving FoxO, NF-κB, and the UPS. This could be a fundamentally important finding because, in addition to muscle wasting, aberrant regulation of FoxO, NF-κB and the UPS has been implicated in the development of numerous diseases (e.g., diabetes, cancer, inflammation, neurodegeneration, aging, etc.) (211-213). Therefore, our investigation not only identifies DGKζ as a potential therapeutic target for preventing muscle wasting, but also suggests that DGKζ could play an important role in a broad range of clinically relevant conditions. In the future, it will be important to further define how DGKζ inhibits the UPS and its upstream regulators such as FoxO and NF-κB. The resulting knowledge should expand our understanding of the mechanisms that control skeletal muscle plasticity and potentially many other prevalent diseases.

Methods

Antibodies and Plasmid constructs. - Rabbit anti-p70^{S6k} (#2708), anti-4EBP1 (#9644), anti-phospho-4EBP1 (T36/47; #2855), anti-eIF4G (#2469), anti-eIF4E (#2067), anti-eIF2a (#5324), anti-eEF2 (#2332), anti-FoxO3a (#2497), anti-HA (#3724), anti-GFP (#2555), and anti-LDHA (#3558) antibodies were purchased from Cell Signaling (Danvers, MA). Rabbit anti-phospho p70^{S6k} (T389), anti-DGKδ (sc66860), and anti-DGKε (sc98729), mouse anti-Ubiquitin (sc8017) and anti-UBF (sc13125), goat anti-DGKζ (sc8722, C-terminus specific), and FITC-conjugated anti-chicken IgY (sc2431) antibodies, and normal goat IgG (sc2028), were purchased from Santa Cruz Biotechnologies (Santa Cruz, CA). Rabbit anti-eIF3f (#600-401-934) was purchased from Rockland Immunochemicals (Limerick, PA). Rabbit anti-DGKζ antibody (N-terminus specific) was obtained from Dr. Matthew Topham (University of Utah, UT) (214). Mouse anti-puromycin antibody was obtained from Dr. Philippe Pierre (Centre d'Immunologie de

Marseille-Luminy, France) (215). Mouse anti-eIF4E antibody was obtained from Dr. Scot Kimball (Pennsylvania State University, PA) (216).(215) Rabbit anti-MAFbx and mouse anti-MuRF1 antibodies were obtained from Regeneron Pharmaceuticals Inc. (Tarrytown, NY). Rabbit anti-laminin (L9393) and anti-FLAG (F7425) antibodies were purchased from Sigma-Aldrich (St. Louis, MO). Mouse IgG1 anti-type 2a MHC (clone SC-71), mouse IgM anti-type 2b MHC (clone BF-F3), and mouse IgM anti-type 2x MHC (clone 6H1) antibodies were purchased from the Developmental Studies Hybridoma Bank (Ames, IA). Mouse IgG1 anti-dystrophin antibody (NCL-DYS2; Novocastra) was purchased from Leica Biosystems (Buffalo Grove, IL). Chicken IgY anti-β-Galactosidase (LacZ; ab9361) was purchased from Abcam (Cambridge, MA). Rat anti-HA IgG1 antibody (#11867431001) was purchased from Roche Applied Science (Indianapolis, IN). HRP-conjugated anti-rabbit IgG (PI-1000), anti-mouse IgG (PI-2000), and anti-goat IgG (PI-9500) antibodies were purchased from Vector Laboratories (Burlingame, CA). HRP-conjugated anti-mouse IgG 2a (#115-035-206), Alexa-Fluor-488-conjugated anti-mouse IgG1 (#115-545-205) and anti-rat IgG (#112-545-167), AMCA-conjugated anti-mouse IgM (#115-155-075), and Dylight 594-conjugated anti-rabbit IgG (#711-515-152) antibodies were purchased from Jackson ImmunoResearch Laboratories Inc. (West Grove, PA). Alexa-Fluor-350-conjugated anti-rabbit IgG antibody (A-11046) was purchased from Invitrogen (Carlsbad, CA).

pEGFP-C3 (GFP) was purchased from Clontech (Mountain View, CA). pCMVβ (LacZ) was purchased from Marker Gene Technologies Inc. (Eugene, OR). pHA3-DGKζ (WT-DGKζ), pcDNA1-FLAG-DGKζ (WT-DGKζ), and pcDNA1-FLAG-DGKζ with K/R→A in the MARCK-PDS-homology domain of DGKζ2 (aa256-273) (ΔNLS-DGKζ) (160) were obtained from Dr. Matthew Topham (University of Utah, UT). KD-DGKζ was generated from pHA3-DGKζ as previously described (109). pECE-HA-FoxO3a (wtFoxO3a) and pECE-HA-FoxO3a with three PKB phosphorylation sites mutations (T32A/S253A/S315A) (caFoxO3a) were obtained from Dr. Paul Coffer (University Medical Center Utrecht, The Netherlands). pCMV2-FLAG-IKK-2 with two phosphomimetic mutations in the kinase activation loop (S177E/S181E) (caIKKβ; #11105) was purchased from Addgene. pGL3-Forkhead response element firefly luciferase was obtained from Dr. Alex Toker (Harvard University, MA). pGL3-

NF-κB response element firefly luciferase was obtained from Dr. Susan Kandarian (Boston University, MA). pGL3-MAFbx promoter firefly luciferase and pGL2-MuRF1 promoter firefly luciferase were obtained from Dr. Marco Sandri (University of Padova, Italy). pGL3-myostatin promoter firefly luciferase was obtained from Dr. David Allen (University of Colorado, CO). pRL-SV40 *Renilla* luciferase was purchased from Promega (Madison, WI). All plasmid DNA was grown in DH5α Escherichia coli, purified with an EndoFree plasmid kit (QIAGEN, Valencia, CA), and re-suspended in sterile PBS.

Animals and Sampling. - Female Sprague-Dawley rats weighing 250-270g were purchased from Harlan Sprague Dawley Inc. (Indianapolis, IN) and used for OV studies. WT C57BL/6 mice were purchased from The Jackson Laboratory (Bar Harbor, MA) and DGK$\zeta^{-/-}$ C57BL/6 mice were kindly provided by Dr. Xiao-Ping Zhong (Duke University, Durham, NC) (217). Male C57BL/6 mice were used for mechanical overload and food deprivation studies, and female C57BL/6 mice were used for denervation and other studies. All mice were 8-10 weeks of age at the initiation of the studies. All animals were housed in a room maintained at 25 °C with a 12-h:12-h light:dark cycle and received food and water *ad libitum* except in the food deprivation study. Before all surgical procedures, animals were anesthetized with an i.p. injection of ketamine (100 mg/kg body weight) and xylazine (10 mg/kg body weight). At the end of the experimental procedures, muscles were collected, and either immediately frozen in liquid nitrogen for non-histochemical analyses or submerged in OCT (Tissue-Tek; Sakura Finetek, Torrance, CA) at resting length and frozen in liquid nitrogen-chilled isopentane for histochemical analyses. Mice were then euthanized by cervical dislocation under anesthesia.

OV, Denervation, and Food deprivation. - Bilateral OV of the PLT muscle was induced by synergist ablation surgery that involved the removal of the soleus and distal one third of the gastrocnemius muscles in both legs, leaving the PLT as the sole plantar flexor muscle. Unilateral denervation of the hind limb muscles was achieved by a small excision (0.5 cm) of the sciatic nerve in the right leg. Mice in the control group received a sham surgery that involved only an incision in the skin where the synergist ablation or denervation surgery would have occurred. Following the surgeries, the

skin incisions were closed with a 5-0 polysorb suture (SL-1614-G; Covidien, Mansfield, MA). For food deprivation, mice had food withdrawn for 48 h, with *ad libitum* access to water.

Skeletal muscle transfection. - Mouse TA or PLT muscles were transfected by electroporation as previously described (218). In brief, a plasmid DNA solution was injected into proximal and distal ends of the muscle belly with a 27-gauge needle. After the injections, two stainless steel pin electrodes (1-cm gap) connected to an ECM 830 electroporation unit (BTX/Harvard Apparatus, Holliston, MA) were laid on top of the proximal and distal myotendinous junctions of the TA or gastrocnemius (for PLT). Then, eight 20 ms square-wave electric pulses were delivered onto the muscle at a frequency of 1 Hz with a field strength of 160 V/cm. In some cases, the electroporation procedure was preceded by OV, denervation, or food deprivation. Following the electroporation, the incisions were closed with a 5-0 polysorb suture.

Sample preparation and Fractionation. - For DGK activity assay, frozen muscles were homogenized with a Polytron in ice-cold buffer A [20 mM Tris (pH 7.5), 250mM sucrose, 1mM EDTA, 1mM EGTA, 1mM DTT, 50 mM NaF, 1 mM Na_3VO_4, 1 mM PMSF, and 20 μg/ml each leupeptin, pepstatin, aprotinin, and soybean trypsin inhibitor], and the homogenates were precleared by centrifugation at 1000 *g* for 10 min (4 °C). The precleared supernatants (whole homogenate) were further centrifuged at 100,000 *g* for 1 h (4 °C) to separate the soluble supernatants (cytosolic fraction) and insoluble pellets (crude membrane fraction) as demonstrated previously (109). The membrane pellets were washed once and resuspended in the ice-cold buffer A.

For Western blot analysis, frozen muscles were homogenized with a Polytron in ice-cold buffer B [40 mM Tris (pH 7.5), 1 mM EDTA, 5 mM EGTA, 0.5% Triton X-100, 25 mM β-glycerolphosphate, 25 mM NaF, 1 mM Na_3VO_4, 1 mM PMSF, and 10μg/ml leupeptin], and the whole homogenate was subjected to further analysis. When nuclear fractionation was needed, frozen muscles were homogenized with a Polytron in ice-cold buffer C [20 mM HEPES (pH 7.5), 10 mM NaCl, 1.5 mM $MgCl_2$, 20% glycerol, 0.1% Triton X-100, 1mM DTT, 25 mM β-glycerolphosphate, 25 mM NaF, 1 mM Na_3VO_4, 1 mM PMSF, and 10μg/ml leupeptin], and the homogenates (whole homogenate) were centrifuged at 900 *g*

for 5 min (4 °C) as previously described (219). The resulting supernatants (cytoplasmic fraction) were further cleared from the residual nuclei by centrifugation at 900 *g* three times, and the pellets (crude nuclear fraction) were washed three times with the ice-cold buffer C. The nuclear pellets were then resuspended in the ice-cold buffer C containing approximately 600 mM NaCl and incubated for 1 h (4 °C) to lyse the nuclei. The resuspended pellets were centrifuged at 22,000 *g* for 15 min (4 °C) to obtain nuclear protein-containing supernatants.

The protein concentration in each homogenate was determined with the DC protein assay kit (Bio-Rad, Hercules, CA) and used to control the loading amounts of whole / cytosolic / membrane protein in the DGK activity assay or whole / cytoplasmic / nuclear protein in the Western blot analyses.

DGK activity assay. - DGK activity was measured *in vitro* by the standard octyl glucoside (OG)/phosphatidylserine (PS)-mixed micelle assay. In brief, OG/PS-mixed micelles were prepared by resuspending dried DAG (1,2-dioleoyl-*sn*-glycerol) and PS (1,2-dipalmitoyl-*sn*-glycero-3-phosphoserine) in 5× OG buffer [275 mM OG, 1 mM diethylenetriaminepentaacetic acid (DTPA)]. The reaction was then initiated by combining 10 µl of each diluted sample or protein G agarose beads (see *Immunoprecipitation*) with 20 µl of the OG/PS-mixed micelles and 70 µl of reaction mixture, which yielded a final concentration of [55 mM OG, 0.25 mM DAG (0.87 mol% in micelles), 1 mM PS, 50 mM imidazole (pH 6.6), 50 mM NaCl, 12.5 mM $MgCl_2$, 1 mM EGTA, 0.2 mM DTPA, 1 mM DTT, 500 µM ATP, and 1 µCi [γ-^{32}P]ATP]. In some cases, R59949 (12 mol% in micelles) was pre-incubated in the mixture of sample and OG/PS-mixed micelles for 10 min before the start of the reaction. After a 30 min incubation at 25 °C, the reaction was terminated by the addition of 0.45 ml of chloroform-methanol 1:2 (v/v) and 0.15 ml of 1% perchloric acid. [γ-^{32}P]PA was then extracted and separated by TLC with a solvent system consisting of ethyl acetate-isooctane-acetic acid-dH_2O 11:5:2:10 (v/v) as previously described (109). The amount of [γ-^{32}P]PA was visualized and quantified with a Storm PhosphorImager (GE Healthcare).

Immunoprecipitation and Western blotting. - For immunoprecipitation of DGKζ and subsequent DGK activity assay, equal amounts of protein from each whole homogenate that was prepared in ice-cold buffer A, or membrane fractions that were derived from equal amounts of whole homogenate protein,

were incubated with goat anti-DGKζ antibody (1:13) (4 h, 4 °C) followed by 20 µl of Protein G agarose beads (Santa Cruz Biotechnologies) (overnight, 4 °C). Following the incubation, DGKζ-depleted supernatants were collected and the beads were washed three times with fresh ice-cold buffer A. For immunoprecipitation of eIF4E and subsequent Western blotting, whole homogenates prepared in ice-cold buffer B were precleared by centrifugation at 10,000 *g* for 10 min (4 °C). Then, equal amounts of protein from each sample were incubated with mouse anti-eIF4E antibody (1:10) (2 h, 4 °C) followed by 20 µl of Protein A agarose beads (Santa Cruz Biotechnologies) (2 h, 4 °C) that were pre-blocked with 1% BSA (1 h, 4 °C). Following the incubations, the beads were washed three times with fresh ice-cold buffer B. Western blot analyses were performed as previously described (109).

Measurements of protein synthesis and protein degradation. - The rate of protein synthesis was measured *in vivo* with the surface sensing of translation technique as previously described (80). In brief, mice were given an i.p. injection of 0.04 µmol/g puromycin (EMD Millipore, Billerica, MA) dissolved in 200 µl of PBS, and exactly 30 min post injection, muscles were collected and subjected to Western blotting for the detection of puromycin-labeled peptides.

The rate of protein degradation was measured *ex vivo* by monitoring the rate of tyrosine release according to previously described methods with minor modifications (109, 220). Briefly, PLT muscles were placed in an organ culture system, which consisted of a refined myograph apparatus (Kent Scientific, Torrington, CT) and an organ culture bath, and incubated at 37 °C in Krebs-Henseleit buffer (120 mM NaCl, 4.8 mM KCl, 25 mM $NaHCO_3$, 2.5 mM $CaCl_2$, 1.2 mM KH_2PO_4, 2 mM $MgSO_4$, and 5 mM HEPES) supplemented with 1× MEM amino acid mixture (Invitrogen), 25 mM glucose, and a continuous 95% O_2 and 5% CO_2 gassing. The medium was refreshed every 10 min during initial 30 min of pre-incubation period and then remained unchanged for 2 h in the presence of 0.5 mM cyclohexamide (Acros Organics, Morris Plains, NJ) to allow tyrosine accumulation in the medium. In some cases, the activity of the proteasome was inhibited by incubating the muscles with 30 µM of MG132 (Cayman Chemical, Ann Arbor, MI) during the last 10 min of the pre-incubation period and throughout the 2 h release period. After collections, the medium was mixed with an equal volume of nitrosonaphthol-nitric acid reagent

50:50 (v/v) and incubated at 55 °C for 30 min. Ethylene dichloride was then added to the mixture, centrifuged briefly, and a fluorescent tyrosine derivative in the upper aqueous phase was quantified by FLUOstar Optima fluorimeter (BMG Labtech, Durham, NC) with excitation at 485 nm and emission at 520 nm, using 0.3-10 μM of tyrosine standards.

Immunohistochemistry. - Cross-sections (10 μm thick) from the mid-belly of the muscles frozen in OCT were obtained with a cryostat and fixed in acetone for 10 min at −30 °C. The sections were warmed to room temperature for 5 min and rehydrated with PBS for 15 min. The sections were then incubated in solution A (PBS containing 0.5% BSA and 0.5% Triton X-100) for 20 min and probed with the indicated primary antibodies (dissolved in solution A) for 45 min at room temperature. After washing with PBS, the sections were incubated with the appropriate fluorophore-conjugated secondary antibodies (dissolved in solution A) for 1 h at room temperature. When nuclei staining was needed, the sections were subsequently incubated with 20 μg/ml of propidium iodine (PI) for 5 min. After a final wash with PBS, florescent signals from each secondary antibody or PI were captured with a DS-QiMc camera on an 80i epifluorescence microscope (both from Nikon, Tokyo, Japan), and the resulting monochrome images were merged with NIS-Elements D image analysis software (Nikon). Investigators that were blinded to the sample identification then used NIS-Elements D to measure the total fiber number per muscle cross-section, average fiber CSA, myonuclei per fiber, and myonuclear localization.

Luciferase activity assay. - Muscles transfected with plasmid DNA encoding a luciferases reporter were homogenized with a Polytron in passive lysis buffer (Promega, Madison, WI), and firefly and *Renilla* luciferase activities were measured by a FLUOstar Optima luminometer using the Dual-Luciferase Reporter Assay kit (Promega) as described in the manufacturer's instructions. Firefly luciferase activity was normalized to the *Renilla* luciferase activity in the same sample.

Measurements of [DAG] and [PA]. - Total lipids were extracted from a 160 mg portion of powdered muscle as previously described (56). The samples were then separated by TLC with a solvent system consisting of hexane-diethyl ether-acetic acid 50:50:1 (v/v) for DAG or ethyl acetate-isooctane-acetic acid-dH_2O 11:5:2:10 (v/v) for PA. The amount of lipids was visualized by 2 h of staining in [30%

methanol, 0.03% (w/v) Coomassie Blue R250 and 100mM NaCl], followed by 5 min of destaining in (30% methanol and 100mM NaCl), and then quantified by transmission densitometry using 1-30 μg of DAG or 0.5-5.0 μg of PA standards.

Real-time qRCR. - Frozen muscles were homogenized with an RNAse-free pestle in ice-cold TRIzol (Ambion, Life Technologies, Grand Island, NY), and total RNA was isolated with a PureLink RNA Mini Kit (Ambion) according to the manufacturer's instructions. The purity and integrity of RNA samples were checked by the ratio of A260/A280 and of 28S/18S rRNA, respectively. cDNA was synthesized from 0.5 μg of total RNA by using the Superscript III First-Strand Synthesis System (Invitrogen) and analyzed for gene expression by quantitative PCR using Fast SYBR Green Master Mix on a StepOnePlus Real-Time PCR System (Applied Biosystems, Foster City, CA). The sequence of primers used are 5'-CAATGCATTAAGCAGCTGGA-3' (forward) and 5'-GGTGAACTTCTGCTGGAAGC-3' (reverse) for DGKζ, and 5'-CCAGCCTCGTCCCGTAGAC-3' (forward) and 5'-ATGGCAACAATCTCCACTTTGC-3' (reverse) for GAPDH as an internal control.

Statistics. - All values were expressed as mean (+SEM in graphs). A sample value that was more than three times deviated from the mean in a given group was excluded as an outlier. Statistical significance was determined by an unpaired, 2-tailed Student's *t* test for single comparison, or one- or two-way ANOVA followed by a post-hoc test for multiple comparisons. Differences between groups were considered significant when $P < 0.05$. All statistical analyses were performed using Excel and SigmaStat (San Jose, CA).

Study approval. - All methods were approved by the Institutional Animal Care and Use Committee of the University of Wisconsin-Madison under protocol # V01324.

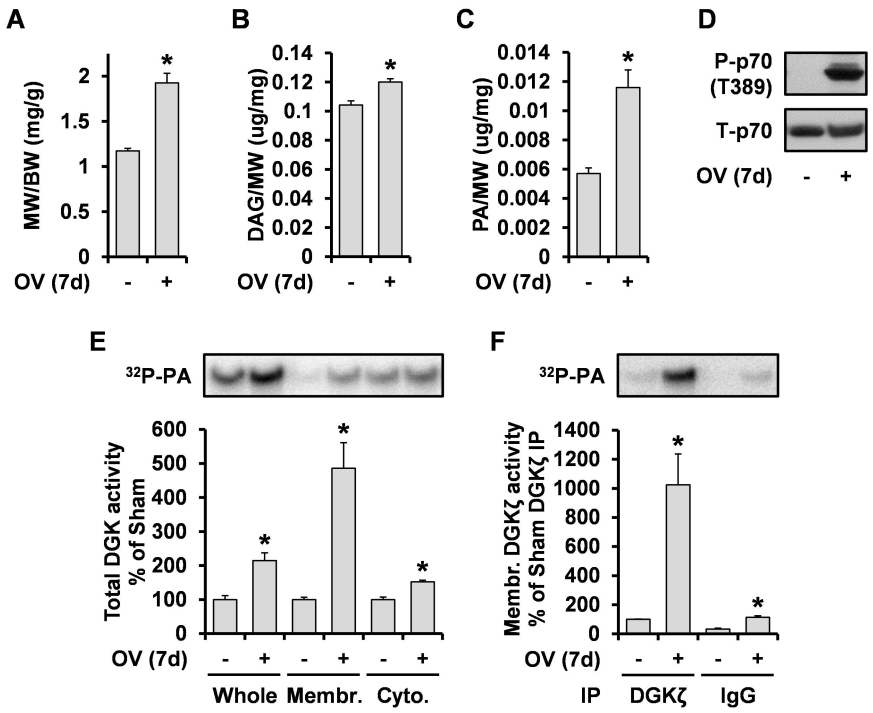

Figure 5-1. OV activates DAG-PA-mTOR signaling and increases DGKζ activity. Rats were subjected to mechanical overload (OV+) or sham (OV-) surgery and the plantaris muscles were collected at 7 days post-surgery. (**A**) Muscle weight (MW) to body weight (BW) ratio (n = 6-8). (**B-C**) TLC-based measurements of (**B**) diacylglycerol (DAG) (n = 3) and (**C**) phosphatidic acid (PA) (n = 4). (**D**) Western blotting to detect phosphorylated (P) and total (T) p70 (n = 4). (**E-F**) DGK activity assay in (**E**) whole homogenate (Whole), membrane fraction (Membr.), or cytosolic fraction (Cyto.) (n = 3-4) or in (**F**) immunoprecipitates (IP) from the membrane fraction (n = 3). *P < 0.05 vs. sham within the same conditions, Student's t test.

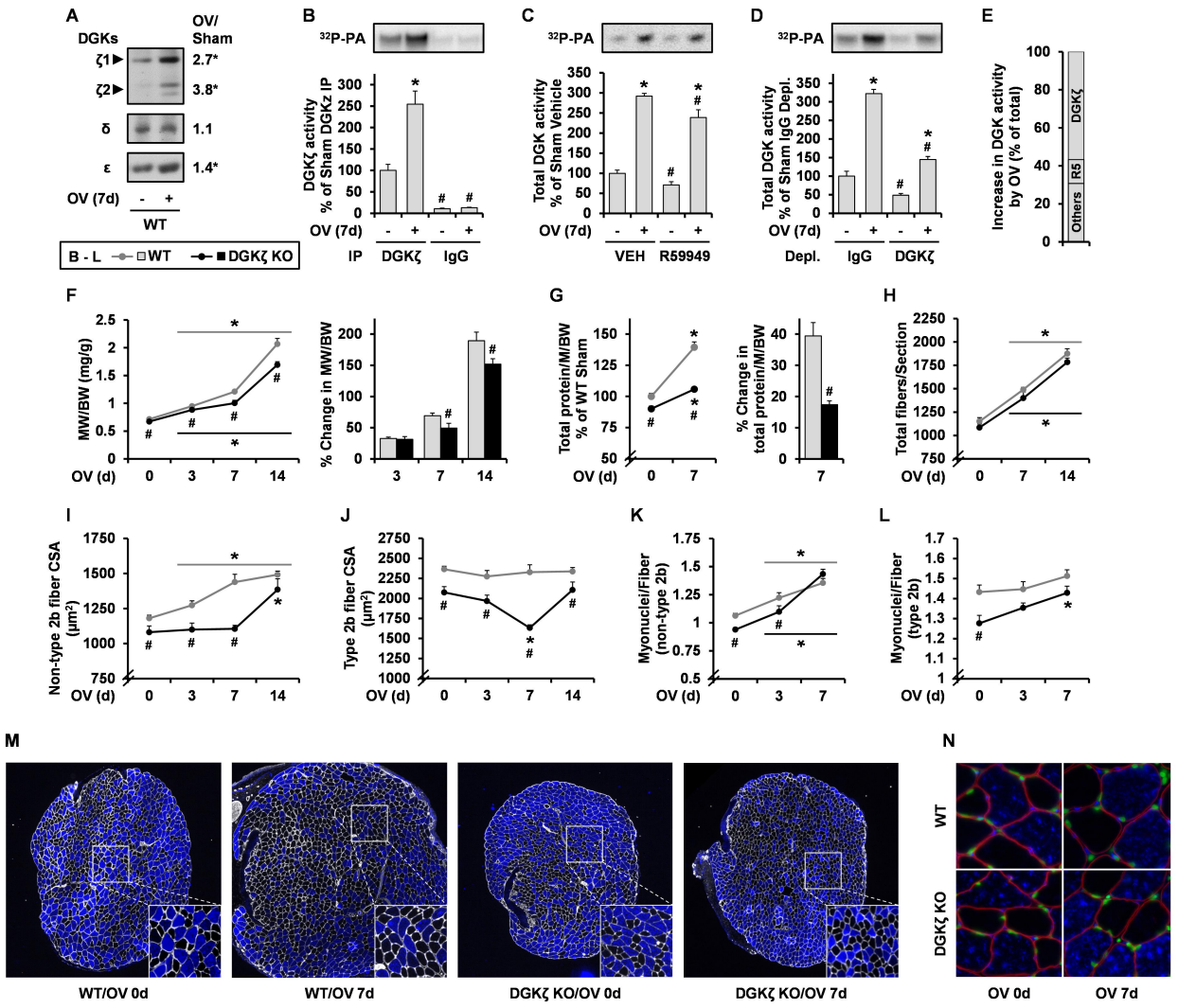

Figure 5-2. During OV, DGKζ is predominantly increased among DGK isoforms and is required for rapid muscle growth. WT and DGKζ KO mice were subjected to mechanical overload (OV+ or OV 3-14d) or sham (OV- or OV 0d) surgery and the plantaris muscles were collected at 3-14 days post-surgery. (**A**) Western blotting to detect the indicated proteins (n = 4). (**B-D**) DGK activity assay following (**B**) immunoprecipitation (IP) of DGKζ (n = 3-4), (**C**) *in-vitro* treatment of R59949 (n = 3-4), and (**D**) immunodepletion (Depl.) of DGKζ (n = 3-4). (**E**) Contribution to the OV-induced increase in total DGK activity by DGKζ, R59949-sensitive DGKs (R5), and other DGKs. (**F**) Muscle weight (MW) to body weight (BW) ratio (n = 6-18). (**G**) Total protein content per muscle (M) normalized by BW (n = 5-6). (**H-J**) Immunohistochemistry on cross-sections with antibodies against laminin and type 2b myosin heavy chain (MHC) to measure (**H**) total fiber number per section, and cross-sectional area (CSA) in (**I**) non-type 2b fibers and (**J**) type 2b fibers (n = 5-16). (**K-L**) Immunohistochemistry on cross-sections with propidium iodine and antibodies against dystrophin and type 2b MHC to measure myonuclei number per fiber cross-section in (**K**) non-type 2b fibers (n = 5-8) and (**L**) type 2b fibers (n = 5-8). (**M-N**) Representative images from the conditions in H-J (white: laminin; blue: type 2b MHC) (**M**) or K-L (red: dystrophin; blue: type 2b MHC; green: propidium iodine) (**N**). Note: sham muscles between different time points were not significantly different in any measurement and thus pooled together to represent 0 day. *P < 0.05 vs. sham within the same conditions, #P < 0.05 vs. DGKζ (B), VEH (C), IgG (D), or WT (F-L), within the same surgery, Student t test (A, the right panels in F-G) or 2-way ANOVA (B-L).

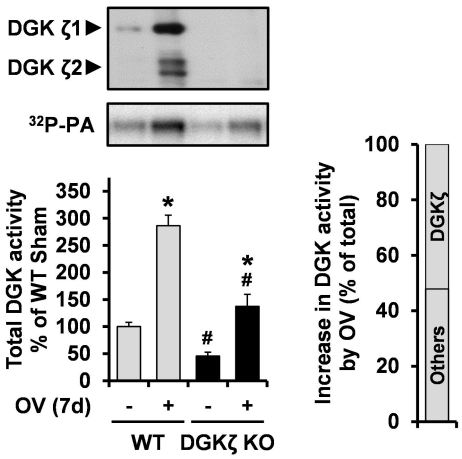

Figure 5-3. During OV, DGKζ is predominantly increased among DGK isoforms. WT and DGKζ KO mice were subjected to mechanical overload (OV+) or sham (OV-) surgery and the plantaris muscles were collected at 7 days post-surgery. The samples were subjected to Western blotting to detect DGKζ protein (top panel), or to DGK activity assay (the right panel shows the contribution of DGKζ and other DGKs to the OV-induced increase in total DGK activity) (n = 4-6). *P < 0.05 vs. sham within the same genotype, #P < 0.05 vs. WT within the same surgery, 2-way ANOVA.

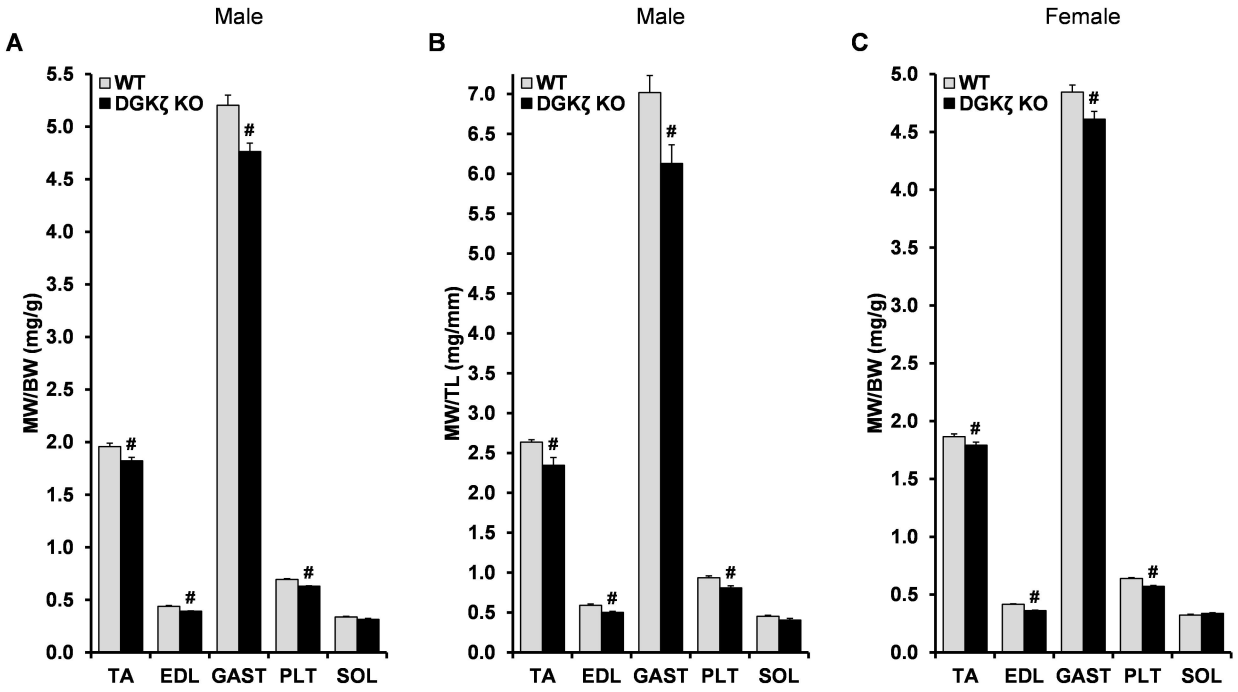

Figure 5-4. DGKζ KO mice exhibit a reduction in skeletal muscle mass. Tibialis anterior (TA), extensor digitorum longus (EDL), gastrocnemius (GAST), plantaris (PLT), and soleus (SOL) muscles from WT and DGKζ KO mice were collected at 8-11 wks of age. (**A**) Muscle weight (MW) to body weight (BW) ratio in male (n = 6). (**B**) MW to tibia length (TL) ratio in male (n = 6). (**C**) MW to BW ratio in female (n = 13-18). #$P < 0.05$ vs. WT, Student t test.

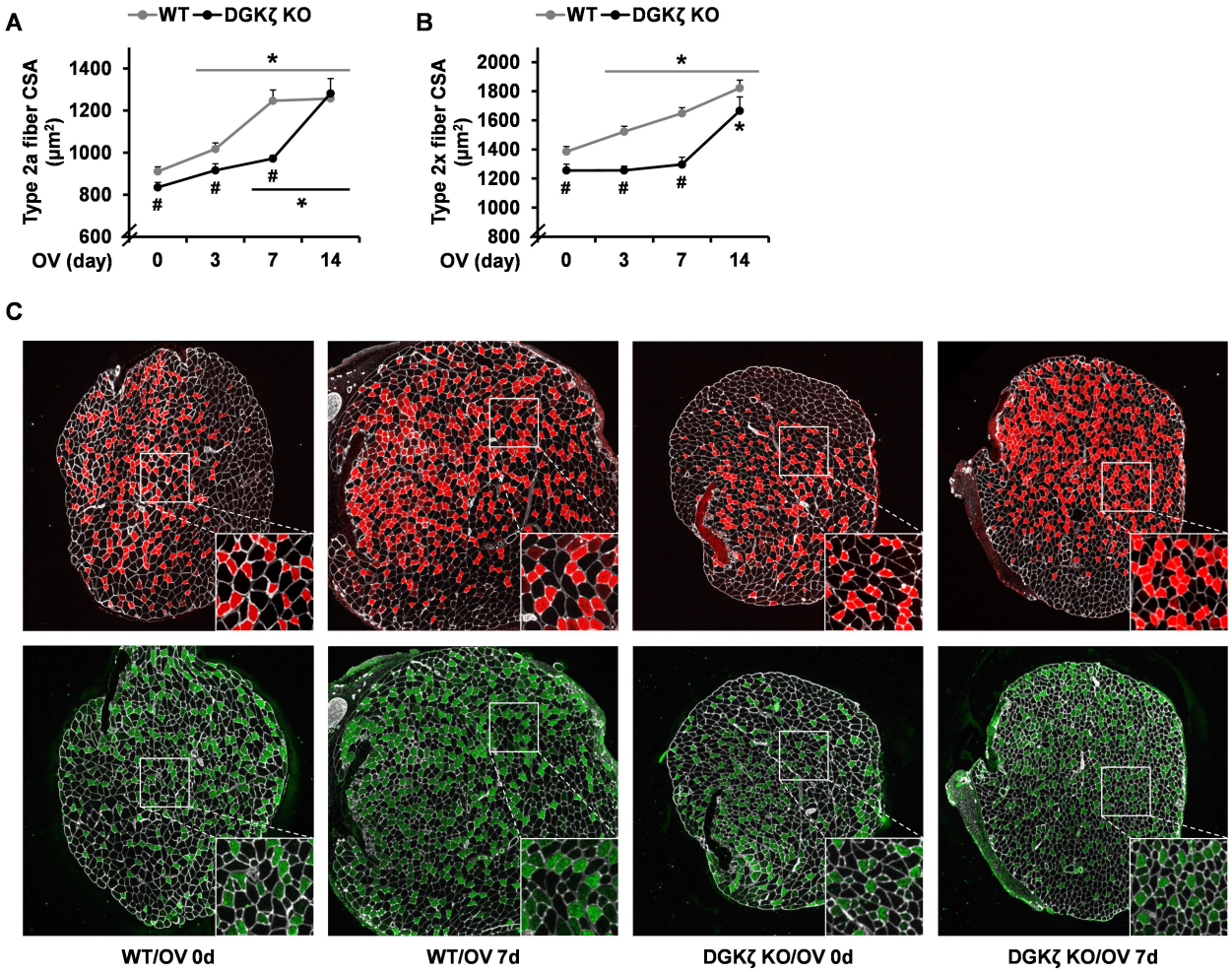

Figure 5-5. During OV, DGKζ is predominantly increased among DGKs and is required for rapid non-type 2b fiber hypertrophy. WT and DGKζ KO mice were subjected to mechanical overload (OV 3-14d) or sham (OV 0d) surgery and the plantaris muscles were collected at 3-14 days post-surgery. Cross-sections of the muscles were subjected to immunohistochemistry with antibodies against laminin and type 2a myosin heavy chain (MHC) or type 2x MHC to measure cross-sectional area (CSA) in (**A**) type 2a MHC fibers and (**B**) type 2x MHC fibers (n = 5-15). (**C**) Representative images from the conditions in A and B (white: laminin; red: type 2a MHC; green: type 2x MHC). Note: sham muscles between different time points were not significantly different in any measurement and thus pooled together to represent 0 day. *P < 0.05 vs. sham within the same genotype, #P < 0.05 vs. WT within the same surgery, 2-way ANOVA.

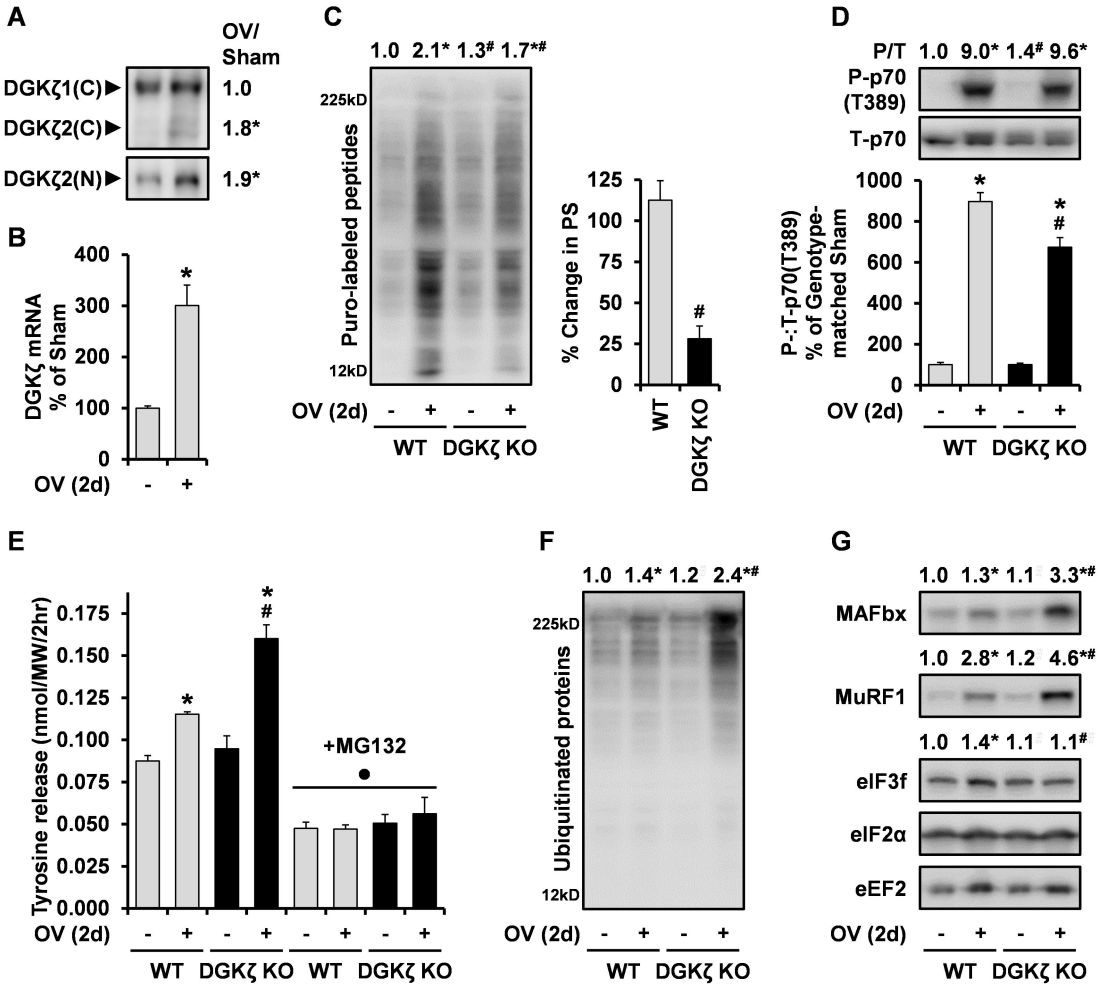

Figure 5-6. DGKζ contributes to the activation of mTOR signaling and protein synthesis, and attenuates the activation of UPS-dependent protein degradation during the early period of OV. WT and DGKζ KO mice were subjected to mechanical overload (OV+) or sham (OV-) surgery and the plantaris muscles were collected at 2 day post-surgery. (**A**) Western blotting to detect DGKζ protein with antibodies against the C-terminus (upper panel) or N-terminus of DGKζ (lower panel; splice variant 2-specific) (n = 6). (**B**) qRT-PCR to measure mRNA levels of DGKζ (n = 5-6). (**C**) Measurement of protein synthesis (PS) rate as assessed by Western blotting of puromycin (puro)-labeled peptides (n = 5-6). (**D**) Western blotting to detect phosphorylated (P) and total (T) p70 (n = 5-6). (**E**) Measurement of protein degradation rate as assessed by tyrosine release (n = 3-5). (**F-G**) Western blotting to detect the indicated proteins (n = 5-8). *P < 0.05 vs. sham within the same genotype, #P < 0.05 vs. WT within the same surgery, •P < 0.05 vs. non-MG132 within the same genotype and surgery, Student t test (A-B, the right panel in C) or 2-way ANOVA (C-G).

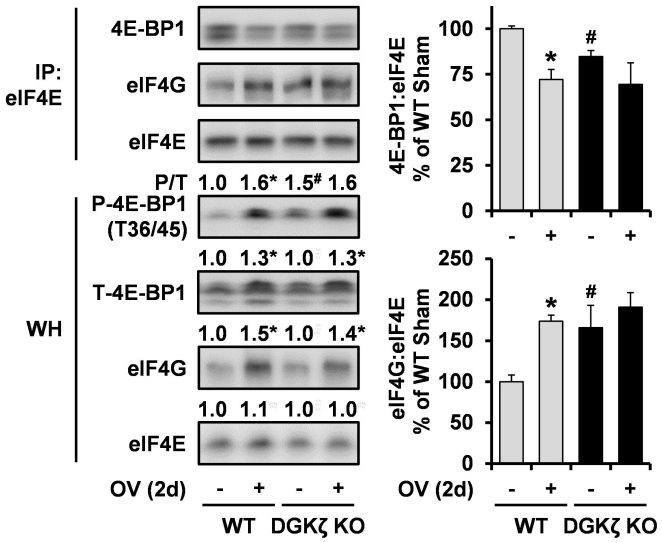

Figure 5-7. DGKζ contributes to the activation of mTOR signaling events during the early period of OV. WT and DGKζ KO mice were subjected to mechanical overload (OV+) or sham (OV-) surgery and the plantaris muscles were collected at 2 days post-surgery. Whole homogenates (WH) and immunoprecipitates (IP) of eIF4E were subjected to Western blotting to detect the indicated proteins (n = 5-6). *P < 0.05 vs. sham within the same genotype, #P < 0.05 vs. WT within the same surgery, 2-way ANOVA.

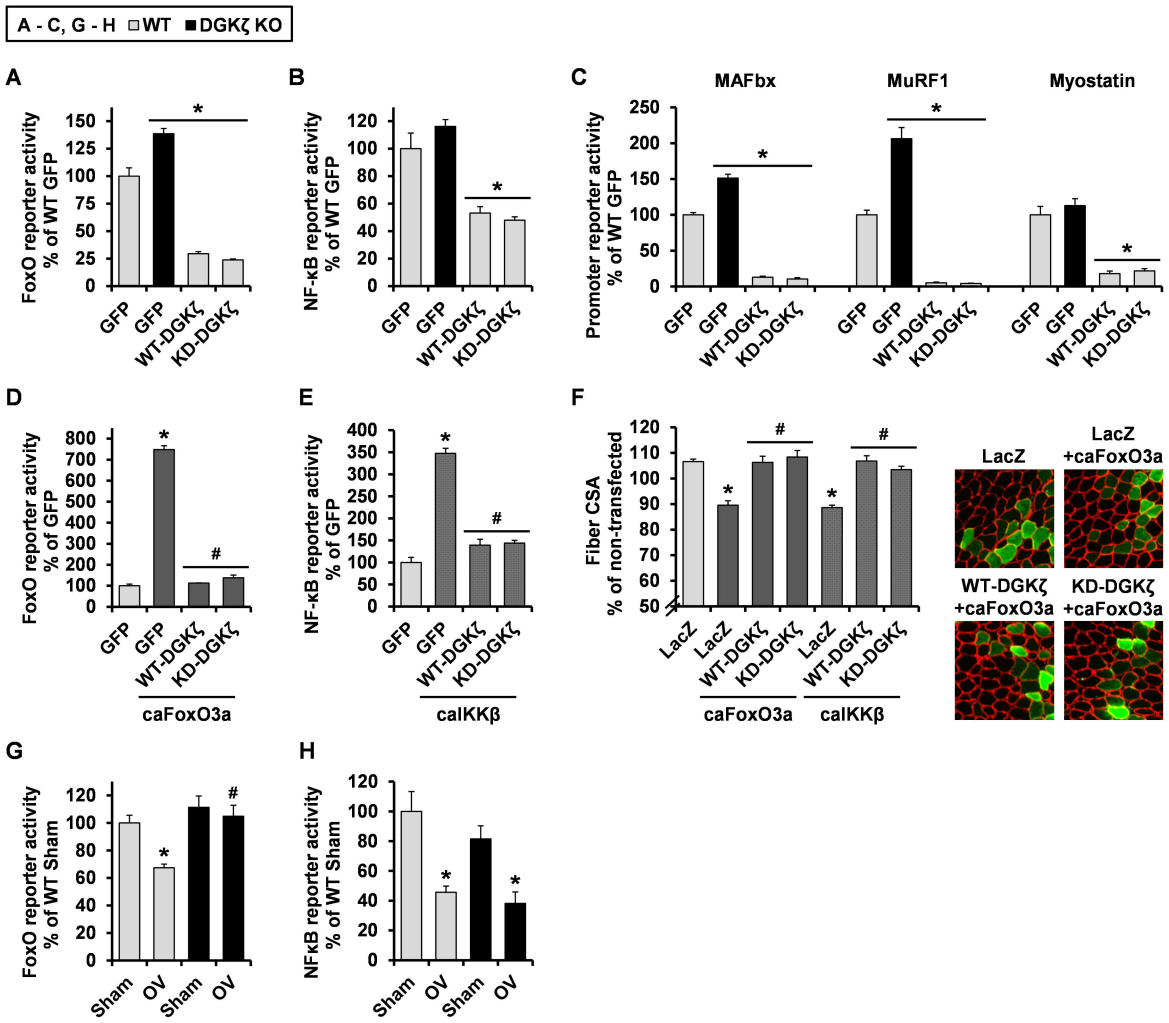

Figure 5-8. DGKζ negatively regulates FoxO and NF-κB activity independent of its kinase activity. **(A-C)** Tibialis anterior (TA) muscles from WT and DGKζ KO mice were co-transfected with GFP, HA-WT-DGKζ, or HA-kinase dead (KD)-DGKζ and pRL-SV40 *Renilla* luciferase (pRL), as well as, (**A**) FoxO response element (RE) firefly luciferase reporter (FF), (**B**) NF-κB RE FF, or (**C**) MAFbx, MuRF1, or Myostatin promoter FF. Muscles were collected at 2 days post-transfection and subjected to dual-luciferase reporter assay (n = 3-8). (**D-E**) TA muscles from WT mice were co-transfected with GFP, HA-WT-DGKζ, or HA-KD-DGKζ and pRL, as well as, (**D**) FoxO RE FF ± constitutively active (ca) FoxO3a or (**E**) NF-κB RE FF ± caIKKβ. Muscles were collected at 2 days post-transfection and subjected to dual-luciferase reporter assay (n = 3-8) (GFP groups present the same data as in A/D and B/E). (**F**) TA muscles from WT mice were transfected with LacZ, HA-WT-DGKζ, or HA-KD-DGKζ ± caFoxO3a or caIKKβ, and collected at 7 days post-transfection. Cross-sections of the muscles were subjected to immunohistochemistry with antibodies against laminin (red), and LacZ (green) or HA (green) to measure cross-sectional area (CSA) of the transfected and non-transfected fibers (the right panel shows representative images from the caFoxO3a conditions) (n = 4). (**G-H**) Plantaris muscles from WT and DGKζ KO mice were co-transfected with pRL, and (**G**) FoxO RE FF or (**H**) NF-κB RE FF, immediately after being subjected to a mechanical overload (OV) or sham surgery. The muscles were collected at 2 days post-surgery and subjected to dual-luciferase reporter assay (n = 4-6). *P < 0.05 vs. WT GFP (A-C), GFP (D-E), LacZ (F), or sham within the same genotype (G-H), #P < 0.05 vs. GFP + caFoxO3a (D), GFP + caIKKβ (E), LacZ + caFoxO3a or LacZ + caIKKβ (F), or WT OV(G), 1-way ANOVA (A-F) or 2-way ANOVA (G-H).

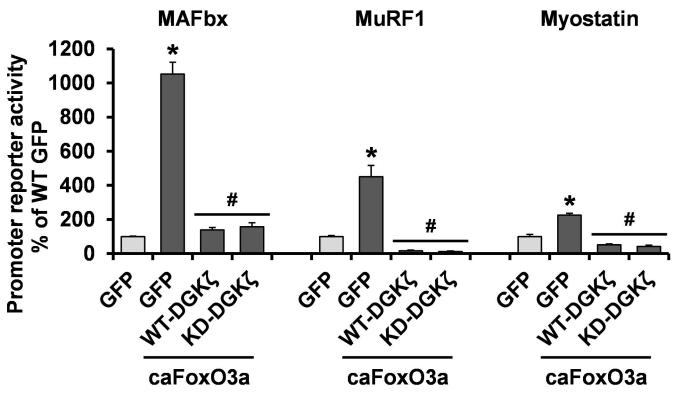

Figure 5-9. DGKζ inhibits the promoter activity of FoxO target genes independent of its kinase activity. Tibialis anterior muscles were co-transfected, in the presence or absence of constitutively active (ca) FoxO3a, with one of the indicated promoter firefly luciferase reporters, pRL-SV40 *Renilla* luciferase reporter, and GFP, HA-WT-DGKζ, or HA-kinase dead (KD)-DGKζ. The muscles were collected at 2 days post-transfection and subjected to dual-luciferase reporter assay (n = 4-8) (GFP groups present the same data as in Figure 3C). *$P < 0.05$ vs. GFP, #$P < 0.05$ vs. GFP + caFoxO3a, 1-way ANOVA.

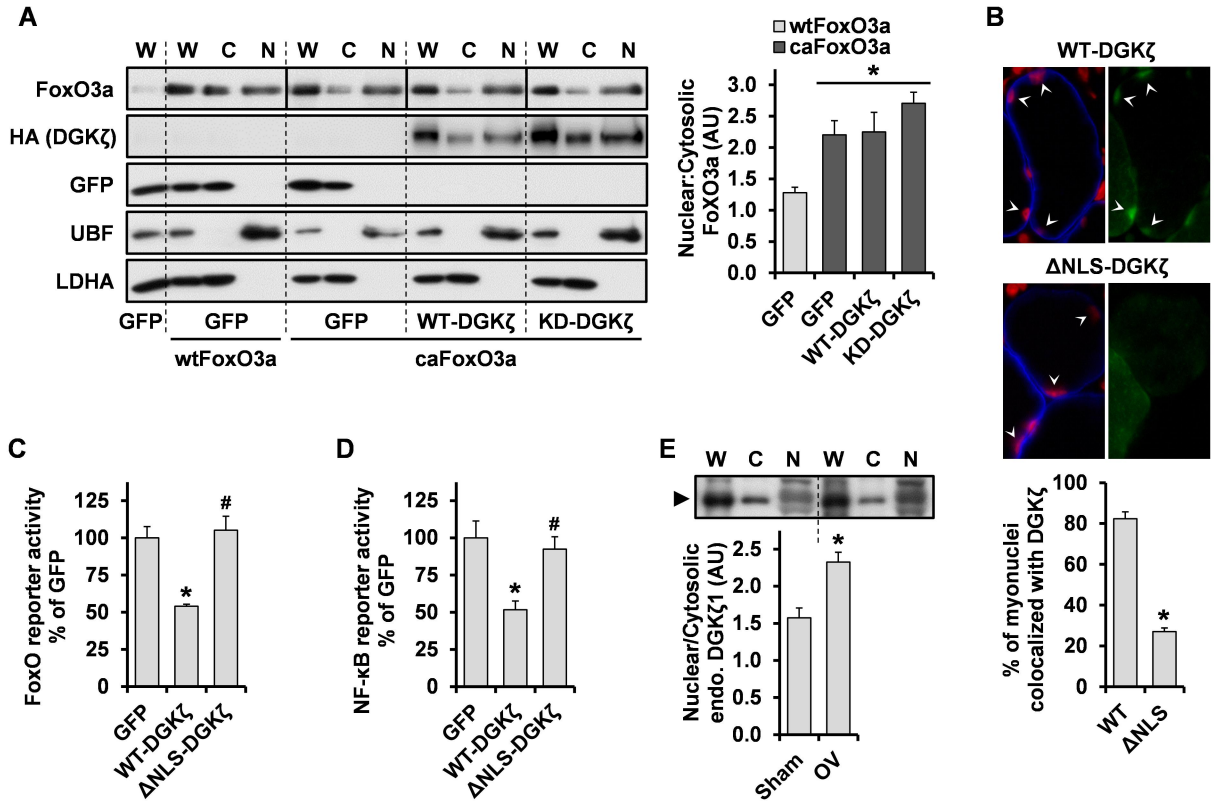

Figure 5-10. The nuclear-localization signal of DGKζ is required for the inhibition of FoxO and NF-κB activity. (**A**) Tibialis anterior (TA) muscles were co-transfected with wild-type (wt) FoxO3a or constitutively active (ca) FoxO3a, and GFP, HA-WT-DGKζ, or HA-KD-DGKζ. The muscles were collected at 2 days post-transfection and subjected to Western blotting to detect FoxO3a, HA (DGKζ), GFP, UBF (nuclear marker), and LDHA (cytosolic marker), in whole homogenates (W), cytosolic fractions (C), and nuclear fractions (N) (solid lines distinguish images from different gels) (n = 4). (**B**) TA muscles were transfected with FLAG-WT-DGKζ or FLAG-nuclear localization signal mutated (ΔNLS)-DGKζ and collected at 2 days post-transfection. Cross-sections of the muscles were subjected to immunohistochemistry with propidium iodine (red) and antibodies against dystrophin (blue) and FLAG (green) to measure myonuclei that colocalized with DGKζ (n = 4). (**C**-**D**) TA muscles were co-transfected with GFP, FLAG-WT-DGKζ, or FLAG-ΔNLS-DGKζ and pRL-SV40 *Renilla* luciferase, as well as, (**C**) FoxO response element (RE) firefly luciferase reporter (FF) or (**D**) NF-κB RE FF. Muscles were collected at 2 days post-transfection and subjected to dual-luciferase reporter assay (n = 4-8) (GFP groups present the same data as in Figure 3, A-B). (**E**) Mice were subjected to mechanical overload (OV) or sham surgery, and the plantaris muscles were collected at 2 days post-surgery and subjected to Western blotting to detect DGKζ protein in different fractions as described in (A) (n = 5). AU, arbitrary unit. *P < 0.05 vs. GFP + wtFoxO3a (A), WT-DGKζ (B), GFP (C-D), or Sham (E), #P < 0.05 vs. WT-DGKζ, 1-way ANOVA (A, C-D) or Student t test (B, E).

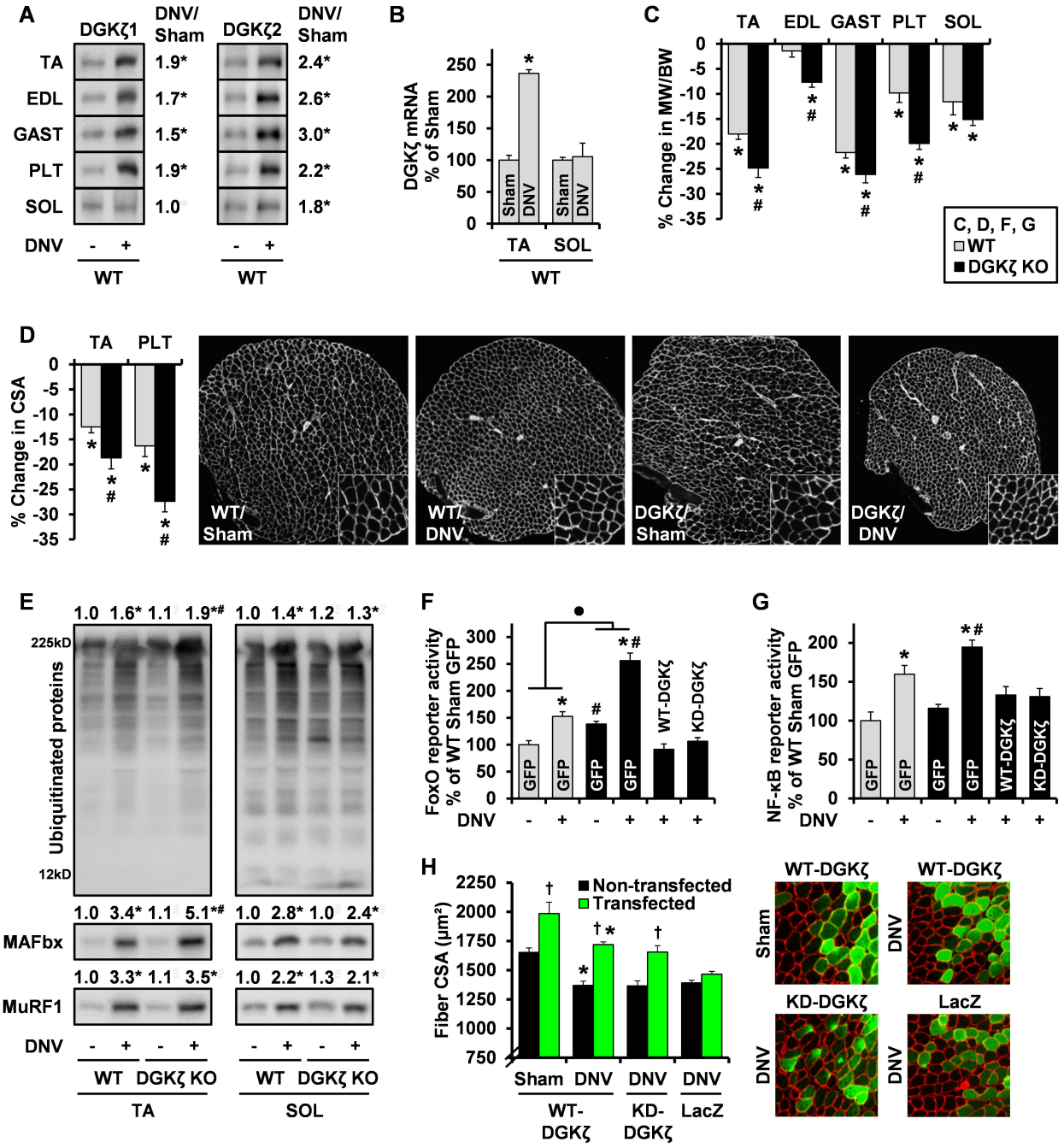

Figure 5-11. DGKζ inhibits the activation of the FoxO/NF-κB/ubiquitin pathway and atrophy during denervation. WT and DGKζ KO mice were subjected to denervation (DNV+) or sham (DNV-) surgery, and the tibialis anterior (TA), extensor digitorum longus (EDL), gastrocnemius (GAST), plantaris (PLT), and soleus (SOL) muscles were collected at 7 days post-surgery. (**A**) Western blotting to detect DGKζ protein with antibodies against C-terminus of DGKζ1 or N-terminus of DGKζ2 (n = 4-6). (**B**) qRT-PCR to measure mRNA levels of DGKζ (n = 4-6). (**C**) Denervation-induced changes in the muscle weight (MW) to body weight (BW) ratio (n = 9-13). (**D**) Immunohistochemistry on cross-sections with an antibody against laminin (white) to measure fiber cross-sectional area (CSA) (the right panel shows representative images of the PLT muscles) (n = 3-6). (**E**) Western blotting to detect the indicated proteins (n = 4-6). (**F-G**) TA muscles were co-transfected with GFP, HA-WT-DGKζ, or HA-kinase dead

(KD)-DGKζ and pRL-SV40 *Renilla* luciferase (pRL), as well as, (**F**) FoxO response element (RE) firefly luciferase reporter (FF) or (**G**) NF-κB RE FF, at 5 days post-DNV or sham surgery. Upon collection, the muscles were subjected to dual-luciferase reporter assay (n = 3-8). (**H**) TA muscles from WT mice were transfected with HA-WT-DGKζ, HA-KD-DGKζ, or LacZ immediately after DNV or sham surgery. Upon collection, cross-sections of the muscles were subjected to immunohistochemistry and analyzed as described in Figure 3F (the right panel shows representative images) (n = 4-6). *$P < 0.05$ vs. sham (within the same genotype in C-G or transfection in H), #$P < 0.05$ vs. WT (within the same surgery in E-G), • $P < 0.05$ in the magnitude of the DNV effect between genotypes, †$P < 0.05$ vs. Non-transfected within the same surgery and DNA, Student t test (A-D; • F) or 2-way ANOVA (E-H).

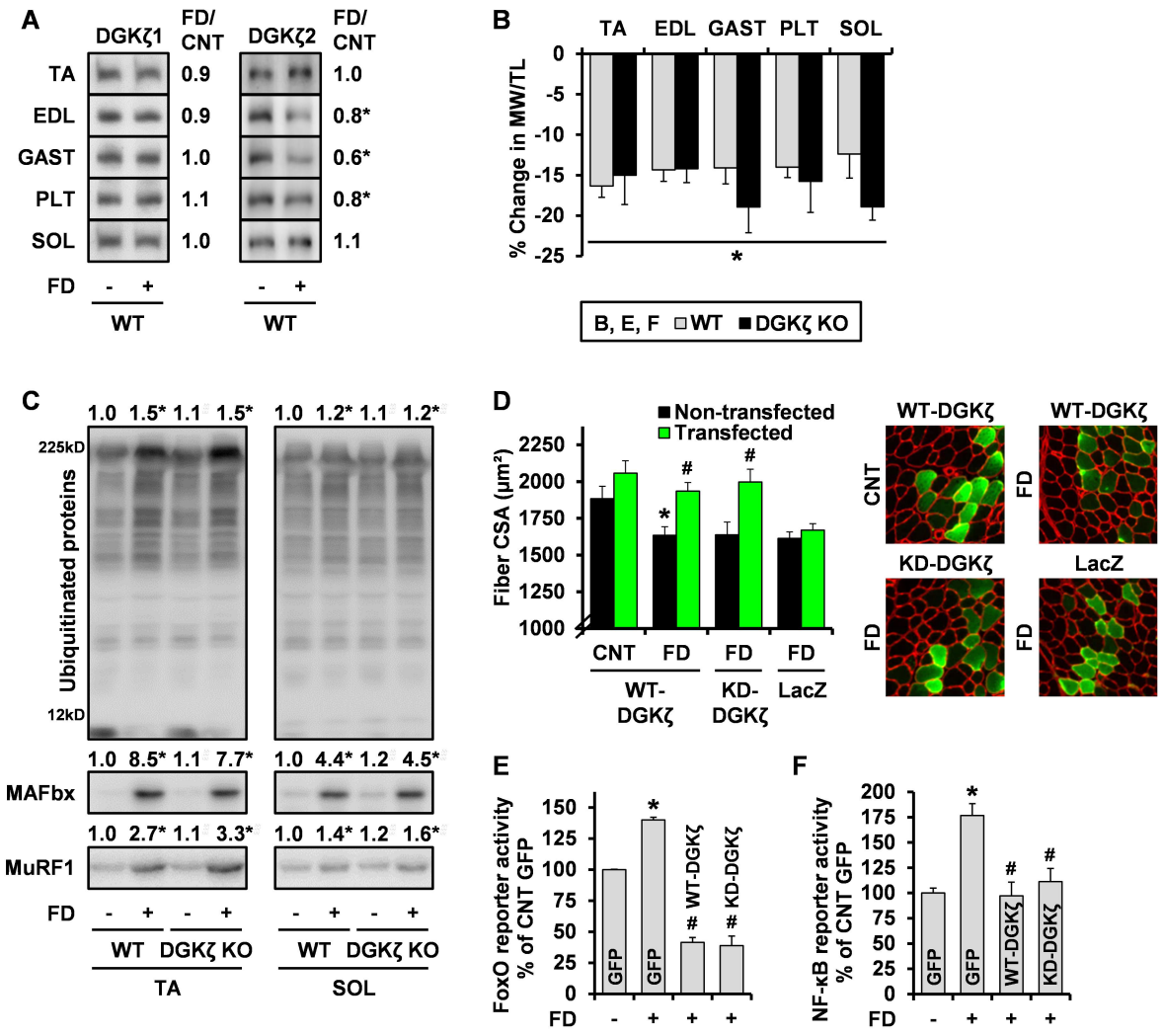

Figure 5-12. Overexpression of DGKζ inhibits the activation of the FoxO/NF-κB and atrophy during food deprivation. WT and DGKζ KO mice were subjected to food deprivation (FD+) or control conditions (FD-), and the tibialis anterior (TA), extensor digitorum longus (EDL), gastrocnemius (GAST), plantaris (PLT), and soleus (SOL) muscles were collected at 2 days post-FD. (**A**) Western blotting to detect DGKζ protein with antibodies against C-terminus of DGKζ1 or N-terminus of DGKζ2 (n = 5-6). (**B**) FD-induced changes in the muscle weight (MW) to tibia length (TL) ratio (n = 5-6). (**C**) Western blotting to detect the indicated proteins (n = 4-6). (**D**) TA muscles from WT mice were transfected with HA-WT-DGKζ, HA-kinase dead (KD)-DGKζ, or LacZ, immediately before being subjected to 2 days of FD or the control condition. Upon collection, cross-sections of the muscles were subjected to immunohistochemistry and analyzed as described in Figure 3F (the right panel shows representative images) (n = 4-5). (**E-F**) TA muscles were co-transfected with GFP, HA-WT-DGKζ, or HA-KD-DGKζ and pRL-SV40 *Renilla* luciferase (pRL), as well as, (**E**) FoxO response element (RE) firefly luciferase reporter (FF) or (**F**) NF-κB RE FF, immediately before being subjected to 2 days of FD or the control condition. Upon collection, the muscles were subjected to dual-luciferase reporter assay (n = 3-5). *P < 0.05 vs. control (within the same genotype in B-C or transfection in D), #P < 0.05 vs. Non-transfected within the same feeding and DNA (D) or GFP + FD (E-F), Student t test (A-B), 2-way ANOVA (C-D), or 1-way ANOVA (E-F).

Chapter 6

Summary and Future Directions

Summary

Skeletal muscle undergoes dynamic remodeling in response to a variety of stimuli, and the resulting changes in muscle mass can profoundly influence health and issues associated with quality of life. It has been well recognized that skeletal muscle mass is largely regulated by changes in mechanical loading and that signaling by the mammalian/mechanistic target of rapamycin (mTOR) is a critical component of the mechanotransduction pathway that regulates protein synthesis and muscle mass in response to the changes in mechanical loading. For example, studies employing rapamycin, an inhibitor of mTOR, have shown that the activation of mTOR signaling is necessary for the mechanically-induced increase in protein synthesis and muscle mass. Accordingly, it has been expected that identifying the mechanisms through which mechanical stimuli activate mTOR signaling would facilitate the development of therapies that can mimic the effects of mechanical loading and, in turn, preserve muscle mass during atrophic conditions such as physical inactivity and aging. However, whether the regulation of mTOR signaling can actually prevent muscle atrophy remains unclear. Furthermore, the mechanisms involved in the mechanical activation of mTOR signaling are poorly understood. Therefore, this study was aimed to determine the role of mTOR signaling in the regulation of protein synthesis and muscle mass during immobilization-induced muscle disuse (Chapter 2) and to define mechanisms that contribute to the mechanically-induced increase in mTOR signaling, protein synthesis, and muscle mass. (Chapter 3-5).

In Chapter 2, I first confirmed that unilateral hindlimb immobilization in mice induces a decrease in the global rates of protein synthesis and muscle mass. Interestingly, in this model, I found that immobilization also induces an increase in mTOR signaling, eukaryotic initiation factor 4F complex formation, and cap-dependent translation. Blocking mTOR signaling during immobilization with rapamycin not only impaired the increase in eukaryotic initiation factor 4F complex formation, but also augmented the decreases in global protein synthesis and muscle mass. On the other hand, stimulating immobilized muscles with isometric contractions enhanced mTOR signaling and rescued the immobilization-induced decrease in global protein synthesis through a rapamycin-sensitive mechanism. Similar to isometric contractions, overexpression of Rheb in immobilized muscles enhanced mTOR

signaling, cap-dependent translation, and global protein synthesis, and prevented the loss of fiber size. Taken together, these results demonstrate that the activation of mTOR signaling is both necessary and sufficient to alleviate the immobilization-induced decreases in protein synthesis and muscle mass.

Having established that the activation of mTOR signaling is a viable target for therapies for preventing muscle atrophy, I began to interrogate the mechanisms through which mechanical stimuli activate mTOR signaling. Based on previous studies, it has been suggested that mechanical stimuli activate mTOR signaling through a phospholipase D (PLD)-dependent increase in the concentration of phosphatidic acid (PA). It has also been suggested that mechanical stimuli, and PA, utilize extracellular regulated kinase (ERK) to induce mTOR signaling. Hence, in Chapter 3, I tested if a mechanically-induced increase in PA promotes mTOR signaling via an ERK-dependent mechanism. To this end, I subjected mouse skeletal muscles to an *ex vivo* passive stretch model of mechanical stimulation, in the presence or absence of an ERK inhibitor. The results revealed that mechanical stimulation induces mTOR signaling, and protein synthesis, through an ERK-independent mechanism. Similar to mechanical stimulation, exogenous PA also induced mTOR signaling via an ERK-independent mechanism. Moreover, PA was able to directly activate mTOR signaling *in vitro*. Combined, these results indicate that mechanical stimuli activate mTOR signaling, and protein synthesis, via an ERK-independent mechanism that potentially involves a direct interaction of PA with mTOR.

In Chapter 4, using the same *ex vivo* passive stretch model, I obtained evidence which further suggests that mechanical stimuli utilize PA as a direct upstream activator of mTOR signaling. Unexpectedly though, in this study, the activation of PLD was not necessary for the mechanically-induced increases in PA or mTOR signaling. Instead, mechanical stimulation increased the concentration of diacylglycerol and the activity of diacylglycerol kinases (DGKs) in membranous structures. Using KO mice, I found that the zeta isoform of DGK (DGKζ) is necessary for the mechanically-induced increase in PA-mTOR signaling. Furthermore, the overexpression of DGKζ was sufficient to induce muscle fiber hypertrophy through an mTOR-dependent mechanism that requires DGKζ kinase activity (i.e. the

synthesis of PA). Overall, these results indicate that DGKζ, but not PLD, plays an important role in the mechanically-induced increases in PA and mTOR signaling.

The studies in Chapter 3 and 4 suggest that DGKζ could be a fundamental component of the mechanism(s) through which mechanical loading increases mTOR signaling, protein synthesis, and skeletal muscle mass. Thus, in Chapter 5, I set out to explore this possibility by employing mechanical overload (OV) model, which induces rapid muscle hypertrophy *in vivo*. The results showed that, during OV, DGKζ expression is elevated in both cytosolic and membranous structures, and required for a rapid hypertrophic response. Surprisingly, during the early period of OV, DGKζ not only promoted the activation of mTOR signaling and protein synthesis, but it also attenuated the induction of proteasome-dependent protein degradation and the ubiquitin-proteasome-system (UPS), including global ubiquitination and muscle-specific E3 ubiquitin ligases. Subsequent experiments revealed that nuclear DGKζ is a potent inhibitor of the Forkhead box O (FoxO) transcription factor, which promotes the induction of the UPS. When a denervation model of muscle atrophy was employed, DGKζ expression was also increased and required for mitigating atrophic response as well as the activation of the UPS and FoxO activity. Likewise, the overexpression of DGKζ was sufficient to prevent the atrophy that occurs during denervation and food deprivation. Collectively, these results demonstrate that DGKζ is a critical component of the mechanism through which mechanical stimuli not only promote the activation of mTOR signaling and protein synthesis, but also attenuate the induction of the UPS and protein degradation, to facilitate skeletal muscle hypertrophy.

In conclusion, the findings from this study unravel a novel mechanotransduction pathway through which mechanical stimuli promote skeletal muscle hypertrophy. I conclude that DGKζ is a critical component of this pathway because DGKζ *i*) contributes to the mechanically-induced activation of PA-mTOR signaling and protein synthesis, *ii*) when overexpressed, is sufficient to induce muscle hypertrophy through an mTOR-dependent mechanism that requires the synthesis of PA, *iii*) attenuates the mechanically-induced activation of the UPS and protein degradation, and *iv*) promotes the mechanically-induced muscle hypertrophy (Figure 6). Importantly, the results from this study also demonstrate that

these effects of DGKζ can help to preserve muscle mass during various atrophic conditions, such as denervation and food deprivation. Therefore, this study identifies DGKζ as a critical component of the mechanotransduction pathway that exhibits a significant clinical implication for the potential treatment of muscle atrophy.

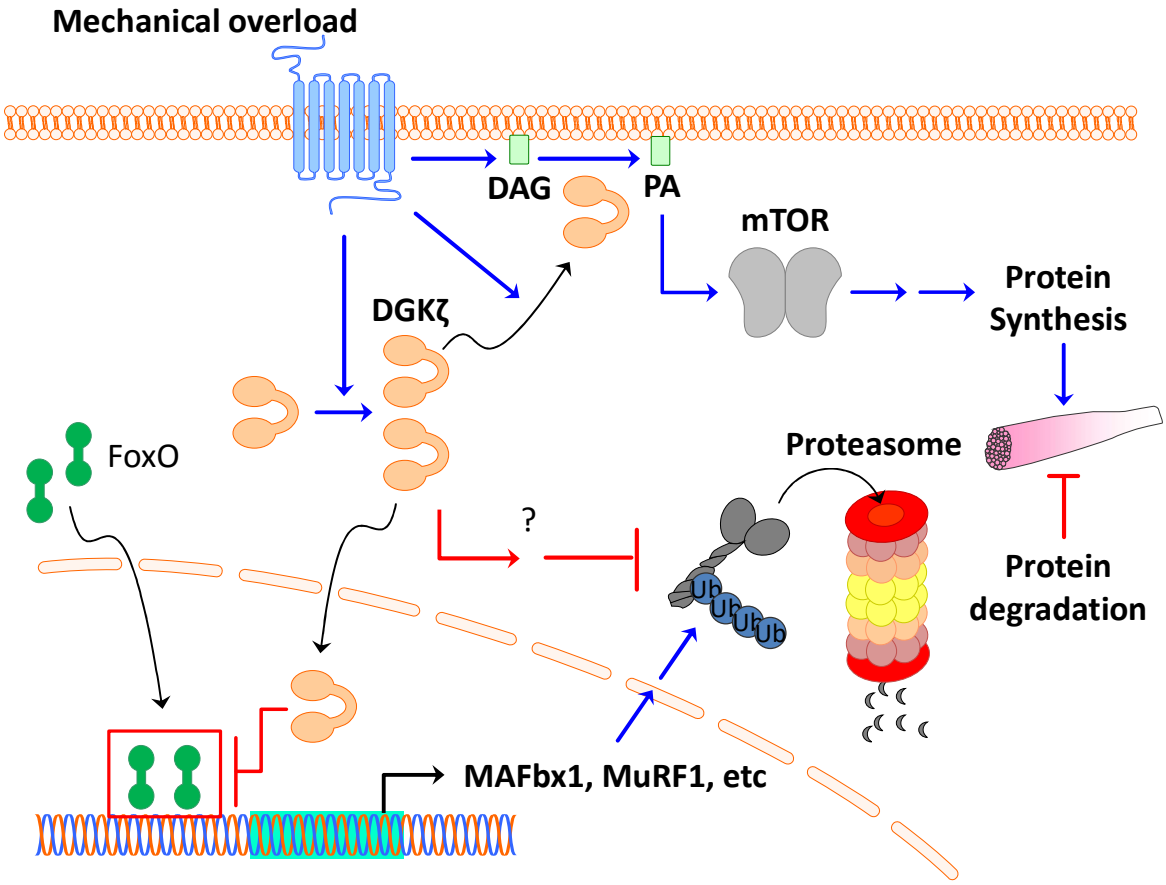

Figure 6. A proposed model for the DGKζ-mediated mechanotransduction pathway.

Future Directions

The studies in this dissertation explored the mechanisms through which mechanical stimuli regulate skeletal muscle mass. Although these studies discovered numerous novel findings, there are several questions that need to be addressed in future studies. The resulting knowledge should expand our understanding of how mechanical stimuli regulate skeletal muscle mass and facilitate the development of therapies that are aimed at preserving muscle mass during various atrophic conditions.

Q1) Is DGKζ necessary for the OV-induced increase in PA?

In this study, I demonstrated that both *ex vivo* passive stretch (Chapter 3) and OV (Chapter 4, using rats) increase the concentration of PA. Furthermore, in Chapter 3, by using DGKζ KO mice, I demonstrated that DGKζ is necessary for the stretch-induced increase in PA. This result was possible to obtain because the *ex vivo* system allows rapid and stable radiolabeling of total lipids which is needed to measure very low amount of a lipid species (e.g. PA) in a small mouse muscle. On the other hand, in Chapter 4, I was not able to test if DGKζ is necessary for the OV-induced increase in PA. This was because the currently validated technique for measuring the concentration of PA *in vivo* requires approximately 160 mg of a muscle tissue which would not be obtainable in mice (DGKζ KO animals are only available in mice) (56). Therefore, it remains undetermined whether DGKζ is necessary for the OV-induced increase in PA. In order to address this question under the current technical limitation, it may be considered to measure PA in a pooled mouse plantaris muscle (e.g., 6-8 muscles for n = 1). If this approach works and is used to test Q1, the resulting knowledge will not only assess the conclusion obtained from the *ex vivo* system, but will also enable us to answer the questions outlined below.

Q2) Is DGKζ-dependent synthesis of PA necessary to promote the OV-induced increase in mTOR signaling, protein synthesis, and muscle mass?

In Chapter 4, by using DGKζ KO mice, I demonstrated that DGKζ significantly contributes to the OV-induced increase in mTOR signaling, protein synthesis, and muscle mass. However, it was not

determined whether these effects of DGKζ require its kinase activity (i.e., synthesis of PA). Answers to this question will depend on the results from Q1. In other words, if DGKζ is not necessary for the OV-induced increase in PA, it will indicate that the effects of DGKζ are mediated by PA-independent mechanisms. On the other hand, if DGKζ is necessary for the OV-induced increase in PA, it will indicate that the effects of DGKζ are mediated by PA-dependent or PA-independent mechanisms (i.e., kinase activity-independent function of DGKζ). In this case, a rescue experiment may be needed to determine the involvement of PA. For example, DGKζ KO muscles can be transfected with a vector that can stably express either WT-DGKζ or kinase-dead (KD)-DGKζ, to create WT muscles (complete rescue) or muscles that only express KD-DGKζ (defective rescue), respectively. If this approach works and is used to test Q2, the resulting knowledge will help to define how DGKζ contributes to the OV-induced increase in mTOR signaling, protein synthesis, and muscle mass.

Q3) Is DGKζ-dependent synthesis of PA necessary to attenuate the OV-induced activation of the UPS and protein degradation?

In Chapter 4, I also demonstrated that DGKζ attenuate the OV-induced activation of the UPS (e.g., global ubiquitination and the expression of E3 ligases) and protein degradation. However, it was not determined whether these effects of DGKζ are mediated by its ability to synthesize PA. As described in Q2, answers to this question will also depend on the results from Q1 and may require the rescue experiment outlined in Q2. If tested, the resulting knowledge will help to define how DGKζ attenuates the OV-induced activation of the UPS and protein degradation.

Q4) Is overexpression of DGKζ sufficient to inhibit the activation of the UPS during denervation and food deprivation?

The identification of DGKζ as a positive regulator of muscle fiber size during OV has a significant clinical implication because it suggests that increasing the level of DGKζ expression could be a therapeutic strategy to combat muscle atrophy. Indeed, in Chapter 4, I demonstrated that the

overexpression of DGKζ is sufficient to attenuate the atrophy that occurs during denervation and food deprivation. Furthermore, these effects of DGKζ did not require its kinase activity. However, it is not clear whether the anti-atrophic effects of DGKζ are associated with its inhibitory role on the UPS (e.g., global ubiquitination and the expression of E3 ligases). In order to address this question, WT muscles that stably overexpress either WT-DGKζ or KD-DGKζ will be needed. If tested, the resulting knowledge will increase the therapeutic potential of DGKζ for preventing muscle atrophy.

Q5) How DGKζ inhibits FoxO transcriptional activity?

In Chapter 4, I demonstrated that DGKζ can potently inhibit FoxO transcriptional activity and this effect of DGKζ requires its nuclear translocation, but not its kinase activity. These findings potentiate the clinical significance of DGKζ because it is well established that the FoxO transcription factor is a tumor suppressor as well as an inducer of muscle atrophy (221, 222). Therefore, a more comprehensive understanding of the molecular mechanism by which DGKζ inhibits FoxO activity will not only increase the therapeutic potential of DGKζ for preventing muscle atrophy, but also benefit the ongoing efforts that are aimed at treating cancer.

References

1. Bentzinger, C.F., Wang, Y.X., and Rudnicki, M.A. 2012. Building muscle: molecular regulation of myogenesis. *Cold Spring Harb Perspect Biol* 4.

2. Buller, A.J., Eccles, J.C., and Eccles, R.M. 1960. Differentiation of fast and slow muscles in the cat hind limb. *J Physiol* 150:399-416.

3. Buller, A.J., Eccles, J.C., and Eccles, R.M. 1960. Interactions between motoneurones and muscles in respect of the characteristic speeds of their responses. *J Physiol* 150:417-439.

4. Miller, J.B., and Stockdale, F.E. 1986. Developmental origins of skeletal muscle fibers: clonal analysis of myogenic cell lineages based on expression of fast and slow myosin heavy chains. *Proc Natl Acad Sci U S A* 83:3860-3864.

5. Miller, J.B., and Stockdale, F.E. 1986. Developmental regulation of the multiple myogenic cell lineages of the avian embryo. *J Cell Biol* 103:2197-2208.

6. National Geographic Society (U.S.). 1986. *The Incredible machine*. Washington, D.C.: National Geographic Society. 384 p. pp.

7. Izumiya, Y., Hopkins, T., Morris, C., Sato, K., Zeng, L., Viereck, J., Hamilton, J.A., Ouchi, N., LeBrasseur, N.K., and Walsh, K. 2008. Fast/Glycolytic muscle fiber growth reduces fat mass and improves metabolic parameters in obese mice. *Cell Metab* 7:159-172.

8. Atlantis, E., Martin, S.A., Haren, M.T., Taylor, A.W., and Wittert, G.A. 2009. Inverse associations between muscle mass, strength, and the metabolic syndrome. *Metabolism* 58:1013-1022.

9. Srikanthan, P., and Karlamangla, A.S. 2011. Relative muscle mass is inversely associated with insulin resistance and prediabetes. Findings from the third National Health and Nutrition Examination Survey. *J Clin Endocrinol Metab* 96:2898-2903.

10. Evans, W.J. 2010. Skeletal muscle loss: cachexia, sarcopenia, and inactivity. *Am J Clin Nutr* 91:1123S-1127S.

11. Janssen, I., Shepard, D.S., Katzmarzyk, P.T., and Roubenoff, R. 2004. The healthcare costs of sarcopenia in the United States. *J Am Geriatr Soc* 52:80-85.

12. Srikanthan, P., and Karlamangla, A.S. 2014. Muscle mass index as a predictor of longevity in older adults. *Am J Med* 127:547-553.

13. Okumura, S., Kaido, T., Hamaguchi, Y., Fujimoto, Y., Masui, T., Mizumoto, M., Hammad, A., Mori, A., Takaori, K., and Uemoto, S. 2015. Impact of preoperative quality as well as quantity of skeletal muscle on survival after resection of pancreatic cancer. *Surgery* 157:1088-1098.

14. Du, Y., Karvellas, C.J., Baracos, V., Williams, D.C., and Khadaroo, R.G. 2014. Sarcopenia is a predictor of outcomes in very elderly patients undergoing emergency surgery. *Surgery* 156:521-527.

15. Goldberg, A.L., Etlinger, J.D., Goldspink, D.F., and Jablecki, C. 1975. Mechanism of work-induced hypertrophy of skeletal muscle. *Med Sci Sports* 7:185-198.

16. Adams, G.R., and Bamman, M.M. 2012. Characterization and regulation of mechanical loading-induced compensatory muscle hypertrophy. *Compr Physiol* 2:2829-2870.

17. Spangenburg, E.E. 2009. Changes in muscle mass with mechanical load: possible cellular mechanisms. *Appl Physiol Nutr Metab* 34:328-335.

18. Goldspink, D.F. 1977. The influence of immobilization and stretch on protein turnover of rat skeletal muscle. *J Physiol* 264:267-282.

19. McCall, G.E., Byrnes, W.C., Dickinson, A., Pattany, P.M., and Fleck, S.J. 1996. Muscle fiber hypertrophy, hyperplasia, and capillary density in college men after resistance training. *J Appl Physiol (1985)* 81:2004-2012.

20. Hurley, B.F., Hanson, E.D., and Sheaff, A.K. 2011. Strength training as a countermeasure to aging muscle and chronic disease. *Sports Med* 41:289-306.

21. Churchward-Venne, T.A., Breen, L., and Phillips, S.M. 2014. Alterations in human muscle protein metabolism with aging: Protein and exercise as countermeasures to offset sarcopenia. *Biofactors* 40:199-205.

22. Seguin, R., and Nelson, M.E. 2003. The benefits of strength training for older adults. *Am J Prev Med* 25:141-149.

23. Hirose, T., Shiozaki, T., Shimizu, K., Mouri, T., Noguchi, K., Ohnishi, M., and Shimazu, T. 2013. The effect of electrical muscle stimulation on the prevention of disuse muscle atrophy in patients with consciousness disturbance in the intensive care unit. *J Crit Care* 28:536 e531-537.

24. Gibson, J.N., Smith, K., and Rennie, M.J. 1988. Prevention of disuse muscle atrophy by means of electrical stimulation: maintenance of protein synthesis. *Lancet* 2:767-770.

25. Lieber, R.L. 2002. *Skeletal muscle structure, function & plasticity : the physiological basis of rehabilitation*. Philadelphia: Lippincott Williams & Wilkins. xii, 369 p. pp.

26. Kimball, S.R., Farrell, P.A., and Jefferson, L.S. 2002. Invited Review: Role of insulin in translational control of protein synthesis in skeletal muscle by amino acids or exercise. *J Appl Physiol* 93:1168-1180.

27. Meyuhas, O. 2000. Synthesis of the translational apparatus is regulated at the translational level. *Eur J Biochem* 267:6321-6330.

28. Chen, Y.W., Nader, G.A., Baar, K.R., Fedele, M.J., Hoffman, E.P., and Esser, K.A. 2002. Response of rat muscle to acute resistance exercise defined by transcriptional and translational profiling. *J Physiol* 545:27-41.

29. Jefferies, H.B., Fumagalli, S., Dennis, P.B., Reinhard, C., Pearson, R.B., and Thomas, G. 1997. Rapamycin suppresses 5'TOP mRNA translation through inhibition of p70s6k. *EMBO J* 16:3693-3704.

30. Drummond, M.J., Fry, C.S., Glynn, E.L., Dreyer, H.C., Dhanani, S., Timmerman, K.L., Volpi, E., and Rasmussen, B.B. 2009. Rapamycin administration in humans blocks the contraction-induced increase in skeletal muscle protein synthesis. *J Physiol* 587:1535-1546.

31. Hornberger, T.A., Stuppard, R., Conley, K.E., Fedele, M.J., Fiorotto, M.L., Chin, E.R., and Esser, K.A. 2004. Mechanical stimuli regulate rapamycin-sensitive signalling by a phosphoinositide 3-kinase-, protein kinase B- and growth factor-independent mechanism. *Biochem J* 380:795-804.

32. Kubica, N., Bolster, D.R., Farrell, P.A., Kimball, S.R., and Jefferson, L.S. 2005. Resistance exercise increases muscle protein synthesis and translation of eukaryotic initiation factor 2Bepsilon mRNA in a mammalian target of rapamycin-dependent manner. *J Biol Chem* 280:7570-7580.

33. Gundermann, D.M., Walker, D.K., Reidy, P.T., Borack, M.S., Dickinson, J.M., Volpi, E., and Rasmussen, B.B. 2014. Activation of mTORC1 signaling and protein synthesis in human muscle following blood flow restriction exercise is inhibited by rapamycin. *Am J Physiol Endocrinol Metab* 306:E1198-1204.

34. Bodine, S.C., Stitt, T.N., Gonzalez, M., Kline, W.O., Stover, G.L., Bauerlein, R., Zlotchenko, E., Scrimgeour, A., Lawrence, J.C., Glass, D.J., et al. 2001. Akt/mTOR pathway is a crucial regulator of skeletal muscle hypertrophy and can prevent muscle atrophy in vivo. *Nat Cell Biol* 3:1014-1019.

35. Goodman, C.A., Frey, J.W., Mabrey, D.M., Jacobs, B.L., Lincoln, H.C., You, J.S., and Hornberger, T.A. 2011. The role of skeletal muscle mTOR in the regulation of mechanical load-induced growth. *J Physiol* 589:5485-5501.

36. Chen, J., Zheng, X.F., Brown, E.J., and Schreiber, S.L. 1995. Identification of an 11-kDa FKBP12-rapamycin-binding domain within the 289-kDa FKBP12-rapamycin-associated protein and characterization of a critical serine residue. *Proc Natl Acad Sci U S A* 92:4947-4951.

37. Yip, C.K., Murata, K., Walz, T., Sabatini, D.M., and Kang, S.A. 2010. Structure of the human mTOR complex I and its implications for rapamycin inhibition. *Mol Cell* 38:768-774.

38. Lorenz, M.C., and Heitman, J. 1995. TOR mutations confer rapamycin resistance by preventing interaction with FKBP12-rapamycin. *J Biol Chem* 270:27531-27537.

39. Brown, E.J., Beal, P.A., Keith, C.T., Chen, J., Shin, T.B., and Schreiber, S.L. 1995. Control of p70 s6 kinase by kinase activity of FRAP in vivo. *Nature* 377:441-446.

40. Adams, G.R., and Haddad, F. 1996. The relationships among IGF-1, DNA content, and protein accumulation during skeletal muscle hypertrophy. *J Appl Physiol* 81:2509-2516.

41. Adams, G.R., and McCue, S.A. 1998. Localized infusion of IGF-I results in skeletal muscle hypertrophy in rats. *J Appl Physiol* 84:1716-1722.

42. Rommel, C., Bodine, S.C., Clarke, B.A., Rossman, R., Nunez, L., Stitt, T.N., Yancopoulos, G.D., and Glass, D.J. 2001. Mediation of IGF-1-induced skeletal myotube hypertrophy by PI(3)K/Akt/mTOR and PI(3)K/Akt/GSK3 pathways. *Nat Cell Biol* 3:1009-1013.

43. Bolster, D.R., Kubica, N., Crozier, S.J., Williamson, D.L., Farrell, P.A., Kimball, S.R., and Jefferson, L.S. 2003. Immediate response of mammalian target of rapamycin (mTOR)-mediated signalling following acute resistance exercise in rat skeletal muscle. *J Physiol* 553:213-220.

44. Hornberger, T.A., McLoughlin, T.J., Leszczynski, J.K., Armstrong, D.D., Jameson, R.R., Bowen, P.E., Hwang, E.S., Hou, H., Moustafa, M.E., Carlson, B.A., et al. 2003. Selenoprotein-deficient transgenic mice exhibit enhanced exercise-induced muscle growth. *J Nutr* 133:3091-3097.

45. Sakamoto, K., Aschenbach, W.G., Hirshman, M.F., and Goodyear, L.J. 2003. Akt signaling in skeletal muscle: regulation by exercise and passive stretch. *Am J Physiol Endocrinol Metab* 285:E1081-1088.

46. Atherton, P.J., Babraj, J., Smith, K., Singh, J., Rennie, M.J., and Wackerhage, H. 2005. Selective activation of AMPK-PGC-1alpha or PKB-TSC2-mTOR signaling can explain specific adaptive responses to endurance or resistance training-like electrical muscle stimulation. *Faseb J* 19:786-788.

47. Deshmukh, A., Coffey, V.G., Zhong, Z., Chibalin, A.V., Hawley, J.A., and Zierath, J.R. 2006. Exercise-induced phosphorylation of the novel Akt substrates AS160 and filamin A in human skeletal muscle. *Diabetes* 55:1776-1782.

48. Haddad, F., and Adams, G.R. 2006. Aging-sensitive cellular and molecular mechanisms associated with skeletal muscle hypertrophy. *J Appl Physiol* 100:1188-1203.

49. Carlson, C.J., Fan, Z., Gordon, S.E., and Booth, F.W. 2001. Time course of the MAPK and PI3-kinase response within 24 h of skeletal muscle overload. *J Appl Physiol* 91:2079-2087.

50. Spangenburg, E.E., and McBride, T.A. 2006. Inhibition of stretch-activated channels during eccentric muscle contraction attenuates p70S6K activation. *J Appl Physiol* 100:129-135.

51. Lockhart, N.C., Baar, K., Mazzeo, R.S., and Brooks, S.V. 2006. Activation of Akt as a potential mediator of adaptations that reduce muscle injury. *Med Sci Sports Exerc* 38:1058-1064.

52. Bruss, M.D., Arias, E.B., Lienhard, G.E., and Cartee, G.D. 2005. Increased phosphorylation of Akt substrate of 160 kDa (AS160) in rat skeletal muscle in response to insulin or contractile activity. *Diabetes* 54:41-50.

53. Varma, S., and Khandelwal, R.L. 2007. Effects of rapamycin on cell proliferation and phosphorylation of mTOR and p70(S6K) in HepG2 and HepG2 cells overexpressing constitutively active Akt/PKB. *Biochim Biophys Acta* 1770:71-78.

54. Pallafacchina, G., Calabria, E., Serrano, A.L., Kalhovde, J.M., and Schiaffino, S. 2002. A protein kinase B-dependent and rapamycin-sensitive pathway controls skeletal muscle growth but not fiber type specification. *Proc Natl Acad Sci U S A* 99:9213-9218.

55. Spangenburg, E.E., Le Roith, D., Ward, C.W., and Bodine, S.C. 2008. A functional insulin-like growth factor receptor is not necessary for load-induced skeletal muscle hypertrophy. *J Physiol* 586:283-291.

56. O'Neil, T.K., Duffy, L.R., Frey, J.W., and Hornberger, T.A. 2009. The role of phosphoinositide 3-kinase and phosphatidic acid in the regulation of mammalian target of rapamycin following eccentric contractions. *J Physiol* 587:3691-3701.

57. Hornberger, T.A., Sukhija, K.B., Wang, X.R., and Chien, S. 2007. mTOR is the rapamycin-sensitive kinase that confers mechanically-induced phosphorylation of the hydrophobic motif site Thr(389) in p70(S6k). *FEBS Lett* 581:4562-4566.

58. Smith, E.M., Finn, S.G., Tee, A.R., Browne, G.J., and Proud, C.G. 2005. The tuberous sclerosis protein TSC2 is not required for the regulation of the mammalian target of rapamycin by amino acids and certain cellular stresses. *J Biol Chem* 280:18717-18727.

59. Bar-Peled, L., and Sabatini, D.M. 2014. Regulation of mTORC1 by amino acids. *Trends Cell Biol* 24:400-406.

60. Vandenburgh, H.H., and Kaufman, S. 1981. Stretch-induced growth of skeletal myotubes correlates with activation of the sodium pump. *J Cell Physiol* 109:205-214.

61. MacKenzie, M.G., Hamilton, D.L., Murray, J.T., Taylor, P.M., and Baar, K. 2009. mVps34 is activated following high-resistance contractions. *J Physiol* 587:253-260.

62. Hornberger, T.A., and Chien, S. 2006. Mechanical stimuli and nutrients regulate rapamycin-sensitive signaling through distinct mechanisms in skeletal muscle. *J Cell Biochem* 97:1207-1216.

63. Hornberger, T.A., Chu, W.K., Mak, Y.W., Hsiung, J.W., Huang, S.A., and Chien, S. 2006. The role of phospholipase D and phosphatidic acid in the mechanical activation of mTOR signaling in skeletal muscle. *Proc Natl Acad Sci U S A* 103:4741-4746.

64. Cleland, P.J., Appleby, G.J., Rattigan, S., and Clark, M.G. 1989. Exercise-induced translocation of protein kinase C and production of diacylglycerol and phosphatidic acid in rat skeletal muscle in vivo. Relationship to changes in glucose transport. *J Biol Chem* 264:17704-17711.

65. Yoon, M.S., Sun, Y., Arauz, E., Jiang, Y., and Chen, J. 2011. Phosphatidic acid activates mammalian target of rapamycin complex 1 (mTORC1) kinase by displacing FK506 binding protein 38 (FKBP38) and exerting an allosteric effect. *J Biol Chem* 286:29568-29574.

66. Veverka, V., Crabbe, T., Bird, I., Lennie, G., Muskett, F.W., Taylor, R.J., and Carr, M.D. 2008. Structural characterization of the interaction of mTOR with phosphatidic acid and a novel class of inhibitor: compelling evidence for a central role of the FRB domain in small molecule-mediated regulation of mTOR. *Oncogene* 27:585-595.

67. Hornberger, T.A. 2011. Mechanotransduction and the regulation of mTORC1 signaling in skeletal muscle. *Int J Biochem Cell Biol* 43:1267-1276.

68. Zhou, X., Wang, J.L., Lu, J., Song, Y., Kwak, K.S., Jiao, Q., Rosenfeld, R., Chen, Q., Boone, T., Simonet, W.S., et al. 2010. Reversal of cancer cachexia and muscle wasting by ActRIIB antagonism leads to prolonged survival. *Cell* 142:531-543.

69. Wall, B.T., and van Loon, L.J. 2013. Nutritional strategies to attenuate muscle disuse atrophy. *Nutr Rev* 71:195-208.

70. de Boer, M.D., Selby, A., Atherton, P., Smith, K., Seynnes, O.R., Maganaris, C.N., Maffulli, N., Movin, T., Narici, M.V., and Rennie, M.J. 2007. The temporal responses of protein synthesis, gene expression and cell signalling in human quadriceps muscle and patellar tendon to disuse. *J Physiol* 585:241-251.

71. Goodman, C.A., Mayhew, D.L., and Hornberger, T.A. 2011. Recent progress toward understanding the molecular mechanisms that regulate skeletal muscle mass. *Cell Signal* 23:1896-1906.

72. Bodine, S.C. 2013. Disuse-induced muscle wasting. *Int J Biochem Cell Biol* 45:2200-2208.

73. Rennie, M.J., Selby, A., Atherton, P., Smith, K., Kumar, V., Glover, E.L., and Philips, S.M. 2010. Facts, noise and wishful thinking: muscle protein turnover in aging and human disuse atrophy. *Scand J Med Sci Sports* 20:5-9.

74. Kimball, S.R., and Jefferson, L.S. 2010. Control of translation initiation through integration of signals generated by hormones, nutrients, and exercise. *J Biol Chem* 285:29027-29032.

75. Ma, X.M., and Blenis, J. 2009. Molecular mechanisms of mTOR-mediated translational control. *Nat Rev Mol Cell Biol* 10:307-318.

76. Hara, K., Yonezawa, K., Kozlowski, M.T., Sugimoto, T., Andrabi, K., Weng, Q.P., Kasuga, M., Nishimoto, I., and Avruch, J. 1997. Regulation of eIF-4E BP1 phosphorylation by mTOR. *J Biol Chem* 272:26457-26463.

77. Haghighat, A., Mader, S., Pause, A., and Sonenberg, N. 1995. Repression of cap-dependent translation by 4E-binding protein 1: competition with p220 for binding to eukaryotic initiation factor-4E. *EMBO J* 14:5701-5709.

78. Raught, B., Peiretti, F., Gingras, A.C., Livingstone, M., Shahbazian, D., Mayeur, G.L., Polakiewicz, R.D., Sonenberg, N., and Hershey, J.W. 2004. Phosphorylation of eucaryotic translation initiation factor 4B Ser422 is modulated by S6 kinases. *EMBO J* 23:1761-1769.

79. Goodman, C.A., Miu, M.H., Frey, J.W., Mabrey, D.M., Lincoln, H.C., Ge, Y., Chen, J., and Hornberger, T.A. 2010. A phosphatidylinositol 3-kinase/protein kinase B-independent activation of mammalian target of rapamycin signaling is sufficient to induce skeletal muscle hypertrophy. *Mol Biol Cell* 21:3258-3268.

80. Goodman, C.A., Mabrey, D.M., Frey, J.W., Miu, M.H., Schmidt, E.K., Pierre, P., and Hornberger, T.A. 2011. Novel insights into the regulation of skeletal muscle protein synthesis as revealed by a new nonradioactive in vivo technique. *Faseb Journal* 25:1028-1039.

81. Huang, J., and Manning, B.D. 2008. The TSC1-TSC2 complex: a molecular switchboard controlling cell growth. *Biochem J* 412:179-190.

82. Quy, P.N., Kuma, A., Pierre, P., and Mizushima, N. 2013. Proteasome-dependent activation of mammalian target of rapamycin complex 1 (mTORC1) is essential for autophagy suppression and muscle remodeling following denervation. *J Biol Chem* 288:1125-1134.

83. Tang, H., Inoki, K., Lee, M., Wright, E., Khuong, A., Sugiarto, S., Garner, M., Paik, J., DePinho, R.A., Goldman, D., et al. 2014. mTORC1 promotes denervation-induced muscle atrophy through a mechanism involving the activation of FoxO and E3 ubiquitin ligases. *Sci Signal* 7:ra18.

84. Harrington, L.S., Findlay, G.M., and Lamb, R.F. 2005. Restraining PI3K: mTOR signalling goes back to the membrane. *Trends Biochem Sci* 30:35-42.

85. Stitt, T.N., Drujan, D., Clarke, B.A., Panaro, F., Timofeyva, Y., Kline, W.O., Gonzalez, M., Yancopoulos, G.D., and Glass, D.J. 2004. The IGF-1/PI3K/Akt pathway prevents expression of muscle atrophy-induced ubiquitin ligases by inhibiting FOXO transcription factors. *Mol Cell* 14:395-403.

86. Ferrari, S., Bandi, H.R., Hofsteenge, J., Bussian, B.M., and Thomas, G. 1991. Mitogen-activated 70K S6 kinase. Identification of in vitro 40 S ribosomal S6 phosphorylation sites. *J Biol Chem* 266:22770-22775.

87. Terzis, G., Georgiadis, G., Stratakos, G., Vogiatzis, I., Kavouras, S., Manta, P., Mascher, H., and Blomstrand, E. 2008. Resistance exercise-induced increase in muscle mass correlates with p70S6 kinase phosphorylation in human subjects. *Eur J Appl Physiol* 102:145-152.

88. Kumar, V., Selby, A., Rankin, D., Patel, R., Atherton, P., Hildebrandt, W., Williams, J., Smith, K., Seynnes, O., Hiscock, N., et al. 2009. Age-related differences in the dose-response relationship of muscle protein synthesis to resistance exercise in young and old men. *J Physiol* 587:211-217.

89. Baar, K., and Esser, K. 1999. Phosphorylation of p70(S6k) correlates with increased skeletal muscle mass following resistance exercise. *Am J Physiol* 276:C120-127.

90. Chaillou, T., Kirby, T.J., and McCarthy, J.J. 2014. Ribosome biogenesis: emerging evidence for a central role in the regulation of skeletal muscle mass. *J Cell Physiol* 229:1584-1594.

91. Bu, X., Haas, D.W., and Hagedorn, C.H. 1993. Novel phosphorylation sites of eukaryotic initiation factor-4F and evidence that phosphorylation stabilizes interactions of the p25 and p220 subunits. *J Biol Chem* 268:4975-4978.

92. Carlberg, U., Nilsson, A., and Nygard, O. 1990. Functional properties of phosphorylated elongation factor 2. *Eur J Biochem* 191:639-645.

93. Wang, X., Li, W., Williams, M., Terada, N., Alessi, D.R., and Proud, C.G. 2001. Regulation of elongation factor 2 kinase by p90(RSK1) and p70 S6 kinase. *EMBO J* 20:4370-4379.

94. Goodman, C.A., Kotecki, J.A., Jacobs, B.L., and Hornberger, T.A. 2012. Muscle fiber type-dependent differences in the regulation of protein synthesis. *PLoS One* 7:e37890.

95. Phillips, S.M., Glover, E.I., and Rennie, M.J. 2009. Alterations of protein turnover underlying disuse atrophy in human skeletal muscle. *J Appl Physiol (1985)* 107:645-654.

96. Kelleher, A.R., Kimball, S.R., Dennis, M.D., Schilder, R.J., and Jefferson, L.S. 2013. The mTORC1 signaling repressors REDD1/2 are rapidly induced and activation of p70S6K1 by leucine is defective in skeletal muscle of an immobilized rat hindlimb. *Am J Physiol Endocrinol Metab* 304:E229-236.

97. You, J.S., Park, M.N., Song, W., and Lee, Y.S. 2010. Dietary fish oil alleviates soleus atrophy during immobilization in association with Akt signaling to p70s6k and E3 ubiquitin ligases in rats. *Appl Physiol Nutr Metab* 35:310-318.

98. Hornberger, T.A., Hunter, R.B., Kandarian, S.C., and Esser, K.A. 2001. Regulation of translation factors during hindlimb unloading and denervation of skeletal muscle in rats. *Am J Physiol Cell Physiol* 281:C179-187.

99. Marimuthu, K., Murton, A.J., and Greenhaff, P.L. 2011. Mechanisms regulating muscle mass during disuse atrophy and rehabilitation in humans. *J Appl Physiol (1985)* 110:555-560.

100. Lin, J., Wu, H., Tarr, P.T., Zhang, C.Y., Wu, Z., Boss, O., Michael, L.F., Puigserver, P., Isotani, E., Olson, E.N., et al. 2002. Transcriptional co-activator PGC-1 alpha drives the formation of slow-twitch muscle fibres. *Nature* 418:797-801.

101. Russell, A.P., Feilchenfeldt, J., Schreiber, S., Praz, M., Crettenand, A., Gobelet, C., Meier, C.A., Bell, D.R., Kralli, A., Giacobino, J.P., et al. 2003. Endurance training in humans leads to fiber type-specific increases in levels of peroxisome proliferator-activated receptor-gamma coactivator-1 and peroxisome proliferator-activated receptor-alpha in skeletal muscle. *Diabetes* 52:2874-2881.

102. Sandri, M., Lin, J., Handschin, C., Yang, W., Arany, Z.P., Lecker, S.H., Goldberg, A.L., and Spiegelman, B.M. 2006. PGC-1alpha protects skeletal muscle from atrophy by suppressing FoxO3 action and atrophy-specific gene transcription. *Proc Natl Acad Sci U S A* 103:16260-16265.

103. Kang, C., and Ji, L.L. 2013. Muscle immobilization and remobilization downregulates PGC-1alpha signaling and the mitochondrial biogenesis pathway. *J Appl Physiol (1985)* 115:1618-1625.

104. Kline, W.O., Panaro, F.J., Yang, H., and Bodine, S.C. 2007. Rapamycin inhibits the growth and muscle-sparing effects of clenbuterol. *J Appl Physiol (1985)* 102:740-747.

105. Dyle, M.C., Ebert, S.M., Cook, D.P., Kunkel, S.D., Fox, D.K., Bongers, K.S., Bullard, S.A., Dierdorff, J.M., and Adams, C.M. 2014. Systems-based discovery of tomatidine as a natural small molecule inhibitor of skeletal muscle atrophy. *J Biol Chem* 289:14913-14924.

106. Ito, N., Ruegg, U.T., Kudo, A., Miyagoe-Suzuki, Y., and Takeda, S. 2013. Activation of calcium signaling through Trpv1 by nNOS and peroxynitrite as a key trigger of skeletal muscle hypertrophy. *Nat Med* 19:101-106.

107. Kazi, A.A., Hong-Brown, L., Lang, S.M., and Lang, C.H. 2011. Deptor knockdown enhances mTOR Activity and protein synthesis in myocytes and ameliorates disuse muscle atrophy. *Mol Med* 17:925-936.

108. Zhang, Y., Nicholatos, J., Dreier, J.R., Ricoult, S.J., Widenmaier, S.B., Hotamisligil, G.S., Kwiatkowski, D.J., and Manning, B.D. 2014. Coordinated regulation of protein synthesis and degradation by mTORC1. *Nature* 513:440-443.

109. You, J.S., Lincoln, H.C., Kim, C.R., Frey, J.W., Goodman, C.A., Zhong, X.P., and Hornberger, T.A. 2014. The Role of Diacylglycerol Kinase zeta and Phosphatidic Acid in the Mechanical

Activation of Mammalian Target of Rapamycin (mTOR) Signaling and Skeletal Muscle Hypertrophy. *J Biol Chem* 289:1551-1563.

110. Carter, M.S., and Sarnow, P. 2000. Distinct mRNAs that encode La autoantigen are differentially expressed and contain internal ribosome entry sites. *J Biol Chem* 275:28301-28307.

111. You, J.S., Frey, J.W., and Hornberger, T.A. 2012. Mechanical Stimulation Induces mTOR Signaling via an ERK-Independent Mechanism: Implications for a Direct Activation of mTOR by Phosphatidic Acid. *PLoS One* 7:e47258.

112. Proctor, D.N., Balagopal, P., and Nair, K.S. 1998. Age-related sarcopenia in humans is associated with reduced synthetic rates of specific muscle proteins. *J Nutr* 128:351S-355S.

113. Pahor, M., and Kritchevsky, S. 1998. Research hypotheses on muscle wasting, aging, loss of function and disability. *J Nutr Health Aging* 2:97-100.

114. Fitts, R.H., Riley, D.R., and Widrick, J.J. 2000. Physiology of a microgravity environment invited review: microgravity and skeletal muscle. *J Appl Physiol* 89:823-839.

115. Vandenburgh, H.H., Hatfaludy, S., Sohar, I., and Shansky, J. 1990. Stretch-induced prostaglandins and protein turnover in cultured skeletal muscle. *Am J Physiol* 259:C232-240.

116. Zoncu, R., Efeyan, A., and Sabatini, D.M. 2011. mTOR: from growth signal integration to cancer, diabetes and ageing. *Nat Rev Mol Cell Biol* 12:21-35.

117. Miyazaki, M., McCarthy, J.J., Fedele, M.J., and Esser, K.A. 2011. Early activation of mTORC1 signalling in response to mechanical overload is independent of phosphoinositide 3-kinase/Akt signalling. *J Physiol* 589:1831-1846.

118. Ma, L., Chen, Z., Erdjument-Bromage, H., Tempst, P., and Pandolfi, P.P. 2005. Phosphorylation and functional inactivation of TSC2 by Erk implications for tuberous sclerosis and cancer pathogenesis. *Cell* 121:179-193.

119. Roux, P.P., Ballif, B.A., Anjum, R., Gygi, S.P., and Blenis, J. 2004. Tumor-promoting phorbol esters and activated Ras inactivate the tuberous sclerosis tumor suppressor complex via p90 ribosomal S6 kinase. *Proc Natl Acad Sci U S A* 101:13489-13494.

120. Carriere, A., Romeo, Y., Acosta-Jaquez, H.A., Moreau, J., Bonneil, E., Thibault, P., Fingar, D.C., and Roux, P.P. 2011. ERK1/2 phosphorylate Raptor to promote Ras-dependent activation of mTOR complex 1 (mTORC1). *J Biol Chem* 286:567-577.

121. Tee, A.R., Anjum, R., and Blenis, J. 2003. Inactivation of the tuberous sclerosis complex-1 and -2 gene products occurs by phosphoinositide 3-kinase/Akt-dependent and -independent phosphorylation of tuberin. *J Biol Chem* 278:37288-37296.

122. Fang, Y., Vilella-Bach, M., Bachmann, R., Flanigan, A., and Chen, J. 2001. Phosphatidic acid-mediated mitogenic activation of mTOR signaling. *Science* 294:1942-1945.

123. Winter, J.N., Fox, T.E., Kester, M., Jefferson, L.S., and Kimball, S.R. 2010. Phosphatidic acid mediates activation of mTORC1 through the ERK signaling pathway. *Am J Physiol Cell Physiol* 299:C335-344.

124. Ghosh, S., Strum, J.C., Sciorra, V.A., Daniel, L., and Bell, R.M. 1996. Raf-1 kinase possesses distinct binding domains for phosphatidylserine and phosphatidic acid. Phosphatidic acid regulates the translocation of Raf-1 in 12-O-tetradecanoylphorbol-13-acetate-stimulated Madin-Darby canine kidney cells. *J Biol Chem* 271:8472-8480.

125. Rizzo, M.A., Shome, K., Vasudevan, C., Stolz, D.B., Sung, T.C., Frohman, M.A., Watkins, S.C., and Romero, G. 1999. Phospholipase D and its product, phosphatidic acid, mediate agonist-dependent raf-1 translocation to the plasma membrane and the activation of the mitogen-activated protein kinase pathway. *J Biol Chem* 274:1131-1139.

126. Rizzo, M.A., Shome, K., Watkins, S.C., and Romero, G. 2000. The recruitment of Raf-1 to membranes is mediated by direct interaction with phosphatidic acid and is independent of association with Ras. *J Biol Chem* 275:23911-23918.

127. Zhao, C., Du, G., Skowronek, K., Frohman, M.A., and Bar-Sagi, D. 2007. Phospholipase D2-generated phosphatidic acid couples EGFR stimulation to Ras activation by Sos. *Nat Cell Biol* 9:706-712.

128. Ge, Y., Wu, A.L., Warnes, C., Liu, J., Zhang, C., Kawasome, H., Terada, N., Boppart, M.D., Schoenherr, C.J., and Chen, J. 2009. mTOR regulates skeletal muscle regeneration in vivo through kinase-dependent and kinase-independent mechanisms. *Am J Physiol Cell Physiol* 297:C1434-1444.

129. Ikenoue, T., Hong, S., and Inoki, K. 2009. Monitoring mammalian target of rapamycin (mTOR) activity. *Methods Enzymol* 452:165-180.

130. Magnuson, B., Ekim, B., and Fingar, D.C. 2012. Regulation and function of ribosomal protein S6 kinase (S6K) within mTOR signalling networks. *Biochem J* 441:1-21.

131. Mukhopadhyay, N.K., Price, D.J., Kyriakis, J.M., Pelech, S., Sanghera, J., and Avruch, J. 1992. An array of insulin-activated, proline-directed serine/threonine protein kinases phosphorylate the p70 S6 kinase. *J Biol Chem* 267:3325-3335.

132. Jeno, P., Ballou, L.M., Novak-Hofer, I., and Thomas, G. 1988. Identification and characterization of a mitogen-activated S6 kinase. *Proc Natl Acad Sci U S A* 85:406-410.

133. Pende, M., Um, S.H., Mieulet, V., Sticker, M., Goss, V.L., Mestan, J., Mueller, M., Fumagalli, S., Kozma, S.C., and Thomas, G. 2004. S6K1(-/-)/S6K2(-/-) mice exhibit perinatal lethality and rapamycin-sensitive 5'-terminal oligopyrimidine mRNA translation and reveal a mitogen-activated protein kinase-dependent S6 kinase pathway. *Mol Cell Biol* 24:3112-3124.

134. Roux, P.P., Shahbazian, D., Vu, H., Holz, M.K., Cohen, M.S., Taunton, J., Sonenberg, N., and Blenis, J. 2007. RAS/ERK signaling promotes site-specific ribosomal protein S6 phosphorylation via RSK and stimulates cap-dependent translation. *J Biol Chem* 282:14056-14064.

135. Gingras, A.C., Kennedy, S.G., O'Leary, M.A., Sonenberg, N., and Hay, N. 1998. 4E-BP1, a repressor of mRNA translation, is phosphorylated and inactivated by the Akt(PKB) signaling pathway. *Genes Dev* 12:502-513.

136. Gingras, A.C., Gygi, S.P., Raught, B., Polakiewicz, R.D., Abraham, R.T., Hoekstra, M.F., Aebersold, R., and Sonenberg, N. 1999. Regulation of 4E-BP1 phosphorylation: a novel two-step mechanism. *Genes Dev* 13:1422-1437.

137. Mothe-Satney, I., Brunn, G.J., McMahon, L.P., Capaldo, C.T., Abraham, R.T., and Lawrence, J.C., Jr. 2000. Mammalian target of rapamycin-dependent phosphorylation of PHAS-I in four (S/T)P sites detected by phospho-specific antibodies. *J Biol Chem* 275:33836-33843.

138. Karim, M.M., Hughes, J.M., Warwicker, J., Scheper, G.C., Proud, C.G., and McCarthy, J.E. 2001. A quantitative molecular model for modulation of mammalian translation by the eIF4E-binding protein 1. *J Biol Chem* 276:20750-20757.

139. Osman, B., Doller, A., Akool el, S., Holdener, M., Hintermann, E., Pfeilschifter, J., and Eberhardt, W. 2009. Rapamycin induces the TGFbeta1/Smad signaling cascade in renal mesangial cells upstream of mTOR. *Cell Signal* 21:1806-1817.

140. Wang, T., and Donahoe, P.K. 2004. The immunophilin FKBP12: a molecular guardian of the TGF-beta family type I receptors. *Front Biosci* 9:619-631.

141. Avila, G., Lee, E.H., Perez, C.F., Allen, P.D., and Dirksen, R.T. 2003. FKBP12 binding to RyR1 modulates excitation-contraction coupling in mouse skeletal myotubes. *J Biol Chem* 278:22600-22608.

142. Goodman, C.A., Mabrey, D.M., Frey, J.W., Miu, M.H., Schmidt, E.K., Pierre, P., and Hornberger, T.A. 2011. Novel insights into the regulation of skeletal muscle protein synthesis as revealed by a new nonradioactive in vivo technique. *FASEB J* 25:1028-1039.

143. Anjum, R., and Blenis, J. 2008. The RSK family of kinases: emerging roles in cellular signalling. *Nat Rev Mol Cell Biol* 9:747-758.

144. Hou, J., Lam, F., Proud, C., and Wang, S. 2012. Targeting Mnks for cancer therapy. *Oncotarget* 3:118-131.

145. Vilella-Bach, M., Nuzzi, P., Fang, Y., and Chen, J. 1999. The FKBP12-rapamycin-binding domain is required for FKBP12-rapamycin-associated protein kinase activity and G1 progression. *J Biol Chem* 274:4266-4272.

146. Martineau, L.C., and Gardiner, P.F. 2001. Insight into skeletal muscle mechanotransduction: MAPK activation is quantitatively related to tension. *J Appl Physiol* 91:693-702.

147. Sancak, Y., Thoreen, C.C., Peterson, T.R., Lindquist, R.A., Kang, S.A., Spooner, E., Carr, S.A., and Sabatini, D.M. 2007. PRAS40 is an insulin-regulated inhibitor of the mTORC1 protein kinase. *Mol Cell* 25:903-915.

148. Yoon, M.S., Du, G., Backer, J.M., Frohman, M.A., and Chen, J. 2011. Class III PI-3-kinase activates phospholipase D in an amino acid-sensing mTORC1 pathway. *J Cell Biol* 195:435-447.

149. Yonezawa, K., Yoshino, K.I., Tokunaga, C., and Hara, K. 2004. Kinase activities associated with mTOR. *Curr Top Microbiol Immunol* 279:271-282.

150. Thoreen, C.C., Chantranupong, L., Keys, H.R., Wang, T., Gray, N.S., and Sabatini, D.M. 2012. A unifying model for mTORC1-mediated regulation of mRNA translation. *Nature* 485:109-113.

151. Gingras, A.C., Raught, B., Gygi, S.P., Niedzwiecka, A., Miron, M., Burley, S.K., Polakiewicz, R.D., Wyslouch-Cieszynska, A., Aebersold, R., and Sonenberg, N. 2001. Hierarchical phosphorylation of the translation inhibitor 4E-BP1. *Genes Dev* 15:2852-2864.

152. Zhang, D., Contu, R., Latronico, M.V., Zhang, J., Rizzi, R., Catalucci, D., Miyamoto, S., Huang, K., Ceci, M., Gu, Y., et al. 2010. MTORC1 regulates cardiac function and myocyte survival through 4E-BP1 inhibition in mice. *J Clin Invest* 120:2805-2816.

153. Walsh, D., and Mohr, I. 2004. Phosphorylation of eIF4E by Mnk-1 enhances HSV-1 translation and replication in quiescent cells. *Genes Dev* 18:660-672.

154. Aviles Mendoza, G.J., Seidel, N.E., Otsu, M., Anderson, S.M., Simon-Stoos, K., Herrera, A., Hoogstraten-Miller, S., Malech, H.L., Candotti, F., Puck, J.M., et al. 2001. Comparison of five retrovirus vectors containing the human IL-2 receptor gamma chain gene for their ability to restore T and B lymphocytes in the X-linked severe combined immunodeficiency mouse model. *Mol Ther* 3:565-573.

155. Toschi, A., Lee, E., Xu, L., Garcia, A., Gadir, N., and Foster, D.A. 2009. Regulation of mTORC1 and mTORC2 complex assembly by phosphatidic acid: competition with rapamycin. *Mol Cell Biol* 29:1411-1420.

156. Fang, Y.M., Vilella-Bach, M., Bachmann, R., Flanigan, A., and Chen, J. 2001. Phosphatidic acid-mediated mitogenic activation of mTOR signaling. *Science* 294:1942-1945.

157. Su, W., Yeku, O., Olepu, S., Genna, A., Park, J.S., Ren, H., Du, G., Gelb, M.H., Morris, A.J., and Frohman, M.A. 2009. 5-Fluoro-2-indolyl des-chlorohalopemide (FIPI), a phospholipase D pharmacological inhibitor that alters cell spreading and inhibits chemotaxis. *Mol Pharmacol* 75:437-446.

158. Yanase, Y., Carvou, N., Frohman, M.A., and Cockcroft, S. 2010. Reversible bleb formation in mast cells stimulated with antigen is Ca2+/calmodulin-dependent and bleb size is regulated by ARF6. *Biochem J* 425:179-193.

159. Sato, T., Hongu, T., Sakamoto, M., Funakoshi, Y., and Kanaho, Y. 2013. Molecular mechanisms of N-formyl-methionyl-leucyl-phenylalanine-induced superoxide generation and degranulation in mouse neutrophils: phospholipase D is dispensable. *Mol Cell Biol* 33:136-145.

160. Topham, M.K., Bunting, M., Zimmerman, G.A., McIntyre, T.M., Blackshear, P.J., and Prescott, S.M. 1998. Protein kinase C regulates the nuclear localization of diacylglycerol kinase-zeta. *Nature* 394:697-700.

161. Zhong, X.P., Hainey, E.A., Olenchock, B.A., Jordan, M.S., Maltzman, J.S., Nichols, K.E., Shen, H., and Koretzky, G.A. 2003. Enhanced T cell responses due to diacylglycerol kinase xi deficiency. *Nature Immunology* 4:882-890.

162. Jacobs, B.L., You, J.S., Frey, J.W., Goodman, C.A., Gundermann, D.M., and Hornberger, T.A. 2013. Eccentric contractions increase the phosphorylation of tuberous sclerosis complex-2 (TSC2)

and alter the targeting of TSC2 and the mechanistic target of rapamycin to the lysosome. *J Physiol* 591:4611-4620.

163. Chibalin, A.V., Leng, Y., Vieira, E., Krook, A., Bjornholm, M., Long, Y.C., Kotova, O., Zhong, Z., Sakane, F., Steiler, T., et al. 2008. Downregulation of diacylglycerol kinase delta contributes to hyperglycemia-induced insulin resistance. *Cell* 132:375-386.

164. Goodman, C.A., McNally, R.M., Hoffmann, F.M., and Hornberger, T.A. 2013. Smad3 induces atrogin-1, inhibits mTOR and protein synthesis, and promotes muscle atrophy in vivo. *Mol Endocrinol* 27:1946-1957.

165. Eaton, J.M., Mullins, G.R., Brindley, D.N., and Harris, T.E. 2013. Phosphorylation of lipin 1 and charge on the phosphatidic acid head group control its phosphatidic acid phosphatase activity and membrane association. *J Biol Chem* 288:9933-9945.

166. Harris, T.E., Huffman, T.A., Chi, A., Shabanowitz, J., Hunt, D.F., Kumar, A., and Lawrence, J.C., Jr. 2007. Insulin controls subcellular localization and multisite phosphorylation of the phosphatidic acid phosphatase, lipin 1. *J Biol Chem* 282:277-286.

167. Kim, D.H., Sarbassov, D.D., Ali, S.M., King, J.E., Latek, R.R., Erdjument-Bromage, H., Tempst, P., and Sabatini, D.M. 2002. mTOR interacts with raptor to form a nutrient-sensitive complex that signals to the cell growth machinery. *Cell* 110:163-175.

168. el Bawab, S., Macovschi, O., Thevenon, C., Goncalves, A., Nemoz, G., Lagarde, M., and Prigent, A.F. 1996. Contribution of phosphoinositides and phosphatidylcholines to the production of phosphatidic acid upon concanavalin A stimulation of rat thymocytes. *J Lipid Res* 37:2098-2108.

169. Sadoshima, J., and Izumo, S. 1993. Mechanical stretch rapidly activates multiple signal transduction pathways in cardiac myocytes: potential involvement of an autocrine/paracrine mechanism. *Embo J* 12:1681-1692.

170. Jiang, Y., Sakane, F., Kanoh, H., and Walsh, J.P. 2000. Selectivity of the diacylglycerol kinase inhibitor 3-[2-(4-[bis-(4-fluorophenyl)methylene]-1-piperidinyl)ethyl]-2, 3-dihydro-2-thioxo-4(1H)quinazolinone (R59949) among diacylglycerol kinase subtypes. *Biochem Pharmacol* 59:763-772.

171. Baldanzi, G., Alchera, E., Imarisio, C., Gaggianesi, M., Dal Ponte, C., Nitti, M., Domenicotti, C., van Blitterswijk, W.J., Albano, E., Graziani, A., et al. 2010. Negative regulation of diacylglycerol kinase theta mediates adenosine-dependent hepatocyte preconditioning. *Cell Death Differ* 17:1059-1068.

172. van Blitterswijk, W.J., and Houssa, B. 2000. Properties and functions of diacylglycerol kinases. *Cell Signal* 12:595-605.

173. Avila-Flores, A., Santos, T., Rincon, E., and Merida, I. 2005. Modulation of the mammalian target of rapamycin pathway by diacylglycerol kinase-produced phosphatidic acid. *J Biol Chem* 280:10091-10099.

174. Gorentla, B.K., Wan, C.K., and Zhong, X.P. 2011. Negative regulation of mTOR activation by diacylglycerol kinases. *Blood* 117:4022-4031.

175. Ballou, L.M., Jiang, Y.P., Du, G., Frohman, M.A., and Lin, R.Z. 2003. Ca(2+)- and phospholipase D-dependent and -independent pathways activate mTOR signaling. *FEBS Lett* 550:51-56.

176. Yoon, M.S., and Chen, J. 2008. PLD regulates myoblast differentiation through the mTOR-IGF2 pathway. *J Cell Sci* 121:282-289.

177. Jaafar, R., De Larichaudy, J., Chanon, S., Euthine, V., Durand, C., Naro, F., Bertolino, P., Vidal, H., Lefai, E., and Nemoz, G. 2013. Phospholipase D regulates the size of skeletal muscle cells through the activation of mTOR signaling. *Cell Commun Signal* 11:55.

178. Sancak, Y., Bar-Peled, L., Zoncu, R., Markhard, A.L., Nada, S., and Sabatini, D.M. 2010. Ragulator-Rag complex targets mTORC1 to the lysosomal surface and is necessary for its activation by amino acids. *Cell* 141:290-303.

179. Saito, K., Araki, Y., Kontani, K., Nishina, H., and Katada, T. 2005. Novel role of the small GTPase Rheb: its implication in endocytic pathway independent of the activation of mammalian target of rapamycin. *J Biochem* 137:423-430.

180. Jacobs, B.L., Goodman, C.A., and Hornberger, T.A. 2013. The mechanical activation of mTOR signaling: an emerging role for late endosome/lysosomal targeting. *J Muscle Res Cell Motil*.

181. Zhao, K., Zhou, H., Zhao, X., Wolff, D.W., Tu, Y., Liu, H., Wei, T., and Yang, F. 2012. Phosphatidic acid mediates the targeting of tBid to induce lysosomal membrane permeabilization and apoptosis. *J Lipid Res* 53:2102-2114.

182. Rincon, E., Santos, T., Avila-Flores, A., Albar, J.P., Lalioti, V., Lei, C., Hong, W., and Merida, I. 2007. Proteomics identification of sorting nexin 27 as a diacylglycerol kinase zeta-associated protein: new diacylglycerol kinase roles in endocytic recycling. *Mol Cell Proteomics* 6:1073-1087.

183. Nelson, C.D., Perry, S.J., Regier, D.S., Prescott, S.M., Topham, M.K., and Lefkowitz, R.J. 2007. Targeting of diacylglycerol degradation to M1 muscarinic receptors by beta-arrestins. *Science* 315:663-666.

184. Truschel, S.T., Wang, E., Ruiz, W.G., Leung, S.M., Rojas, R., Lavelle, J., Zeidel, M., Stoffer, D., and Apodaca, G. 2002. Stretch-regulated exocytosis/endocytosis in bladder umbrella cells. *Mol Biol Cell* 13:830-846.

185. Chen, Y., Zheng, Y., and Foster, D.A. 2003. Phospholipase D confers rapamycin resistance in human breast cancer cells. *Oncogene* 22:3937-3942.

186. Thalacker-Mercer, A., Stec, M., Cui, X., Cross, J., Windham, S., and Bamman, M. 2013. Cluster analysis reveals differential transcript profiles associated with resistance training-induced human skeletal muscle hypertrophy. *Physiol Genomics* 45:499-507.

187. Evangelisti, C., Riccio, M., Faenza, I., Zini, N., Hozumi, Y., Goto, K., Cocco, L., and Martelli, A.M. 2006. Subnuclear localization and differentiation-dependent increased expression of DGK-zeta in C2C12 mouse myoblasts. *J Cell Physiol* 209:370-378.

188. Abramovici, H., and Gee, S.H. 2007. Morphological changes and spatial regulation of diacylglycerol kinase-zeta, syntrophins, and Rac1 during myoblast fusion. *Cell Motil Cytoskeleton* 64:549-567.

189. Guerci, A., Lahoute, C., Hebrard, S., Collard, L., Graindorge, D., Favier, M., Cagnard, N., Batonnet-Pichon, S., Precigout, G., Garcia, L., et al. 2012. Srf-dependent paracrine signals produced by myofibers control satellite cell-mediated skeletal muscle hypertrophy. *Cell Metab* 15:25-37.

190. Sun, Y., Ge, Y., Drnevich, J., Zhao, Y., Band, M., and Chen, J. 2010. Mammalian target of rapamycin regulates miRNA-1 and follistatin in skeletal myogenesis. *J Cell Biol* 189:1157-1169.

191. Schiaffino, S., Dyar, K.A., Ciciliot, S., Blaauw, B., and Sandri, M. 2013. Mechanisms regulating skeletal muscle growth and atrophy. *FEBS J* 280:4294-4314.

192. Murton, A.J., Constantin, D., and Greenhaff, P.L. 2008. The involvement of the ubiquitin proteasome system in human skeletal muscle remodelling and atrophy. *Biochim Biophys Acta* 1782:730-743.

193. Bodine, S.C., and Baehr, L.M. 2014. Skeletal muscle atrophy and the E3 ubiquitin ligases MuRF1 and MAFbx/atrogin-1. *Am J Physiol Endocrinol Metab* 307:E469-484.

194. Yoon, M.S., Sun, Y.T., Arauz, E., Jiang, Y., and Chen, J. 2011. Phosphatidic Acid Activates Mammalian Target of Rapamycin Complex 1 (mTORC1) Kinase by Displacing FK506 Binding Protein 38 (FKBP38) and Exerting an Allosteric Effect. *Journal of Biological Chemistry* 286:29568-29574.

195. Mobley, C.B., Hornberger, T.A., Fox, C.D., Healy, J.C., Ferguson, B.S., Lowery, R.P., McNally, R.M., Lockwood, C.M., Stout, J.R., Kavazis, A.N., et al. 2015. Effects of oral phosphatidic acid feeding with or without whey protein on muscle protein synthesis and anabolic signaling in rodent skeletal muscle. *J Int Soc Sports Nutr* 12:32.

196. McCarthy, J.J., Mula, J., Miyazaki, M., Erfani, R., Garrison, K., Farooqui, A.B., Srikuea, R., Lawson, B.A., Grimes, B., Keller, C., et al. 2011. Effective fiber hypertrophy in satellite cell-depleted skeletal muscle. *Development* 138:3657-3666.

197. Lagirand-Cantaloube, J., Offner, N., Csibi, A., Leibovitch, M.P., Batonnet-Pichon, S., Tintignac, L.A., Segura, C.T., and Leibovitch, S.A. 2008. The initiation factor eIF3-f is a major target for atrogin1/MAFbx function in skeletal muscle atrophy. *EMBO J* 27:1266-1276.

198. Van Gammeren, D., Damrauer, J.S., Jackman, R.W., and Kandarian, S.C. 2009. The IkappaB kinases IKKalpha and IKKbeta are necessary and sufficient for skeletal muscle atrophy. *Faseb Journal* 23:362-370.

199. Brunet, A., Bonni, A., Zigmond, M.J., Lin, M.Z., Juo, P., Hu, L.S., Anderson, M.J., Arden, K.C., Blenis, J., and Greenberg, M.E. 1999. Akt promotes cell survival by phosphorylating and inhibiting a Forkhead transcription factor. *Cell* 96:857-868.

200. Bodine, S.C., Latres, E., Baumhueter, S., Lai, V.K., Nunez, L., Clarke, B.A., Poueymirou, W.T., Panaro, F.J., Na, E., Dharmarajan, K., et al. 2001. Identification of ubiquitin ligases required for skeletal muscle atrophy. *Science* 294:1704-1708.

201. Milan, G., Romanello, V., Pescatore, F., Armani, A., Paik, J.H., Frasson, L., Seydel, A., Zhao, J., Abraham, R., Goldberg, A.L., et al. 2015. Regulation of autophagy and the ubiquitin-proteasome system by the FoxO transcriptional network during muscle atrophy. *Nat Commun* 6:6670.

202. Lee, D., and Goldberg, A.L. 2015. Muscle wasting in fasting requires activation of NF-kappaB and inhibition of AKT/mTOR by the protein acetylase, GCN5. *J Biol Chem*.

203. Kumar, V., Atherton, P., Smith, K., and Rennie, M.J. 2009. Human muscle protein synthesis and breakdown during and after exercise. *J Appl Physiol (1985)* 106:2026-2039.

204. Sanchez, A.M., Csibi, A., Raibon, A., Docquier, A., Lagirand-Cantaloube, J., Leibovitch, M.P., Leibovitch, S.A., and Bernardi, H. 2013. eIF3f: a central regulator of the antagonism atrophy/hypertrophy in skeletal muscle. *Int J Biochem Cell Biol* 45:2158-2162.

205. Goldberg, A.L. 2003. Protein degradation and protection against misfolded or damaged proteins. *Nature* 426:895-899.

206. Baehr, L.M., Tunzi, M., and Bodine, S.C. 2014. Muscle hypertrophy is associated with increases in proteasome activity that is independent of MuRF1 and MAFbx expression. *Front Physiol* 5:69.

207. Beehler, B.C., Sleph, P.G., Benmassaoud, L., and Grover, G.J. 2006. Reduction of skeletal muscle atrophy by a proteasome inhibitor in a rat model of denervation. *Exp Biol Med (Maywood)* 231:335-341.

208. Krawiec, B.J., Frost, R.A., Vary, T.C., Jefferson, L.S., and Lang, C.H. 2005. Hindlimb casting decreases muscle mass in part by proteasome-dependent proteolysis but independent of protein synthesis. *Am J Physiol Endocrinol Metab* 289:E969-980.

209. Mourkioti, F., Kratsios, P., Luedde, T., Song, Y.H., Delafontaine, P., Adami, R., Parente, V., Bottinelli, R., Pasparakis, M., and Rosenthal, N. 2006. Targeted ablation of IKK2 improves skeletal muscle strength, maintains mass, and promotes regeneration. *J Clin Invest* 116:2945-2954.

210. Cai, D., Frantz, J.D., Tawa, N.E., Jr., Melendez, P.A., Oh, B.C., Lidov, H.G., Hasselgren, P.O., Frontera, W.R., Lee, J., Glass, D.J., et al. 2004. IKKbeta/NF-kappaB activation causes severe muscle wasting in mice. *Cell* 119:285-298.

211. van der Horst, A., and Burgering, B.M. 2007. Stressing the role of FoxO proteins in lifespan and disease. *Nat Rev Mol Cell Biol* 8:440-450.

212. Tak, P.P., and Firestein, G.S. 2001. NF-kappaB: a key role in inflammatory diseases. *J Clin Invest* 107:7-11.

213. Paul, S. 2008. Dysfunction of the ubiquitin-proteasome system in multiple disease conditions: therapeutic approaches. *Bioessays* 30:1172-1184.

214. Abramovici, H., Hogan, A.B., Obagi, C., Topham, M.K., and Gee, S.H. 2003. Diacylglycerol kinase-zeta localization in skeletal muscle is regulated by phosphorylation and interaction with syntrophins. *Mol Biol Cell* 14:4499-4511.

215. Schmidt, E.K., Clavarino, G., Ceppi, M., and Pierre, P. 2009. SUnSET, a nonradioactive method to monitor protein synthesis. *Nat Methods* 6:275-277.

216. Kimball, S.R., Jurasinski, C.V., Lawrence, J.C., Jr., and Jefferson, L.S. 1997. Insulin stimulates protein synthesis in skeletal muscle by enhancing the association of eIF-4E and eIF-4G. *Am J Physiol* 272:C754-759.

217. Zhong, X.P., Hainey, E.A., Olenchock, B.A., Jordan, M.S., Maltzman, J.S., Nichols, K.E., Shen, H., and Koretzky, G.A. 2003. Enhanced T cell responses due to diacylglycerol kinase zeta deficiency. *Nature Immunology* 4:882-890.

218. You, J.S., Anderson, G.B., Dooley, M.S., and Hornberger, T.A. 2015. The role of mTOR signaling in the regulation of protein synthesis and muscle mass during immobilization. *Dis Model Mech*.

219. Rothermel, B., Vega, R.B., Yang, J., Wu, H., Bassel-Duby, R., and Williams, R.S. 2000. A protein encoded within the Down syndrome critical region is enriched in striated muscles and inhibits calcineurin signaling. *J Biol Chem* 275:8719-8725.

220. Waalkes, T.P., and Udenfriend, S. 1957. A fluorometric method for the estimation of tyrosine in plasma and tissues. *J Lab Clin Med* 50:733-736.

221. Fu, Z., and Tindall, D.J. 2008. FOXOs, cancer and regulation of apoptosis. *Oncogene* 27:2312-2319.

222. Bonaldo, P., and Sandri, M. 2013. Cellular and molecular mechanisms of muscle atrophy. *Dis Model Mech* 6:25-39.